



Norwegian University of
Science and Technology

An Investment Model for Energy Systems in Zero Emission Neighborhoods

A Multi-Horizon Stochastic Programming
Approach

Lea Beus

Caroline Eldrup

Ingrid Hammersbøen

Industrial Economics and Technology Management

Submission date: June 2018

Supervisor: Asgeir Tomasgard, IØT

Co-supervisor: Karen Byskov Lindberg, IEL

Norwegian University of Science and Technology

Department of Industrial Economics and Technology Management

Problem formulation

The main objective of the ZEN energy system investment problem is to find the cost-optimal strategic investment decisions of which capacities of different energy technologies that should be installed in each investment period, while considering the optimal operation of the energy system with short-term uncertainties taken into account. It should also fulfill certain emission requirements with regard to the determined level of ZEN.

Preface

This thesis is a continuation of Beus et al. (2018) and comprises the work performed during the spring of 2018 at the Norwegian University of Technology and Science (NTNU). It represents the completion of our Master of Science degree in Industrial Economics and Technology Management and is written as the result of the course *TIØ4905 Managerial Economics and Operations Research, Master's Thesis* at the Department of Industrial Economics and Technology Management. The study is carried out in cooperation with the Research Centre on Zero Emission Neighborhoods in Smart Cities (FME ZEN) and the collaboration has contributed to the motivation behind this thesis and what is enclosed in the following.

We would like to express a great gratitude to the people who have contributed to the content in this thesis. First and foremost, we want to thank our supervisor Asgeir Tomasgard, who has given us academic and technological insights and a high degree of autonomy. We also want to especially thank our co-supervisor Karen Byskov Lindberg, for her unwavering assistance, advice, and motivation. She has also developed a ZEB model that has served as a basis for the design of our model. We would also like to give our gratitude to Stian Backe for his remarkable interest in our study and all the useful help he has provided us with.

Throughout the process of producing this thesis, the FME ZEN and other involved parties have been accommodating in facilitating our research. This thesis contains a case study performed on the pilot project *Ydalir* and we wish to thank Anna-Thekla Tonjer from Elverum Vekst for giving us useful data and insights about the pilot project, as well as Ola T. Dahl from Eidsiva Bioenergi and Einar Hoff from Eidsiva Nett who also have provided useful information.

It is assumed that the readers have some background or central knowledge in operations research to understand the profound material in this thesis.

Trondheim, June 2018

Abstract

This thesis studies an optimization problem regarding investment planning of energy systems in ZENs, and suggests a two-stage multi-horizon stochastic programming approach. It aims to provide a useful decision tool for developers in ZENs, in addition to a model that may be used as a neighborhood module in EMPIRE.

The main objective is to find cost-optimal investment decisions of which capacities of different energy technologies that should be installed in each investment period, while considering the optimal operation of the energy system. Technologies included in the model are district heating, ST-collectors, PV-panels, heat pumps, electric boiler, bio boiler, gas boiler, combined heat and power, heat storage and battery. The high number of included technologies is one of the contributions of the model. Especially the inclusion of combined heat and power and storage technologies for *both* heat and electricity, facilitating load shifting, is important to emphasize. With the use of feed-in-tariffs, the option of exporting electricity is also implemented.

Another important contribution of this work is the integrated optimization of *both* strategic investments and the operation of the energy system, while taking operational uncertainties in PV and ST generation, electricity and heat demand, and electricity and district heating prices into account. The uncertainty is proposed modeled with a multi-horizon information structure, separating the operational and strategic investment horizons of the problem. Accompanied by the proposed scenario generation method, which has proved to be very stable for a number of problem instances, the complexity of the problem is considerably decreased.

An extensive case study of the pilot project Ydalir is also provided, demonstrating and validating the model. The practical analysis emphasizes the behaviour of the model and the considerations that should be taken into account.

This thesis also includes a comprehensive literature review covering research studying strategic and/or operational decision making within energy systems on both small and large scales. To our knowledge there does not exist many studies considering ZENs in particular, implying that the study may be a valuable contribution to the research area.

Sammendrag

Denne oppgaven studerer investeringsproblemet tilknyttet planleggingen av energisystemer i nullutslippsnabolag og foreslår en to-stegs multihorisont stokastisk programmeringstilnærming. Modellen er utviklet med den hensikt å tilby beslutningstakere et nyttig verktøy i planleggingsfasen av nullutslippsnabolag. Den er også utviklet med tanke på å kunne representere en nabolagsmodul i storskalamodellen EMPIRE.

Hovedmålet er å finne kostnadsoptimale investeringsbeslutninger som angir kapasiteten til de energiteknologiene som burde installeres i hver investeringsperiode, tatt i betraktning av en optimal operasjonell drift av energisystemet. Teknologiene inkludert i modellen er fjernvarme, solfanger, solcellepanel, luft- og grunnkildewarmepumper, elektrisk kjel, biokjel, gasskjel, kraftvarme (CHP), varmelager og batteri. Et stort antall teknologier er inkludert, og er en av styrkene til modellen. Inkluderingen av kraftvarme og lagringsteknologier for *både* varme og elektrisitet, noe som muliggjør lastforskyvning, er spesielt viktig å merke seg. Modellen inkluderer også muligheten for å eksportere elektrisitet ved å bruke innmatingstariffer (feed-in-tariffs).

Et annet viktig bidrag er den integrerte optimeringen av *både* de strategiske investeringsbeslutningene og den operasjonelle driften av energisystemet, samtidig som modellen tar hensyn til kortsiktig usikkerhet i solcelle- og solfangerproduksjon, elektrisitet- og varmeeterspørsel og elektrisitet- og fjernvarmepriser. Usikkerheten er modellert ved å ta i bruk en multihorisont informasjonsstruktur, som skiller de to ulike tidshorisontene. I kombinasjon med den foreslåtte scenariogenereringsmetoden, som har vist seg å være stabil for et antall ulike probleminstanser, har problemets kompleksitet blitt redusert. En omfattende casestudie av pilotprosjektet Ydalir validerer modellen. Denne praktiske analysen vektlegger modellens oppførsel og hvilke betraktninger som burde overveies.

Opgaven inkluderer også et omfattende litteratursøk som dekker studier relatert til strategisk og/eller operasjonell beslutningstaking i energisystemer av ulike skalaer. Så vidt vi vet finnes det ikke mange studier som omhandler nullutslippsnabolag, noe som betyr at denne oppgaven kan være et verdifullt bidrag til det aktuelle forskningsområdet.

Contents

1	Introduction	1
2	Background	3
2.1	Introduction to Zero Emission Buildings	3
2.2	Zero Emission Neighborhoods	6
2.2.1	The FME ZEN	7
2.2.2	The pilot project Ydalir	8
2.2.3	Definition of ZEN	9
2.3	Energy technologies	9
3	Related literature	15
3.1	Introduction to stochastic programming	16
3.1.1	Multi-horizon modeling design	17
3.2	Multi-objective optimization	18
3.3	Zero Emission Buildings	20
3.4	Large scale models	24
3.5	Local energy system models	27

3.6	Modeling of battery	28
4	Problem description	31
4.1	Problem statement	31
5	Mathematical model	33
5.1	Model design	33
5.2	Modeling choices	37
5.2.1	Fulfilling the ZEN requirement	38
5.2.2	Binary variables	38
5.2.3	Battery formulation	39
5.2.4	Ramping rate of HS	40
5.2.5	Maximum PV and ST areas	40
5.3	Modeling assumptions	41
5.4	Mathematical formulation	45
5.4.1	Sets and indices	45
5.4.2	Parameters and variables	46
5.4.3	Multi-horizon stochastic model	48
6	Data analysis	61
6.1	Financial data	62
6.2	Fuel prices	62
6.3	Emission factors	63
6.4	Embodied energy	65

6.5	Technological data	65
6.5.1	Technology costs	67
6.5.2	Efficiencies and lifetimes	69
6.6	Length of periods	71
6.7	Probability of scenarios	71
6.8	Seasonal scaling factor	71
6.9	Stochastic operational data	72
6.9.1	Energy demand	72
6.9.2	Electricity prices	76
6.9.3	DH prices	80
6.9.4	ST heat generation	81
6.9.5	PV electricity generation	83
7	Scenario generation and evaluation methods	85
7.1	Scenario generation	85
7.1.1	Selection of method	87
7.1.2	Literature regarding scenario generation	87
7.1.3	Scenario generation method for the IMEZEN	88
7.2	Evaluation of the scenario generation method	93
7.2.1	Stability of the algorithm	94
7.3	Value of stochasticity	96
8	Computational study	99
8.1	Hardware and software	100

8.2	Solver settings	100
8.3	Stability tests of the IMEZEN	101
8.3.1	In-sample stability	101
8.3.2	Out-of-sample stability	105
8.4	Value of the IMEZEN	107
8.4.1	EVPI	107
8.4.2	VSS	108
8.4.3	LUSS	111
8.4.4	LUDS	112
9	Case study – Ydalir	113
9.1	The base case	113
9.2	Different emission factors	120
9.2.1	Total PE factors	120
9.2.2	Non-renewable PE factors	122
9.2.3	Effect of the emission factors	124
9.3	Practical analysis	126
9.3.1	Increased bio fuel price	126
9.3.2	Reduced battery price	127
9.3.3	Maximum export of electricity	128
9.3.4	Maximum PV and ST areas	129
9.3.5	Maximum HS ramping	130
9.4	Different types of neighborhoods	131

<i>CONTENTS</i>	xv
9.4.1 Restricted access to bio fuel	131
9.4.2 Local vs. district heat generation	133
9.5 ZEN vs. ZEB	136
10 Concluding remarks	139
11 Future research	143
Bibliography	145
Appendix A	157
Appendix B	163

Abbreviations

ASHP	Air Source Heat Pump
BB	Bio Boiler
CHP	Combined Heat and Power
COP	Coefficient of Performance
DH	District Heating
DHW	Domestic Hot Water
EB	Electric Boiler
EEV	Expected result of using the Expected Value solution
EIV	Expected Input Value
EMO	Evolutionary Multi-objective Optimization
EPBD	Energy Performance of Buildings Directive
ESSV	Expected Skeleton Solution Value
EV	Expected Value problem
EVPI	Expected Value of Perfect Information
FME ZEN	Research Centre on Zero Emission Neighborhoods in Smart Cities

GB	Gas Boiler
GHG	Green House Gas
GSHP	Ground Source Heat Pump
HP	Heat Pump
HS	Heat Storage
IMEZEN	Investment Model for Energy systems in Zero Emission Neighborhoods
LUDS	Loss of Upgrading the Deterministic Solution
LUSS	Loss of Using the Skeleton Solution
MCDM	Multi-Criteria Decision Making
OM	Operation and Maintenance
PE	Primary Energy
PV	Photovoltaics
RES	Renewable Energy Source
RP	Recourse Problem
SH	Space Heating
SOC	State of Charge
ST	Solar Thermal
VSS	Value of the Stochastic Solution
WS	Wait-and-see Solution
ZCB	Zero Carbon Building
ZEB	Zero Emission Building
ZEB-COM	Zero Emission Building level including Construction,

	Operation and Materials
ZEB-O	Zero Emission Building level including Operation
ZEB-O-EQ	Zero Emission Building level including Operation minus Equipment
ZEB-OM	Zero Emission Building level including Operation and Materials
ZEN	Zero Emission Neighborhood
ZEN-O	Zero Emission Neighborhood level including Operation
ZEN-OM	Zero Emission Neighborhood level including Operation and Materials

List of Figures

- 2.1 Levels of ambition in the proposed ZEB definition obtained from Dokka et al. (2013). 6

- 5.1 Scenario tree for the multi-stage optimization problem. 35
- 5.2 Scenario tree for the multi-horizon optimization problem. 36

- 6.1 Duration curves for mean and peak heat demands, showing sorted demands from highest to lowest during one year. 66
- 6.2 Duration curve for electricity demand, showing sorted demand from highest to lowest during one year. 67
- 6.3 Average daily heat demand for a residential unit of 100 m² 74
- 6.4 Average hourly heat demand for a residential unit of 100 m² 74
- 6.5 Average daily electricity demand for a residential unit of 100 m² 75
- 6.6 Average hourly electricity demand for a residential unit of 100 m² 76
- 6.7 Daily mean electricity price [NOK] for one year 78
- 6.8 Hourly mean electricity price [NOK] for one week 79
- 6.9 Daily mean ST generation and irradiation for one year 82
- 6.10 Hourly mean ST generation for one day 83

8.1	Average coefficient of variation [%] for all problem instance combinations	102
8.2	Average computation time [minutes] for all problem instance combinations	103
8.3	Average objective value deviation from problem instance average for each combination	104
8.4	Relative difference using Equation 8.1 for all combinations with a ZEN degree of 100 %, as well as the objective value obtained on the reference tree	106
9.1	Total installed capacities and costs for increasing degree of ZEN, using carbon factors	114
9.2	Average annual demand covered by on-site energy generation and import, using carbon factors	115
9.3	Electricity balance for a representative week in season 1	116
9.4	Heat balance for a representative week in season 1	117
9.5	Electricity balance for a representative week in season 3	118
9.6	Heat balance for a representative week in season 3	118
9.7	Total installed capacities and costs for increasing degree of ZEN, using total PE factors	121
9.8	Average annual demand covered by on-site energy generation and import, using total PE factors	122
9.9	Total installed capacities and costs for increasing degree of ZEN, using non-renewable PE factors	123
9.10	Average annual demand covered by on-site energy generation and import, using non-renewable PE factors	124
9.11	Total installed capacities and total costs for 100 % ZEN, using different emission factors	125

9.12	Total installed capacities and total costs with and without maximum electricity export limit	128
9.13	Total installed capacities and costs for the base case, CHP with gas, and without bio fuel	132
9.14	Total energy imports and exports and consumption for the base case, CHP with gas and without bio fuel	133
9.15	Total installed capacities and costs for the base case, without DH and for DH only	134
9.16	Total energy imports and exports and consumption for the base case, without DH and for DH only	135
9.17	Total energy imports and exports for a ZEN and for the case of aggregated ZEBs	138

List of Tables

- 5.1 Problem assumptions 37
- 5.2 Modeling assumptions 41
- 5.3 Sets 46
- 5.4 Indices 46
- 5.5 Parameters 47
- 5.6 Variables 48

- 6.1 CO₂ factors 64
- 6.2 Primary energy factors 65
- 6.3 Technology costs - neighborhood size 68
- 6.4 Efficiencies and lifetimes - neighborhood size 70
- 6.5 Grid charges - Eidsiva Nett (Tariff E10, E25 and E65) 77
- 6.6 Electricity prices - Eidsiva Energi (Innlansspot) 78
- 6.7 Grid charges - Eidsiva Bioenergi (Tariff F4) 80
- 6.8 Heat prices - Eidsiva Bioenergi (Tariff F4) 80

- 8.1 Computation time using different algorithms in Xpress, given in minutes 100

8.2	Problem instances tested for in-sample stability	102
8.3	Out-of-sample stability results from pairwise testing using 3 scenarios	107
8.4	VSS for the IMEZEN, calculated for three problem instances	109
8.5	VSS for the IMEZEN with penalty, calculated for three problem instances	110
8.6	LUSS for the IMEZEN, calculated for three problem instances . . .	111
8.7	LUDS for the IMEZEN, calculated for three problem instances . . .	112
9.1	Installed capacities of the included technologies in each investment period	119
9.2	Objective values for a ZEN and for the case of aggregated ZEBs . .	137
9.3	Total installed capacities of technologies for a ZEN and for the case of aggregated ZEBs	137
B.1	Technology costs - building size	164
B.2	Efficiencies and lifetimes - building size	164

Chapter 1

Introduction

The energy industry is currently going through a transition phase, aiming toward a low carbon society which to a high extent exploits the use of renewable energy sources (RESs) and strives for low greenhouse gas (GHG) emissions. The green transition comes along with large changes in both technology and organization of the global energy markets. The liberalization process makes the energy sector more complex and introduces the possibility of competition between different energy carriers. New technologies allow an increasing flexibility in energy systems, which also results in higher complexity within design, operation and maintenance of the systems. Thus, the need for improved methodologies and tools for planning and operation of energy systems are more than ever of great importance.

Buildings stand for 36% of CO₂ emissions and 40% of energy consumption in the EU (European Commission, 2017*a*). The European Commission (2016) treats buildings as an essential part of Europe's green transition and the EU Directive on Energy Performance of Buildings (EPBD) introduced the concept of Zero Emission Buildings (ZEBs) in 2010. The introduction of ZEBs has also led to the idea of establishing energy efficient *neighborhoods* with several interconnected low-carbon buildings and infrastructures, which together constitute a Zero Emission Neighborhood (ZEN).

In international literature one typically find tools for optimization of energy systems which consider either the operational part of the problem or the strategic investment planning. Studies that cover the operation of energy systems are usually modeled for a given design of the studied area, and the investment planning tools are often applicable for regional and global levels and do not consider optimal operation of the systems to a large extent. Many use multi-objective optimization,

because of the large number of stakeholders with different purposes involved. Few studies consider stochastic programming and there is also a lack of studies specifically regarding ZENs.

The goal of this thesis is to provide a two-stage stochastic multi-horizon optimization model for investment planning of energy systems in ZENs, which will serve its purpose to decision makers in ZENs. It handles short-term and long-term dynamics, as well as short-term uncertainties. It enables annual expansion planning of neighborhoods and optimizes on an aggregated level, implying that infrastructure is not considered. It optimizes which technologies and how much capacity to install in each investment period, while considering optimal operation with uncertainties taken into account. Multi-horizon modeling is used to avoid the curse of dimensionality when modeling short-term uncertainty in a long-term model. A big effort is put into developing a stable and representative scenario generation algorithm and several tests are performed to verify this.

In particular, the model is developed to accompany research in the Research Centre on Zero Emission Neighborhoods in Smart Cities (FME ZEN). It should serve as a tool in the research center and a case study on the pilot project *Ydalir* is therefore performed in this thesis. The model should also be constructed in such way, that it is compatible with the European Model for Power system Investment with Renewable Energy (EMPIRE) and may be used on larger scales. We are not aware of other small scale stochastic investment planning models, which optimizes strategic investment decisions while considering optimal operation with short-term uncertainty, that applies to a ZEN.

In order to put our research problem in context, Chapter 2 provides an introduction to ZEBs, a presentation of the FME ZEN and the pilot project *Ydalir*, their definition of a ZEN, in addition to background on relevant energy technologies. Chapter 3 provides theory behind relevant operations research methods and a review of available literature in the appropriate field. Further, the problem studied in this thesis will be described in more detail in Chapter 4. In Chapter 5 we present the model design along with essential modeling assumptions and implications of these, as well as the suggested mathematical formulation of the problem. Chapter 6 presents a data analysis discussing how input data is obtained and handled, while Chapter 7 discusses the choice of scenario generation method and presents relevant evaluation methods. Next, in Chapter 8 we test the stability and value of stochasticity, before the case study is presented in Chapter 9. Finally, Chapter 10 provides a conclusion to our work, while Chapter 11 contains suggestions for further research.

Chapter 2

Background

Before the ZEN energy system investment problem is discussed in more detail in Chapter 4, this chapter provides a context and motivation for the study presented in this thesis. Some of the content in this chapter is taken from the preparatory work for this thesis, found in Beus et al. (2018). First, it provides motivation behind inclusion of buildings in the effort to reduce GHG emissions, as well as an introduction to ZEBs and important definitions accompanying this research area. Next, a presentation of the FME ZEN and the pilot project Ydalir will be introduced, as well as the research center's proposed definition of a ZEN. Lastly, relevant energy technologies will be presented, in order to give the reader better insight in the different technology options our mathematical model includes.

2.1 Introduction to Zero Emission Buildings

This section presents the role of buildings in terms of energy consumption and the importance of studying this area. Further, it provides definitions of nearly and strictly ZEBs, how the energy balance is performed, and how the ZEB ambition levels are differentiated.

Buildings are responsible for 36% of CO₂ emissions and 40% of energy consumption in the EU, and around 75% of today's existing buildings are inefficient (European Commission, 2017a). The European Commission (2016) treats buildings as an essential part of Europe's green transition and the Energy Performance of Buildings Directive (EPBD) introduced the concept of ZEBs in 2010. The EPBD states that

all *new* buildings shall be nearly ZEBs from 2020 in order to make buildings a part of the solution to combat GHG emissions and turn the focus toward energy efficiency (European Commission, 2017a). Thus, the creation of such buildings require decision tools regarding planning of design and operation of energy systems in the buildings.

An overview of existing definitions of ZEBs can be found in Marszal et al. (2011), while Sartori et al. (2012) give a concrete definition framework. The definition of a nearly ZEB is stated in the EPBD as follows: *‘nearly zero-energy building’ means a building that has a very high energy performance. The nearly zero or very low amount of energy required should be covered to a very significant extent by energy from renewable sources, including energy from renewable sources produced on-site or nearby* (European Parliament, 2010). ZEBs are basically low energy demand buildings that to a high extent cover their own demand with on-site generated renewable energy. Because of this, the buildings will automatically become an integrated part of the whole energy system.

The EPBD also gives a framework for how the energy balance should be calculated, which is defined as follows (see Equation 2.1): the annual weighted energy imports to the building, subtracted the annual weighted energy exports from the building, summed over all energy carriers i (European Committee for Standardization, 2013). The balance can also be calculated over the whole lifetime of a building.

$$\sum_i f_i \cdot \text{imported}_i - \sum_i f_i \cdot \text{exported}_i = G, \quad (2.1)$$

where f_i are the weighting factors. When $G = 0$, which is when the net balance of energy consumed and energy generated is zero, the building is considered a ‘strictly’ ZEB. One can relax the strictly zero target to $G > 0$, achieving a ‘nearly’ ZEB. Whenever using ZEB in the following, it refers to strictly ZEB, otherwise ‘nearly’ will be specified.

Even though EPBD has a framework for what a nearly ZEB should be and how to determine the energy balance, each member state must define their own

- ambition level for how near zero the ZEB target should be
- weighting factors
- boundary conditions on what energy consumption to include in the calculation

The weighting factors f_i differs for each energy carrier i and are usually stated as primary energy (PE) factors measured in $\text{kWh}_{PE}/\text{kWh}_f$ or carbon factors (CO_2 emission factors) stated in $\text{gram CO}_2\text{-eq}/\text{kWh}_f$. The primary energy factor is the ratio of all the primary energy used for processing, transporting, extracting and distribution of the delivered energy, divided by the amount of actual delivered energy, whereas carbon factors describe how much CO_2 -equivalent GHGs that are being emitted per unit of energy delivered.

Since the instantaneous on-site generation of electricity may not always correspond to the load, a ZEB may exchange electricity with the local grid. Typically, a building will have the highest energy consumption in the winter, while the on-site generation will usually be highest in the summer, due to use of RESs such as solar energy. Thus, the possibility of export to the grid is necessary to meet the ZEB requirements for the energy balance.

The behaviour of importing electricity at some times and exporting at other times, leads to the differentiation between symmetric and asymmetric PE factors for electricity. For symmetrical PE factors the PE factor of import and export of electricity are equal, whereas for asymmetrical PE factors, the electricity imported from the grid has a higher PE factor than the electricity exported. Hence, to achieve a zero balance of primary energy use, one need to export more electricity than one import.

PE can also be divided into non-renewable PE and total PE, where non-renewable PE denotes PE only based on non-renewable energy, while total PE includes both non-renewable and renewable primary energy. Use of PE lead to a *Zero Energy Building* (ZEB), whereas use of carbon factors lead to a *Zero Emission Building* (ZEB) or *Zero Carbon Building* (ZCB). In the following, whenever using ZEB, it embraces both ZEB and ZCB.

The boundaries for what energy consumption to include in the energy balance is another aspect of defining the ambition level of a ZEB. In Figure 2.1 one can see the four different ambition levels for an “all electric” (all imported and exported energy is electricity) building used by Dokka et al. (2013) in a concept analysis.

The emission on the y-axis has to be balanced by electricity production from RESs in order to meet the different ambition levels. The different levels that are used in their proposed definition are:

- ZEB-O-EQ, which consists of partly operational energy use, excluding energy consumed by equipment such as elevators and computer servers

- ZEB-O containing all operational energy consumption
- ZEB-OM including all operational energy consumption and energy embodied in the materials (included demolition)
- ZEB-COM, which includes all operational energy use and energy embodied in both materials and construction of the buildings

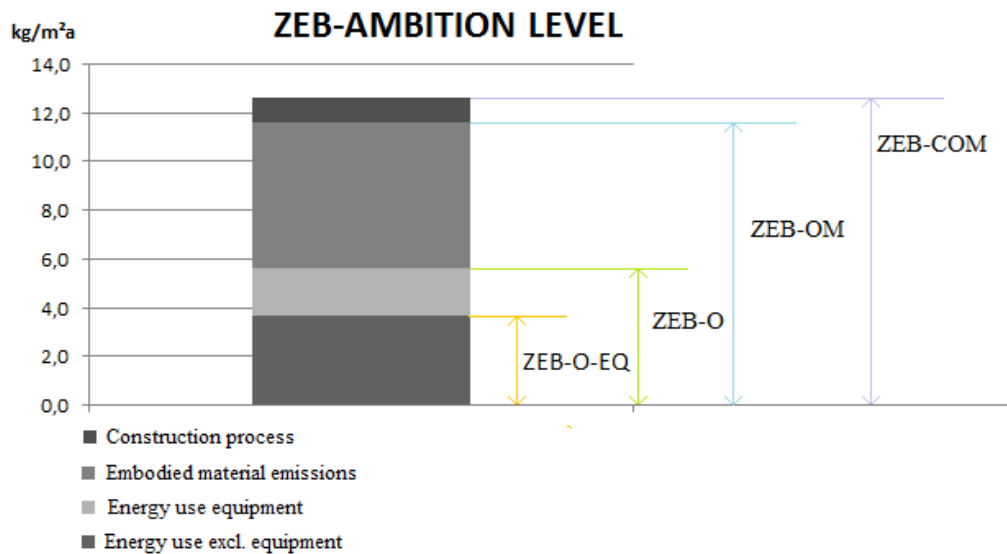


Figure 2.1: Levels of ambition in the proposed ZEB definition obtained from Dokka et al. (2013).

How the ZEB requirement is defined may have a large impact on the choice of energy technologies when considering both economical and environmental aspects of the problem. The weighting factors typically play a big role in the choice of technologies, especially when considering the heat technologies (Noris et al., 2014).

2.2 Zero Emission Neighborhoods

The introduction of ZEBs has also led to the idea of establishing energy efficient *neighborhoods* with several interconnected low-carbon buildings and

infrastructures, which together constitute a ZEN. This section will provide motivation for studying ZENs and a presentation of the FME ZEN, as well as a short description of how ZENs are defined according to the research centre.

The increased environmental pollution that is caused by increasing energy use and waste of energy has contributed to the ongoing green transition process. The concept of ZEN is a relatively new concept and there does not exist much research particularly on ZENs. By looking at several buildings at the same time, synergies between the energy demand profiles of the individual buildings may be realized, meaning when one building has excess energy, other buildings can use it (Fosso and Gustavsen, 2016). Optimizing on a neighborhood scale may also reduce strain on the grid, because more electricity generation will take place on-site where the consumption also takes place.

The neighborhood dimension is large enough to have an impact, but at the same time small enough to consider the different technologies explicitly, as well as the interaction with the users (Fosso and Gustavsen, 2016). In addition, not all buildings can be built or renovated into ZEBs, because buildings for example may be protected or placed at difficult sites, which implies that the synergies may be necessary to reach the desired level of low-carbon societies. The possibility of competition between different energy carriers and the increasing complexity within design, operation and maintenance of local energy systems that are introduced with ZENs provide a basis for the need of improved methodologies and tools for design planning and operation of energy systems in ZENs.

2.2.1 The FME ZEN

The FME ZEN was established the spring of 2017 at the NTNU in Trondheim. The main objective of the research centre is to develop solutions that enable the transition toward a low-carbon society with sustainable neighborhoods that have zero GHG emissions related to their production, operation and transformation (Fosso and Gustavsen, 2016). The FME ZEN is organized in six work packages as follows

- WP1: Analytic framework for design and planning of ZEN
- WP2: Policy measures, innovation and business models
- WP3: Responsive and energy efficient buildings

- WP4: Energy flexible neighborhoods
- WP5: Local energy system optimization within a larger system
- WP6: Pilot projects and living labs

WP6 is dealing with living labs and pilot projects where new tools and methodologies that are developed within the other work packages can be tested on data obtained from real neighborhoods. Most of the pilot projects are only in the planning phase and some have relatively long planning horizons.

2.2.2 The pilot project Ydalir

Ydalir is an area northeast of the city centre in Elverum, located in the county of Hedmark in Norway. This area is about 300 decares large and is currently used as a gravel depot, an activity that will continue in some parts until 2019. Elverum Tomteselskap AS, a semi-public organization, is the project owner and owns 80% of the land in Ydalir. They will develop the area together with a number of other stakeholders, both private and public. The development plan consists of building a school and a kindergarten, as well as approximately 800 new residential units. The Ydalir project has high energy and emission ambitions and will serve as an environmental forerunner project for the city of Elverum (ZEN Research Centre, 2018).

The development will be highly dependent on several factors, among them the housing market in Elverum and the population growth. The idea is that Ydalir will cover half of the need for new houses in Elverum each year during the development period, which means building about 60 houses yearly the next 10-15 years (Tonjer, 2018).

Ydalir is one of the pilot projects in the FME ZEN, enabling them to make use of the competence available. The goal of Ydalir is to reduce the mobile and stationary energy demand and GHG emissions, while at the same time finding new and innovative solutions for developing major neighborhoods. The general idea is that locally produced energy shall offset the carbon emissions of the neighborhood (Elverum Vekst AS, 2017).

The pilot project Ydalir has been chosen as the case study of this master's thesis. This is mainly because of the project's high energy and emission ambitions. At the same time, as this is a pilot project in the FME ZEN, one can expect that later

development projects may make use of the experiences from this pilot project, making it representative for future neighborhoods.

2.2.3 Definition of ZEN

The decision of what to include in the definition of a ZEN is an ongoing process which may change as data from solution testing and tools from the pilot projects are obtained. As provisionally described in an unpublished memo from the FME ZEN, a *neighborhood* can briefly be defined as a cluster of interconnected buildings (existing or new) and infrastructure (water, roads, communication, sewage and data lines) that are located within a defined geographical area and with a restricted boundary to the electrical and thermal grids (Baer and Andresen, 2017). Thus, a ZEN can be described as a low energy demand defined geographical area that to a high extent cover its own demand with on-site generated renewable energy. The energy balance and ambition levels are in this thesis defined according to the same methods as described for ZEBs in Section 2.1. The definition of ZEN used in this thesis will conform to this.

2.3 Energy technologies

This section provides an overview of the different technologies that are included as investment alternatives in our mathematical model. Energy technologies are system components for conversion, transport and storage. Conversion components transform primary energy to secondary energy, transportation components distribute energy, whereas storage components store energy for later use. Energy transformation and energy conversion is considered the same. The section aims to give the reader insight in how the components work and a better basis for understanding the context in which our model operates in. Thus, providing the reader understanding of what choices a decision maker in a ZEN faces.

Combined heat and power

Combined heat and power (CHP) is a conversion component based on the principle of cogeneration, where a single source of energy is used for both the production of electricity and heat (Office of Energy Efficiency and Renewable Energy, 2018a).

Traditional centralized electricity generation wastes a large amount of the energy through heat loss, as well as during the distribution of electricity to end users (U.S. Environmental Protection Agency, 2018). With CHP, the heat that would normally be wasted is instead recovered and used to meet heating requirements, thereby providing a greater fuel efficiency. Additionally, since the power is generated on-site, losses through transmission are avoided.

Solar technologies

Solar photovoltaics (PVs) is the concept of direct conversion of sunlight into electricity (NASA Science, 2018). Solar cells consist of semiconducting materials that have the property of absorbing sunlight, resulting in the release of electrons that flow through the material and generate an electrical current. This process of converting light (photons) into electricity (voltage) is referred to as the PV effect. Solar cells can be combined into a module, and multiple modules can be wired together to form an array. Several arrays can then be connected to form a PV system (Renewable Energy World, 2018). Since the system has a modular structure, it is possible to build it to meet almost any electricity need.

Solar thermal collectors (STs) use solar radiation to provide heat. The collector will absorb solar radiation, convert this into heat, and then transfer this heat to a fluid that circulates through the collector. The energy obtained can either be used directly, or it can be stored in a thermal energy storage tank (Kalogirou, 2004). Solar collectors are either non-concentrating or concentrating. For collectors that are non-concentrating, the area that intercepts the solar radiation is the same as the area that absorbs the radiation, whereas a concentrating collector has the property that the collector area is larger than the absorber area (U.S. Energy Information Administration, 2018). The two most common types of solar collectors are the flat plate collectors and evacuated tube collectors, which both fall in under the category of non-concentrating collectors (Solar Server, 2018).

Heat pumps

Heat pumps (HPs) are designed to transport thermal energy in the opposite direction of spontaneous heat transfer. They use the physical properties of a volatile fluid known as a refrigerant. The refrigerant evaporates and absorbs heat from the external surroundings and is then pressurized and circulated through the system by a compressor. The refrigerant enter a condenser where it is cooled

while exchanging heat with the side of the system to be warmed. The pressure is lowered through an expansion valve and the cycle is repeated (Natural Resources Canada, 2017). Heat pumps have some impact on the environment since they run on electricity, but the heat they extract from air, water or ground is constantly being renewed naturally (Energy Saving Trust, 2018*b*). Today's HPs can reduce the electricity use for heating by approximately 50% compared to other common heating systems (Office of Energy Efficiency and Renewable Energy, 2018*c*).

Air source heat pumps (ASHPs) are HPs that extract heat from the ambient or exhaust air. ASHPs can either be air-to-air, heating the inside air, or air-to-water, heating underfloor heating systems or larger radiators (Energy Saving Trust, 2018*a*). HPs work more efficiently at lower temperatures than boiler systems, giving out low-temperature heat over longer periods of time (Energy Saving Trust, 2018*a*). This makes them suitable for local energy systems. Ground source heat pumps (GSHPs) are geothermal HPs which uses pipes that are buried in the ground to extract heat from down under (Energy Saving Trust, 2018*b*). GSHPs can be either ground source or water source HPs, meaning that they extract heat from the ground itself or a water source to heat water that are carried in the pipes. They are more expensive than ASHPs to install, but have lower operating costs due to the advantage of utilizing the relatively constant ground and water temperatures (Office of Energy Efficiency and Renewable Energy, 2018*c*).

Boilers

Boilers are used to heat water, and provide either hot water or steam for heating. Boilers can use different energy carriers to heat the water through heating elements or use of controlled combustion of fuel (Office of Energy Efficiency and Renewable Energy, 2018*b*). Electric boilers (EBs) heat water using only electricity. The water is heated by running past a heating element in the boiler, often with large surface areas, so as little heat as possible is lost. They are very efficient and easy to install (The Green Age, 2018).

Gas boilers (GBs) often use natural gas as fuel, but they can also use propane (U.S. Department of Energy, 2018). A gas boiler consists of a burner, a combustion chamber, a heat exchanger, and controls. The burner mixes the fuel and oxygen, and is equipped with an ignition device to make combustion occur. The platform of combustion is the combustion chamber and the heat generated here is transferred to the water via the heat exchanger. Controls regulate the ignition, burner firing rate, fuel supply, air supply, exhaust draft, water temperature, steam pressure,

and boiler pressure (Boilers Guide, 2018).

Bio boilers (BBs) burn bio pellets or wood chips to heat water and basically work the same way as a gas boiler. Bio pellets consist of biomass such as agricultural waste like crop stalk and straw materials, forestry residue such as sawmill residue, bark and leaves, or solid waste such as cardboard and waste plastic. Basically any material can be made into bio pellets as long as it burns, but the most common are wood chips and other residue from sawmill or forestry industry. Wood chips can also be used directly as fuel in a bio boiler (Chou, 2016).

District heating

District heating (DH) is a transportation system distributing heat to buildings from one or more heat sources and heat technologies through a network of insulated pipes carrying hot water or steam. The heat generators can be different types of energy technologies such as boilers, STs, HPs, and CHPs, or power stations such as industrial processing power plants that generate heat as a by-product. In this way DH can utilize heat that otherwise might have been wasted and contribute to improved pollution control (Panagiotakopoulou and Papadopoulos, 2015).

Heat storage

A heat storage (HS) is a component that stores thermal energy at large densities, enabling use of the heat at later points in time. The choice of storage material depends on the desired temperature range, application of the heat storage and size of the unit. The shortage of non-renewable sources of energy, the increased gap between energy supply and demand, and the non-uniform distribution of energy generated from RESs, makes energy storage technologies important in order to reduce waste of energy (Dinker et al., 2017).

Battery

The battery works as a temporary local electricity storage or home storage for the smart electricity grid. Here, the electrical energy is stored in the form of chemical energy. The current is generated by electrons and ions moving from the negative to the positive electrodes, and the charging is done when the particles move in

the opposite direction (Vereecken and Bavel, 2016). Increased use of RESs and mismatches in supply and demand lead to voltage rises and drops in low voltage distribution networks. Use of batteries can reduce this problem, especially by storing excess energy and releasing it later when the sun does not shine or when the wind does not blow strongly enough (IRENA, 2017), and the RES hosting capacity of the distribution networks can be intensified (Gavric, 2016).

The technology is developed rapidly as the performance is improving and the costs are decreasing. Simultaneously, the batteries are getting safer and more efficient. One also sees that regulatory barriers and conventional energy structures based on non-RESs are being challenged. Thus, there are several aspects that indicate that the battery will have a key role in the transition to a sustainable energy system (Curry, 2017; IRENA, 2017).

Chapter 3

Related literature

Investment planning of energy systems in ZENs is a complex problem which provides several possible approaches. Most of the content in this chapter is maintained from our preliminary work in Beus et al. (2018), with some additional improvements. The first part of the chapter provides an overview of relevant optimization methods, in particular an introduction to stochastic programming and multi-horizon modeling, which forms a basis for the model design and mathematical formulation proposed in Chapter 5. A presentation of multi-objective optimization will also be given, since this optimization method is widely used in the following presented literature. Further, we introduce relevant research studying strategic and/or operational decision making within energy systems on both small and large scales, to provide a wide selection of different possible approaches that may be applicable to our problem. Specifically, research related to ZEBs will first be presented, subsequently relevant studies concerning larger scale models and lastly literature regarding ZENs. Finally, a review on batteries will be provided.

The main purpose of our model is to plan and design energy systems in ZENs and the literature review will therefore mainly focus on *investment models*. It is limited to only give an overview of what *optimization methods* that have previously been used to solve challenges related to the combination of strategic and operational decisions, such as combining different time scales and various possible objectives. Due to this, literature concerning scenario generation will not be reviewed in this chapter, but rather be introduced as a basis of how we decide to develop our scenario generation algorithm in Chapter 7.

Several studies concerning local energy system planning do not include batteries in

their models. We find it natural to include a storage component for electricity in our model and a review on how batteries may be modeled is therefore also included. The review as a whole aims to give the reader understanding of our decision to use Lindberg, Doorman, Fischer, Korpås, Ånestad and Sartori's (2016) model as a basis, how we have chosen to expand their model to be applicable to neighborhoods, as well as our single-objective, multi-horizon stochastic modeling approach. These modeling choices will be further discussed in section 5.2 in Chapter 5.

3.1 Introduction to stochastic programming

This section gives an introduction to stochastic programming and introduces the concept of multi-horizon modeling and why this method is useful compared to traditional stochastic programming. Multi-horizon stochastic modeling is not commonly used in the research area of ZEBs and ZENs, but as we have seen from the following literature review it may be an applicable approach to the problem presented in this thesis. Hence, this section provides some relevant theory behind the respective optimization approach, aiming to give the reader a basic understanding of the method and why it is applicable to our problem.

A lot of real life decisions (some claim all decisions) are affected by uncertainty. One way of dealing with this uncertainty is stochastic programming. In oppose to deterministic programming, where the problems are formulated in terms of known parameters, some parameters are unknown in stochastic programming. The approach utilizes either known or estimated probability distributions to define these parameters (Shapiro and Philpott, 2007). Kall and Wallace (1994) state that deterministic models often provide good solutions for certain data sets and to certain problems. However, there is no general way to conclude that the solutions are good without comparing them to the respective stochastic solutions (Kall and Wallace, 1994). Stochastic programming is more complex than deterministic programming, but it is in some cases necessary to provide an eligible solution.

In some cases some of the decisions have to be made before relevant information is available, while some decisions can be delayed until afterward. These cases result in recourse models, and refer to the opportunity of adapting the solution to the applicable observed outcome (L. Higle, 2005).

The most widely applied stochastic programming models are two-stage linear models. In these models the decision maker makes a decision in the first stage, and then a random event occurs affecting the outcome of this decision. In the second

stage a recourse decision can be made to compensate for any bad effects of the first decision. Thus, there is a single first stage policy and a collection of recourse decisions defining which second stage decision that should be made according to each random outcome (Shapiro and Philpott, 2007). The model assumes that the second-stage data can be modeled as a random vector with a known (or estimated) probability distribution (Shapiro and Philpott, 2007). A standard representation of the problem is the scenario tree approach. This approach is based on a discretization of the outcome space of the uncertain data. The random vector is assumed to have a finite number of possible realizations, called scenarios (Defourny et al., 2011). A scenario tree is then an explicit distributional representation of the branching process evoked by the stochastic elements and how they may evolve over the period of time represented in the problem.

The two-stage problem with recourse exerts the process where an initial decision is made without knowing the specific outcome of the stochastic parameters, followed by a new decision after this information is revealed. When this pattern is repeated, the problem becomes a multi-stage problem (L. Hige, 2005).

The value of the stochastic approach is associated with the decision maker's opportunity to delay decisions, thus the explicit evaluation of flexibility (Kall and Wallace, 1994). However, with several stages and a great number of scenarios, the stochastic problem quickly becomes large and difficult to solve. Solution methods that exploit the structure of the multi-stage stochastic problems should therefore be used (L. Hige, 2005). Commonly used methods are different types of decomposition methods such as the L-shaped method and stochastic decomposition. Some estimation methods are also increasingly used (L. Hige, 2005). More on solution methods can be found in L. Hige (2005).

3.1.1 Multi-horizon modeling design

Some problems, as investments in energy systems, contain uncertainty both on the investment level and the operational level, in addition to that the uncertainties in the strategic level influence the operational decisions. By solving this type of problems with the traditional scenario-tree-based multistage stochastic programming, the model would be unmanageable large. Another challenge is that the decisions regarding investment strategies will necessarily have a different time scale than the operational decision aspects. The investment strategies are determined by decisions with a time scale of months or years, while the operational decisions are shorter term decisions with time scale of hours or days.

One method commonly used for solving such problems is to separate the strategic and the operational decision models and run them in loop, such that strategic decisions will be updated according to the operational decisions. As it is important to acknowledge how the operational aspects will affect, and be affected by, the strategic decisions, this method faces challenges with coordination and convergence of the different time scales (Kaut et al., 2014).

Kaut et al. (2014) suggest a different way of structuring the scenario-tree in stochastic optimization. This method is called *Multi-Horizon Stochastic Programming*. The method differentiates the scenario tree nodes devoted to the strategic decisions and the ones devoted to the operational decisions. By this, it reduces the size of the scenario tree significantly, compared to the standard scenario tree. The operational nodes are embedded in the respective strategic nodes and check the feasibility and profitability of the strategic decisions.

The structure of the multi-horizon scenario tree is based on the assumption that the strategic decisions are not dependent on a typical operational decision, but rather on the collection of operational decisions made in the previous strategic decision period (Kaut et al., 2014). The multi-horizon scenario tree is therefore solely constructed by the strategic nodes, and the operational nodes are sub-trees associated with the respective strategic nodes. In an investment problem, the sub-trees will be operational scenarios for a particular investment decision. As a consequence of the assumption, the model assumes that the first operational decision after a strategic node does not depend on the last operational decision in the previous strategic period. Thus, there are no connection between operational scenarios of two consecutive strategic nodes (Kaut et al., 2014).

An application of the method is shown in Hellemo et al. (2013) where it is used a multi-horizon stochastic approach when optimizing design and operation of infrastructure components for production of natural gas.

3.2 Multi-objective optimization

This section provides theory related to multi-objective optimization. As the following literature review will show, multi-objective programming is a widely used optimization method in problems considering optimization in ZEBs. Therefore, this section aims to give the reader a basis for understanding the further described research. Only the most relevant solution methods emphasized.

In multi-objective optimization there are multiple objectives to either maximize or minimize. These objectives are often difficult to compare and in conflict with each other (López Jaimes et al., 2011). Therefore, instead of a single optimal solution, one finds a set of trade-off optimal solutions. These solutions are a set of alternative good solutions and are called Pareto-optimal. A solution is Pareto-optimal if none of the other objective functions can be improved without having a negative impact on the other objective values. The set provides a front, called a Pareto-optimal front. How to prioritize the solutions is up to the decision maker. Further, a solution is *weakly* Pareto-optimal when there does not exist another solution where one or more objective values are better (López Jaimes et al., 2011).

There are several solution methods to solve a multi-objective problem, and López Jaimes et al. (2011) distinguish them into two different approaches; Multi-Criteria Decision Making (MCDM) and Evolutionary Multi-objective Optimization (EMO). The former represents a set of mathematical programming techniques in combination with subjective preferences the decision maker may have. The latter represents algorithms of heuristics. MCDM can further be categorized according to *when* the subjective role of the decision maker takes place in the process; a priori, interactive or posteriori (López Jaimes et al., 2011).

Some of the solution methods consist of converting the multi-objective problem into a single objective problem. A widely used method for this is the *weighted sum method*, which is performed by weighting the individual components in the objective vector (objective functions) after their relative importance. The outcome of this method is seen as weakly Pareto-optimal López Jaimes et al. (2011). The *ε -constrained method* converts the multi-objective problem to a single-objective by making all but one objective into constraints, each bounded by a value ε . Next, the problem is solved iteratively for different ε -values. Both of these methods may be priori or posteriori. Another commonly used method is *Goal Programming*. In this method, all the objectives are assigned goals and treated as targets rather than absolute constraints. The problem may then be solved as a single-objective problem (López Jaimes et al., 2011).

Evolutionary algorithms do not guarantee to find the optimal Pareto set, but with a population approach the Pareto-optimal solutions are found simultaneously in a single simulation run. This approach is also less sensitive to the shape of the Pareto front and require less domain information. The *genetic algorithm* is a widely used evolutionary algorithm (Lu et al., 2015). A short review other commonly used evolutionary algorithms can be found in Hamdy et al. (2016).

3.3 Zero Emission Buildings

This section presents relevant literature studying ZEBs. First, it presents literature using multi-objective optimization, before considering study's regarding single-objective modeling and lastly also multi-horizon stochastic programming. The section aims to give the reader an insight in the literature that is used as basis for our model and hence give understanding for the choice of modeling approach applied to our problem.

In optimization of ZEBs there are different areas to focus on, and there may be multiple conflicting objective functions when developing models. One can focus on the emissions, costs, comfort/discomfort, demand/load or life cycle costs, and several models are therefore based on multi-objective optimization, to take into account all these aspects. Sun et al. (2015), Hamdy et al. (2013) and Huws and Jankovic (2014) use a multi-objective approach by step wise varying the design parameters.

Sun et al. (2015) use multi-objective optimization for design of net ZEBs under uncertainties. They consider system initial cost, indoor thermal comfort and grid stress caused by power mismatch. The problem is solved in several steps. In the first step, the peak cooling load is identified using the stochastic inputs and the *Monte Carlo simulation method*. The simulation method is a sample-based method which uses repeated random sampling to acquire numerical research.

In the second step, the size of the air-condition system and the renewable energy system, according to different thresholds from the peak load distribution defined in the previous step, are selected. The thresholds represents the potential risks that the corresponding air-condition system cannot fulfill. The air-condition system sizes are determined and based on this the building's energy demands are estimated. These are further used to determine the size of the corresponding renewable energy systems. In the third step the optimal size of the air-condition system and the renewable system are determined based on the overall performance of the different combinations from the previous step. According to the weighting factors determined by the decision maker, the overall performance scores are obtained and compared to the different thresholds. Hence, the sizes with the highest overall performance are chosen as the optimal ones.

Hamdy et al. (2013) minimize heat demand and life cycle cost in the first step. This step provides different building structures. The operational costs are calculated for each Pareto optimal case in step one, by simulating four different heating and cooling systems. The last step includes on-site renewable energy generation,

such as solar thermal collectors and PV, as a way of improving costs and energy consumption from the cases in the second step.

Huws and Jankovic (2014) use a multi-objective model with three conflicting objectives; carbon emission, cost and comfort. The optimal design is found by comparing emission and cost, cost and discomfort, and discomfort and emission. The building structure is first optimized, before the energy technologies within the building are determined.

There has also been done a performance comparison of different multi-objective optimization algorithms for solving nearly-zero-energy design problems (Hamdy et al., 2016). A review on the different algorithms that are compared can be found in Hamdy et al. (2016). A conclusion from this comparison is that when the number of generations was increased, the solutions were improved. Further, when running each algorithm 20 times with gradually increasing number of evolutions, a two phase optimization approach using the genetic algorithm had high repeatability to explore a large area of the solution space and achieved solutions close to optimal with a great diversity. They also concluded that the minimum required number of evolutions to stabilize the optimization results of the building energy model was 1400-1800.

Palonen et al. (2009) and Wang, Zmeureanu and Rivard (2005) state that in multi-objective optimization there exist an advantage of using the generic algorithm as a solution method, in contrast to the weighted-sum-method, where there is only one optimal solution given the weighting factors (if used as an a priori method). The approach of generating a diverse set of Pareto front values and capturing the extreme solutions to all objective functions is seen as the most optimal (Palonen et al., 2009).

Lu et al. (2015) compare two different methods for optimization of design of renewable energy systems in buildings. They compare a single-objective and a multi-objective optimization method. The multi-objective function is minimizing costs, emissions and grid interaction and the problem is converted to a single-objective problem using the weighted sum method a priori. They conclude that the single-objective optimization model gives the best solution for a given objective, while the multi-objective model provides richer information, enabling a more compromised decision.

Lindberg, Doorman, Fischer, Korpås, Ånestad and Sartori (2016) claim that the outcome of the multi-objective models (also the ones solved with weighted-sum method) depends a lot on the weighting factors between the objectives, making

it difficult to draw a clear conclusion. Lindberg, Doorman, Fischer, Korpås, Ånestad and Sartori (2016) have therefore chosen single-objective optimization when optimizing energy systems in ZEBs. The optimization model used in their research is a dynamic deterministic mixed integer model with hourly time resolution. The objective function minimizes costs during the lifetime of the building, and the zero emission/energy aspect is included as constraints. This also allows the decision maker to set a ZEB-limit, given as a parameter to the model. The model also differs from the previous mentioned ones, due to the combination of considering both the investment problem and the operational problem and not just the investment aspect as the others.

As indicated, within ZEBs there are mostly studies optimizing either the investment aspect regarding the design or the operational aspect, where the energy technologies and design of buildings are given (Lindberg, Doorman, Fischer, Korpås, Ånestad and Sartori, 2016; Milan et al., 2012). The separation of the two aspects may lead to either an operation of a system that is over or under dimensioned, or a design that is based on a operation that is not optimal (Lindberg, Doorman, Fischer, Korpås, Ånestad and Sartori, 2016). In the multi-objective models mentioned above, the operation in the investment models are mostly simulated. The simulation processes are not necessarily a good reflection of the reality nor the cost-optimal operation.

Milan et al. (2012) has a similar approach as Lindberg, Doorman, Fischer, Korpås, Ånestad and Sartori (2016) where both the operational and the strategic aspects are optimized simultaneously. The model is an LP problem that optimizes the size of a 100% renewable supply system by minimizing the overall system costs. The operational level has an hourly resolution. The limitation of the model constructed by Milan et al. (2012) is the few technology options that are available and included in the model.

The model developed by Lindberg, Doorman, Fischer, Korpås, Ånestad and Sartori (2016) have a larger amount of energy technologies to choose from. Both models take the energy loads as input and the building structure as given. The outputs are the optimal system configuration and overall costs of the system as well as expected system performance data, as the operational aspects also are optimized. Both models are deterministic and Milan et al. (2012) have made the model more robust by including a safety margin on the supply system dimensions to compensate for unexpected peaks in demand.

As presented, there are mostly deterministic models existing for optimization of energy system design in ZEBs. However, there are several sources to uncertainties

when optimizing these kind of energy systems. As mentioned, simulation is a commonly used method to handle the uncertainties. Ferrara et al. (2014) are using a simulation-based optimization method for cost-optimal analysis of nearly ZEBs. They have build a simulation model for a French single-family house. The different options for design and the corresponding cost functions are defined. They use a simulation-based method for minimizing the global cost functions and define a set of energy efficiency measures that are being combined in different packages of measures. The energy consumption related to the packages are then calculated by energy simulation and the costs of the different packages are established. The one with the lowest cost is determined as the optimal.

The advantage of this approach is the simplicity, but it is difficult to ensure that all measurements that are relevant are taken into account simultaneously, knowing that more alternatives make it more complex. Therefore, this approach can not guarantee to find the most optimal solution for the design problem.

Another approach to deal with the uncertainties in the operational and the strategic levels is *scenario-tree based stochastic modeling*. This might provide a more accurate result, but the size of the scenario tree becomes unmanageable large very quickly. A decision support system from the *EnRiMa project* contains both a stochastic operational model and a stochastic strategic model when optimizing energy efficiency and risk management in buildings (Cano et al., 2014). This decision-support system assesses retrofits, investments into new equipment and decommissions of obsolete installations.

The model uses a *multi-horizon* stochastic approach to reduce the size of the scenario tree and to combine the two time scales for the operational and strategic levels (Kaut et al., 2014; SINTEF and SU, 2012). The model is a two-stage problem that optimizes both the strategic and operational problem simultaneously. Investments in new energy technologies are first-stage decisions taken before uncertainties are resolved, and the operational decisions are the second-stage decisions that are taken once the values for the uncertain parameters become known. The operational level has hourly resolution like the others mentioned above (Cano et al., 2014).

Lindberg (2016) also states that further work on the investment model should be to apply a stochastic approach to the problem, and by this take the operational uncertainties into account for the investment decisions.

3.4 Large scale models

Studies that consider expansion planning with several energy carriers and technologies are mostly dominated by large scale optimization tools that are developed for national and global levels. This section reviews optimization models for expansion planning and/or operation in energy systems on such levels. Optimization methods used on larger scale models may be relevant to our problem because a neighborhood will presumably also have similar characteristics to even larger areas and model design approaches used for these areas may be useful when expanding a model from being applicable to buildings to neighborhoods. First, deterministic models will be reviewed, while stochastic models or extension of deterministic models will be mentioned toward the end.

MARKAL (Loulou et al., 2004), EFOM (Grohnheit, 1991), TIMES (Loulou et al., 2016) and MESSAGE (Messner and Strubegger, 1995) are all examples of mathematical models designed to optimize energy systems on larger scales. MARKAL (MARKet ALlocation) is a mathematical model for optimization in energy systems in one or several regions, which aims to supply energy services at least global cost (Loulou et al., 2004). Similar to TIMES (The Integrated MARKAL-EFOM System), it calculates at all levels of the energy systems and estimates the energy dynamics over a multi-period horizon, and provides a rich basis of energy technologies (Loulou et al., 2004, 2016).

The input data to the MARKAL model is developed by users in each region and the time horizon is also divided into a number of time periods decided by the user, and may thus differ for each region (Loulou et al., 2004). TIMES may also be used on more local levels, as well as even larger scales like national and global levels (Loulou et al., 2016). TIMES combines two different approaches, a technical engineering one and an economic approach and is used for in-depth energy and environmental analyses. The model is, similar to all the other mentioned models, a single-objective model and produces outputs related to least-cost energy system configurations, which meet the end-use energy demands and fulfills requirements regarding emissions and use of RESs through various constraints (Loulou et al., 2016).

TIMES is a bottom-up model, i.e. a very detailed model identifying each energy technology explicitly by a detailed description of its inputs and outputs and other technical and economic characteristics (Loulou et al., 2016). Both MARKAL and TIMES are economic equilibrium models which assumes perfectly competitive markets for energy carriers. By computing equilibrium on the energy markets,

they ensure to maximize total surplus (sum of producers' and consumers' surplus) over the entire horizon. This means, prices and quantities in each time period, are such that the suppliers produce quantities exactly equal to the demands, to the current price (Loulou et al., 2004, 2016).

EFOM (Energy Flow Optimization Model) is an optimization tool that uses linear programming and finds a minimum cost solution for the energy network, subject to several constraints including regulations on GHG emissions (Grohnheit, 1991). The model is the supply part of the energy model complex of the Commission of the European Communities (der Voort, 1982). Messner and Strubegger (1995) presents in their paper MESSAGE, a Model for Energy Supply Strategy Alternatives and their General Environmental Impact, which similarly to EFOM, is described as a linear programming model for optimization of energy supply and utilization which aims to minimize the total system costs. In oppose to EFOM, but similar to MARKAL and TIMES, MESSAGE also uses dynamic programming and make decisions dynamically.

Grohnheit (1991) describes his energy system as a network where the energy starts in a form of primary energy and is flowing through the network via transportation and conversion components and is lastly transformed into useful energy to satisfy given energy demands. This is similar to MESSAGE, that includes strong technical descriptions of energy carriers and technologies, and structures the energy flow in a so-called chain going from the supply side to the exogenous demand side (Messner and Strubegger, 1995).

Insights generated from both TIMES and EFOM are obtained via scenario analysis. Loulou et al. (2016) compare different scenarios according to a reference energy scenario which is generated by running the model without any policy constraints. The model produces several least-cost scenarios based on simulations of future energy demands and supplies from perfect energy foresight, while applying the policy constraints on the model. When comparing the results, the different energy technologies that deliver the policy constraints at least cost may be identified (Loulou et al., 2016). Loulou et al. (2016) solve the model by simultaneously making investment decisions and operating decisions, as well as decisions regarding primary energy supply and energy trade. In EFOM scenarios for periods of 20-40 years are constructed by energy demand forecasts, energy prices, emission limits etc. and each scenario is solved to obtain an optimal solution for investments in energy technologies (Grohnheit, 1991).

Even though the core paradigms in all the discussed models assume linearity of the objective functions and constraints and perfect foresight over the entire

horizons, TIMES and MESSAGE have several extensions beyond the deterministic LP approaches. The current version of MESSAGE, MESSAGE III, also has the feature to define investment variables as integers and may then be used on mixed integer programming problems. It can also handle nonlinear objective functions, in addition to providing a multi-objective option (Messner and Strubegger, 1995), similar to many of the models designed for ZEBs, mentioned in Section 3.3.

Among the extensions of TIMES one find the Stochastic Programming TIMES extension which assumes certain key model parameters to be random, similar to EMPIRE (European Model for Power system Investment with Renewable Energy) (Skar et al., 2016) which also is a stochastic investment model. The Stochastic Programming TIMES extension is still an LP, but the size become much larger. A multi-stage stochastic program like this, may be solved with complex decomposition approaches such as Dantzig-Wolfe decomposition with dynamic column generation or stochastic decomposition methods, or Benders decomposition algorithm for a two-stage model (Loulou et al., 2016).

However, the current TIMES implementation for stochastic programming is solved by solving the deterministic equivalence problem. As this may lead to very large instances, the stochastic TIMES model is very limited. Skar et al. (2016) solve this by formulating their long-term stochastic power system investment model as a multi-horizon stochastic program. The multi-horizon approach makes the problem tractable, by decoupling here-and-now operational decisions from all future investments and operational decisions, in addition to coordinating the different time scales well. It optimizes long-term investments under short-term operational uncertainty (uncertainties such as renewable energy production and energy demand), while considering both long-term and short-term system dynamics (Skar et al., 2016).

In these models, the energy system is often modeled with one energy balance per energy carrier, with energy generation on one side and energy consumption on the other and several technologies are represented with energy losses and emissions. These approaches are sufficient on large scale levels, but when modeling on a neighborhood level, it is not only a question on which resources and what amounts to use. Questions like *where* and *when* investments should be carried out also arise (Bakken et al., 2007).

3.5 Local energy system models

This section reviews research on local energy systems such as ZENs, where several energy carriers and technologies are integrated and optimal investment planning is needed. It does not exist many studies considering ZENs in particular, but several approaches to include different energy technologies and carriers on local levels have appeared the last years.

MODEST (Henning, 1997) and deeco (Bruckner et al., 1997) are both dynamic linear programming models designed for energy system optimization. MODEST (Model for Optimization of Dynamic Energy Systems with Time-Dependent Components and Boundary Conditions) aims to minimize the capital and operation costs of energy supply and also includes demand-side management (Henning, 1997). deeco (*dynamic energy, emissions, and cost optimization*) may be used for examining competition and interaction between different technologies and for utilizing RESs. It also has the feature to operate under nonlinear and time-dependent impacts of parameters on technology efficiencies such as ambient temperature and insolation.

Both MODEST and deeco may serve as decision support tools for investment decisions in municipal energy systems, whereas MODEST may also be used on national levels. MODEST is used to dimension new installations and optimize the operation of all system components where the various properties are known at each hour (Henning, 1997), similarly to deeco, which calculates the optimal combination of energy conversion technologies for given time-series of electricity and heat demand and energy supply (Bruckner et al., 1997). Hence, both deeco and MODEST are single-objective deterministic models. MODEST uses simulation, similar to TIMES (Loulou et al., 2016) and EFOM (Grohnheit, 1991), to consider different system designs and compare the consequences of different decisions.

Sandou et al. (2005) presents a methodology for short-term optimal scheduling of cogeneration systems considering heat and electricity demands. The initial problem is a large, non-linear mixed integer programming problem, which is highly intractable. Their main idea is to establish an approximate problem, whereas the computation of an exact solution remains tractable, instead of computing an approximate solution to the initial problem. Other papers, such as the one presented by Geidl and Andersson (2005), provides more generalized optimization approaches for power systems including multiple energy carriers. Geidl and Andersson (2005) are focusing on the couplings and interactions between the different power systems and are using the concept of hybrid energy hubs.

None of these approaches consider *expansion* planning for multiple energy infrastructures. Bakken et al. (2007) presents the optimization tool eTransport, which is a tool for expansion planning in local energy supply systems with multiple energy carriers and infrastructures. Geography, topology and timing are taken into account to match the problem on a local level like a municipality or a neighborhood. eTransport is a single-objective model which minimizes total energy system cost (investments, operation and emissions), and consists of two nested models (operational and investment) that run in loop (Bakken et al., 2007). Thus, it calculates both the optimal diurnal operation and an expansion plan for the upcoming 20-30 years.

The model has a modular structure, where the physical components and the flow of energy between them are modelled explicitly. The operational model is using mixed integer programming, with sub-models for each energy carrier and conversion component. The operational planning horizon is usually around 24-72 hours, with typical time-steps of 1 hour. The operational model minimizes operational and environmental costs for different energy loads in different energy systems for each operational period (Bakken et al., 2007). The investment model uses dynamic programming to find an investment plan that minimizes the present value of all future costs during the planning horizon. It receives the pre-calculated annual costs, that are obtained for different energy system designs, demands and periods by solving the operational model repeatedly, as inputs (Bakken et al., 2007).

When optimizing in local energy systems, it is important to identify different infrastructures within the geographical area (Bakken et al., 2007). eTransport does exactly this by considering all physical components and geographical topology for the different energy infrastructures in one model. Transmission distances and alternative locations are geographical details that are accounted for and it also handles the competition between different energy carriers. However, the model is deterministic with predefined demands for electricity and heating, as well as predefined energy system designs. Hence, it lacks the ability to optimize the size of specific components in the system and operate under uncertain energy prices and demand.

3.6 Modeling of battery

For a household or a neighborhood, the storage capacity and the lifetime of the battery are important aspects. The amount of the electrode material mainly determine the storage capacity, and the electrolyte that causes the

ionic conductance between the electrodes determines the power of the battery (Vereecken and Bavel, 2016). The lifetime is however more difficult to anticipate. When planning the energy system it is crucial to estimate the operational costs. These costs are closely connected to the degradation of the battery cells, and the degradation process is again related to the operational behaviour of the battery. As the operational pattern is unknown in the planning period, it becomes difficult to plan the system (Xu et al., 2016).

In order to take the operational costs into account, some studies have been done with the mission to express the process as a function of battery operations. From this work both theoretical and empirical degradation models have been developed (Xu et al., 2016). The theoretical types are based on a degradation due to loss of lithium ions and other active materials, and Xu et al. (2016) claim that it is inadequate to link the observations on the operational level to the molecular level. Thus, it would be incorrect to assume a direct correlation between the process on a molecular level *inside* the battery cell and the behaviour of charging and discharging.

The empirical models are more beneficial for storage planning and operational studies. Nevertheless, these methods need to be done for each specific case of energy systems or storage systems, as they are designed specifically for that application. This is unfortunate, as the process of making the empirical models both take time and are very expensive (Xu et al., 2016). Xu et al. (2016) therefore propose a semi-empirical battery capacity degradation model that is based on a theoretical analysis with experimental observations. Alharbi (2015) has chosen a more simple method by restricting the operational behaviour of the battery in advance. In that way the lifetime becomes easier to model, and it becomes more accurate for those specific patterns proposed. The model is however limited by these pre-selected patterns.

Batteries are usually considered at its end of life when the capacity has reached 80 % of the initial energy capacity. The degradation of the battery is often divided into calendrical aging and cycling aging. The degradation due to calendrical aging happens during the time the battery is not operating. This aging depends on temperature and SOC. Korpås et al. (2017) have modeled a battery where they take battery degradation into account, and also adds the degradation costs due to cycling to the objective function.

Experimental results from Delaille et al. (2008) have shown a linear relationship between battery capacity and the number of equivalent full discharges. Based on this Korpås et al. (2017) calculate the maximum energy throughput of the battery

during its lifetime by multiplying the average of the initial battery capacity and the end of life capacity by the minimum depth of discharge and the number of cycles to failure for the respective depth of discharge. This information can usually be found in the battery's technical specifications. This is then used as a measure of the battery lifetime. They also make sure that the SOC is maintained within a certain region, in order to prolong the battery lifetime (Korpås et al., 2017).

The empirical, theoretical and the semi-empirical models are often complex and created with the intention to optimize battery energy storage systems and not as a part of a larger investment model containing several energy technologies and carriers. Therefore, some design problems do not emphasize this issue that much and make several different simplifications in the modeling of the battery.

EMPIRE has incorporated batteries in the energy system design problem, and sets the lifetime as an input parameter *independent* of operations (Skar et al., 2016). Yang et al. (2007), on the other hand, have chosen to integrate the operational aspect by dividing the lifetime into two variables; one for the overall maximum lifetime, and one for the lifetime associated with the actual operation. The variable that reaches its maximum first decides the lifetime of the battery. Arnesen and Borgen (2017) have modeled a battery as a part of a microgrid design problem. Here, they define a variable that indicates the amount of average energy throughput of the battery. Further, an upper limit is given as an input parameter and the lifetime is determined based on when it reaches this upper limit.

Chapter 4

Problem description

This chapter provides a description of the ZEN energy system investment problem discussed in this thesis.

4.1 Problem statement

The problem studied in this thesis is a single-objective two-stage stochastic multi-horizon problem for investment planning of energy systems in ZENs. The main objective is to find the cost-optimal investment choices of which capacities of different technologies to install in a ZEN energy system each investment period, while considering optimal operation with uncertainties taken into account. The constraints restricting operational behaviour should be fulfilled, as well as the determined level of ZEN, which is ZEN-OM. The degree of ZEN to achieve and the emission weighting factors to use should be input to the model.

The technologies included as investment alternatives in the problem are ST, ASHP, GSHP, EB, BB, GB, and CHP for heat generation, CHP and PV for electricity generation, and heat storage and battery for energy storing. The neighborhood should also have the possibility to be connected to an external DH grid, enabling import of heat. Note that this should not be an investment decision, but rather a choice made beforehand by the decision maker. The neighborhood should also be connected to the electricity grid, permitting both import and export of electricity. As the problem is highly dependent on the technologies included, flexibility with regards to future developments and the inclusion of new technologies should be

considered in the mathematical formulation.

The investment decisions are considered to be first-stage decisions and are made at the beginning of each investment period. The operational decisions are made in the second stage, optimizing the operation of the energy system. All decisions relates to the neighborhood as an aggregated entity, not considering infrastructure.

The costs associated with the energy system, which are to be minimized, are investment costs and operational costs. Operational costs consist of fuel costs and other variable operation and maintenance (OM) costs, import of heat and electricity, less the revenue from export of electricity. All costs should be discounted back to year 0. The operational parameters consist of heat and electricity demand, PV and ST generation, import and export prices, fuel prices and efficiencies, whereas one or more should be modeled as stochastic input.

On-site energy generation in each operational period is restricted by the total available capacity of the installed technologies, and depends on the related efficiencies and amount of fuel consumed. The amount of energy transferred to or from the storage components also depend on the available capacity, as well as the amount of energy currently stored. The operation of the storage components is also restricted by the maximum ramping, the rate at which the storage component can be charged and discharged. Maximum limits on electricity trade, heat import, and total installed PV and ST areas, should also be included.

The aggregated heat and electricity demand have to be met in each operational period. Heat demand must be covered by on-site generation, heat from the heat storage, or import from the DH grid, whereas electricity demand must be met by on-site generation, discharge of the battery, or import from the electricity grid. Loss of excess heat or electricity produced should be allowed.

All technologies have associated investment costs, efficiencies, and lifetimes. The CHP produces both heat and electricity and should have two affiliated efficiencies. The efficiencies related to PV and ST are incorporated in their respective generation parameters, and do not need to be considered explicitly.

The length of the total time horizon, as well as the number of investment periods are given as input to the model and may be chosen by the decision maker. Since the uncertainty only is included in the operational perspective, it implies that the scenarios should have the same length as the investment periods. Each scenario consists of a number of seasons, and each season consists of a number of operational periods. The number of scenarios, seasons, and operational periods are also considered to be input to the model.

Chapter 5

Mathematical model

This chapter provides the proposed formulation of the mathematical model that has been developed to solve the ZEN energy system investment problem described in Chapter 4. The proposed mathematical model is continued from our preparation for this thesis, found in Beus et al. (2018). However, it comprises many important improvements and adjustments that has been made in the final work, both related to superior modeling choices and the specific mathematical formulation. First, a review and justifications of which model design that is chosen will be presented, before other modeling choices are discussed. Further, important modeling assumptions along with their implications will be summarized, before the notation in the model is defined and the mathematical model is presented and explained.

5.1 Model design

The problem stated in Chapter 4, implies that the model should include optimization across several horizons, i.e. operational and strategic horizon. The investment decisions will thereby be directly linked to the operational decisions made under uncertainties. The benefit of this procedure is emphasized in the literature review in Chapter 3.

The problem contains different uncertainties at the operational level. To take these into account we present a scenario-tree based stochastic model. When constructing the scenario tree it is important to determine when relevant information is

revealed. In our problem we assume perfect foresight in terms of the strategic data. Information about the long-term development of electricity and gas prices, prices and efficiencies of different technologies and potential regulations such as subsidies and electricity tariffs, are assumed known in the beginning of each investment period.

The strategic decisions are the first stage decisions in the scenario-tree. In our problem the strategic decisions are investment decisions related to choice of technologies and respective capacities. At this point, the future operational conditions are unknown. After the first stage decisions are made, the operational conditions for a full investment period are revealed as discrete scenarios based on probability distributions related to historical data. This is the beginning of the operational horizon, and the operational decisions are made. These become the second stage decisions in the model, and are restricted by the decisions made in the first stage. The operational decisions represent the interaction between on-site production, export, import and storage.

A investment period is in this thesis defined as five years. Thus, the operational horizon is five years and one operational scenario represents five years. The operational periods are based on an hourly time resolution. The strategic decisions are the same for every investment period, i.e. every fifth year. These decisions are followed by operational decisions for a set of scenarios within the five years. The strategic horizon is equivalent to the planning period. Thus, this two stage structure is repeated every fifth year throughout the planning period, containing both operational and investment decisions.

If we solve the problem using the traditional scenario-tree structure, we get the scenario tree with operational uncertainty illustrated in Figure 5.1. Here, the square nodes represent the strategic decisions, and the circular nodes represent the operational decisions. The figure shows when decisions are made and when information is revealed, as described in the paragraph above. As one investment period lasts for five years, the figure shows the first 15 years of the planning horizon. From the strategic nodes there are two branches representing two scenarios for each investment period. The number of scenarios is set to be two in the figure, only due to simplicity. In practical problems the number of scenarios should be much higher in order to reflect the reality. The operational scenarios are sequences of operational decisions made on hourly basis. Thus, one operational period is one hour. Only the three first periods within an operational scenario are shown in the figure, while the remaining periods are illustrated by dotted lines. This is also done for simplicity.

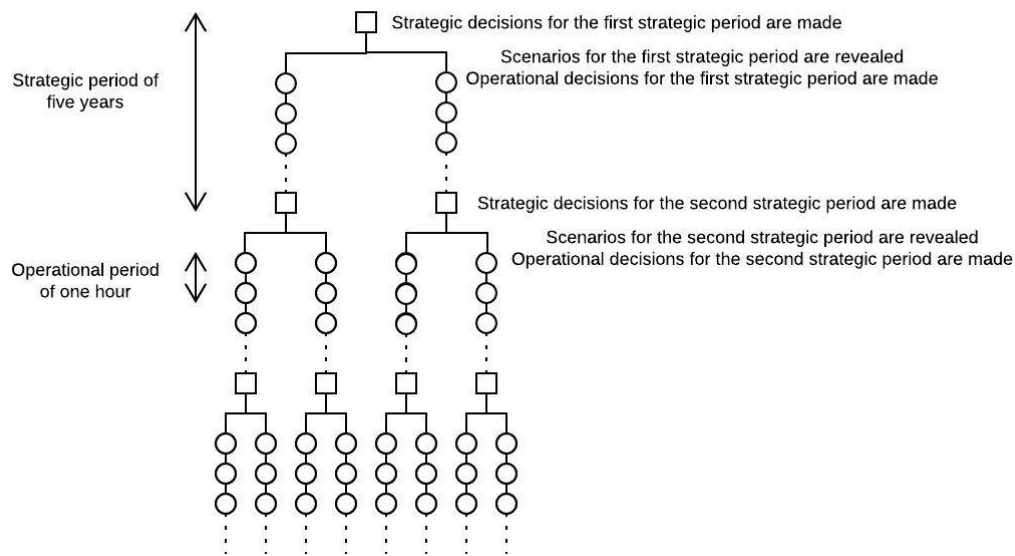


Figure 5.1: Scenario tree for the multi-stage optimization problem.

The figure illustrates the growth of scenarios as the number of investment periods increases. With three investment periods, and two scenarios for each strategic decision, the tree would consist of 2^3 (8) scenarios. This is a manageable number, but as mentioned earlier, in real life problems, the number of scenarios are much higher. The planning horizon would probably be longer as well, closer to 30 years. If we increase the number of scenarios for each strategic decision to 10, and the number of investment periods to 6, the corresponding total number of scenarios would be 10^6 . Hence, this structure provides an explosion in terms of number of scenarios.

Therefore, we use a multi-horizon scenario tree to solve the stochastic problem. Even though this method separates the strategic and operational nodes, it still allows the model to use the operational decisions to evaluate the strategic decisions, but without the extensive branching. The multi-horizon scenario tree is solely constructed by the strategic nodes, and the operational nodes are sub-trees embedded in the respective strategic nodes. This structure is shown in Figure 5.2. The figure illustrates the same problem as earlier with two scenarios for each strategic decision. The strategic horizon is still 15 years with investment periods of five years.

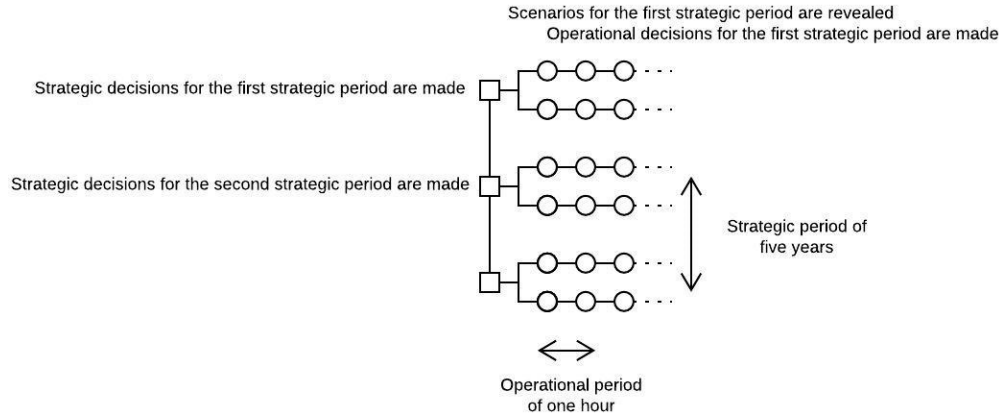


Figure 5.2: Scenario tree for the multi-horizon optimization problem.

As seen in the figure, the number of scenarios decreases significantly. In this case the total number of scenarios goes from 2^3 (8) to $2 \cdot 3$ (6), whereas if we increase the number of embedded scenarios and investment periods as before, the total number of scenarios would go from 10^6 to $10 \cdot 6$. This shows the huge effect the new structure has on the size of the scenario tree.

As mentioned in section 3.1.1 in Chapter 3, the structure of the multi-horizon scenario tree is based on the assumption that the strategic decisions are not dependent on a specific operational decision, but rather on the collection of the operational decisions made in the previous strategic decision period (Kaut et al., 2014). In our problem, the investment decision is not dependent on how the energy system perform in a particular hour, but rather on how the energy system is expected to perform under varying hourly conditions. Thus, this requirement is fulfilled.

However, the model also assumes that the first operational decision after a strategic node do not depend on the last operational decision from the previous period (Kaut et al., 2014). In our problem this is more challenging in the context of short-term energy-storage. The model will therefore be an approximation of the standard stochastic scenario tree. However, it may be assumed that the short-term storages associated with the renewable energy sources will be empty in the winter. The periods of time with daylight are shorter in the winter, implying that production from PV and ST are lower, at the same time as the heat load is higher than for the rest of the year, due to lower temperatures. Thus, to minimize the approximation

error, we place the strategic decisions in the winter time.

The problem assumptions based on the problem statement in Chapter 4 and the modeling design presented in this section are rendered in Table 5.1.

Table 5.1: Problem assumptions

Assumption	Description
Assumption 1	Strategic uncertainties are not considered
Assumption 2	Operating conditions are known prior to each investment period
Assumption 3	The investment decisions are based on the collection of operational decisions made in the previous investment decision period
Assumption 4	There is no connection between operation in the last hour and first hour of consecutive investment periods
Assumption 5	The storage technologies are assumed empty at the beginning of each investment period

5.2 Modeling choices

As stated in our preliminary work in Beus et al. (2018), Lindberg, Doorman, Fischer, Korpås, Ånestad and Sartori's (2016) model for ZEBs serves as a basis for the formulation of the Investment Model for Energy systems in ZENs (IMEZEN), as it combines optimization of both operational and strategic aspects, as well as it includes many components. The components included in their model are also relevant for this thesis, as they study a Norwegian school building, which typically will consist of many of the same components as for a Norwegian neighborhood. Many of the components in this thesis are therefore modeled the same way as in Lindberg, Doorman, Fischer, Korpås, Ånestad and Sartori (2016). See literature review in Chapter 3 for more details about Lindberg, Doorman, Fischer, Korpås, Ånestad and Sartori's (2016) model and deeper understanding of this choice.

The section starts by discussing how the fulfillment of ZEN requirements is included in the mathematical model formulation. Further, other modeling choices that in some way differ from the model in Beus et al. (2018) are discussed. Finally, an overview of all modeling assumptions for the IMEZEN are presented.

5.2.1 Fulfilling the ZEN requirement

In the IMEZEN, both costs and emissions are preferred minimized. However, as emphasized in the literature review in Chapter 3, these objectives are in conflict. We have chosen to develop a single-objective model where costs are minimized and restrictions regarding emissions are included as a constraint, as done in Lindberg, Doorman, Fischer, Korpås, Ånestad and Sartori (2016). This is opposite to multi-objective optimization, which, as seen in the literature review in 3, is heavily dependent on the solution method and might give a compromised solution that is difficult to draw a clear conclusion from. Also, restricting the emissions as a constraint still makes it easy for the decision maker to choose the degree of ZEN, and establish the best trade-off for that specific neighborhood problem.

The ZEN requirement is included as a *hard* constraint in the proposed mathematical modeling formulation. This means that the requirement *must* be fulfilled. In reality this might provide infeasible solutions for higher degrees of ZEN, and one can discuss if the requirement in reality rather will serve as a *soft* constraint. This implies that the requirement of the ZEN degree goes from being something one *must* fulfill to something one *wants* to fulfill. In this case, one minimizes the penalty related to exceeding the required ZEN degree, in addition to the main costs. In the mathematical formulation, this implies adding a variable representing the amount by which the restriction value is exceeded to the right hand side of the ZEN constraint. The variable is also added to the objective function, where it is multiplied by a penalty cost. This method is similar to goal programming, mentioned in Chapter 3 as a multi-objective solution method, as the ZEN degree serves as a goal rather than an absolute requirement.

We have chosen not to use this in the case study, as this alternative approach has the drawback of setting a realistic penalty, which requires a judgmental function that is difficult to establish. Therefore, this area of interest is open to further research.

5.2.2 Binary variables

In Beus et al. (2018) there are three binary variables in the model. Two of these are connected to import and export of electricity, and prohibit import and export in the same hour. This is based on Lindberg, Doorman, Fischer, Korpås, Ånestad and Sartori (2016). Importing electricity from the grid always has a higher cost than what one will earn from exporting to the grid. Because of this, removing

these binary variables from the model will not influence the behaviour related to export and import of electricity. To reduce the run time, we have therefore chosen to model import and export of electricity as continuous variables.

The third binary variable in Beus et al. (2018) is related to whether or not the neighborhood is connected to an external DH grid. To reduce the run time we have chosen to model this as a binary input parameter instead of a variable. This is reasonable because access to an external DH grid may be very case specific and agreements like this might be carried out early in the planning phase. It is therefore easy for a decision maker to give this as input.

5.2.3 Battery formulation

In Beus et al. (2018) we present a battery formulation with lifetime measured in number of full charges, without taking battery degradation into account. This was mainly inspired by work in Arnesen and Borgen (2016). The literature review presented in Chapter 3 suggests different possible ways to model the battery lifetime, with and without degradation of the battery cells. The most common ways to model the lifetime are either in number of years, reflecting the calendrical aging, or the number of equivalent full discharge cycles, reflecting aging due to operation of the battery. One could, as Yang et al. (2007), model the battery lifetime using two variables; one for each of the mentioned lifetime measures. Then, the one that reaches its end of lifetime first, would be applicable.

In order to keep the convexity of the model and avoid non-linear constraints, degradation is not included in the IMEZEN. Further, for simplicity, it is chosen to formulate the battery lifetime in terms of years only. This reflects the formulation used in EMPIRE (Skar et al., 2016), where the battery lifetime also is modeled independent of operation. This assumption is valid as commercial batteries have a guaranteed lifetime and thus would be replaced at zero cost if the usage is damaged before the end of its lifetime. The guarantee is typically based on standard usage of the battery, implying steady cycling. It is legitimate to assume standard usage of the battery in a neighborhood, because we see no reason to expect that the battery will be used less than what is considered as standard, if it shows to be profitable to invest in. The battery is still a very expensive technology and it will presumably not be profitable to invest in unless it is extensive need for it. It is also beneficial to model on the same detail level as EMPIRE, since our model should be compatible with this larger scale model.

In order to keep the convexity of the model and avoid non-linear constraints,

degradation is not included in the IMEZEN. One could for example model the battery the same way as Korpås et al. (2017) to account for degradation, but as the IMEZEN is not an operational problem and the main focus for this model is the investment decisions, this is assumed too detailed. Ramping constraints representing max charge and discharge rates on the battery are included, since these are technical specifications accompanying a battery.

5.2.4 Ramping rate of HS

In Beus et al. (2018) the heat storage is modeled in such way that it is possible to fully charge and equivalently fully discharge in one hour. This implies that very large heat fluxes may occur when the heat storage becomes large. This may cause unrealistic behaviour of the HS, and we choose to introduce a maximum ramping rate. This means that the HS can only be filled and emptied with a certain rate of heat at any time.

We assume this will lead to more realistic and optimal operation of the heat storage. This assumption is justified by Wang, Lin, Chen and Lee (2005), who state that an energy storage device has optimal charge and discharge performance under 35 – 40% fill ratio. This implies that a heat storage is not optimal operated if it is charged or discharged fully within one hour.

However, it might be hard to set a value on this limit, because heat flux depends on many factors such as material, insulation, volume, surface area, temperature differences and type of heating element of the heat storage. This is up to the decision maker to consider if the ramping constraints are chosen to be included.

5.2.5 Maximum PV and ST areas

In some cases there might exist an actual limit on the total area that can be covered by PV-panels and/or ST-collectors. To eliminate the possibility of installing very large capacities of PV and ST to achieve the desired level of ZEN, one can include restrictions on the size of areas of PV and ST based on physical area restrictions in the applicable neighborhood.

5.3 Modeling assumptions

In addition to the problem assumptions, a number of modeling assumptions have been made in order to simplify the the mathematical formulation of the problem considered in this thesis. An overview of the modeling assumptions is rendered in Table 5.2.

Table 5.2: Modeling assumptions

Assumption	Description
Assumption 6	There is no correlation between operation in the last hour and first hour of consecutive seasons
Assumption 7	The storage technologies are assumed empty at the beginning of each season
Assumption 8	Costs related to fuel (natural gas and wood chips) are constant
Assumption 9	Investment costs of technologies are constant
Assumption 10	Salvage values are not accounted for
Assumption 11	Variable OM costs only consist of fuel costs
Assumption 12	There are no direct costs related to consumption of heat from the heat storage, electricity from the battery and on-site generated energy from PV and ST
Assumption 13	The neighborhood has a central heating system
Assumption 14	Domestic hot water demand and space heating demand are not differentiated
Assumption 15	There is no minimum limit on installed capacities
Assumption 16	All technology efficiencies used as input are constant
Assumption 17	The efficiency of the heat storage is only related to the energy loss when the energy is stored
Assumption 18	No degradation of capacities of the different technologies are considered
Assumption 19	All technologies have lifetimes measured in years
Assumption 20	Inverters have the same lifetimes as the associated technologies
Assumption 21	The generation technologies have no maximum rampings
Assumption 22	The technologies bear no restrictions on annual full-time hours
Assumption 23	The CHP may overproduce heat or electricity

The first modeling assumption, given as Assumption 6, states no correlation between the last operational hour of one season and the first operational hour of the following season. This is assumed as a consequence of how the scenario generation algorithm is performed. This assumption also ensures that the main assumption related to the multi-horizon modeling design used in this thesis is fulfilled, implying that the first hour of an investment period always is the first hour of a season.

The HS and the battery are assumed empty at the beginning of each season, as rendered in Assumption 7. This assumption is based on the previous assumption and is made to simplify the problem. This assumption also makes the constraints related to maximum ramping of the HS and the battery unproblematic. However, this simplification also implies that seasonal heat storage will be problematical to include. Because of this, we do not consider a seasonal heat storage in the model.

Assumption 8 concerns the costs related to fuel such as natural gas and wood chips consumed by BB, GB and CHP. These costs are assumed deterministic and constant throughout the time horizon, unlike the other operational parameters. This is a reasonable assumption because the price of wood chips and natural gas delivered in tanks do not fluctuate on an hourly basis. This is a case specific assumption, and may be less applicable if the neighborhood studied is close to a gas grid.

The investment costs are also assumed constant throughout the time horizon. This is rendered as Assumption 9 in the table. In reality some technology prices are expected to have a significant decrease, and this could be reflected by an associated rate. However, constant prices make the problem more tractable, and the time horizon would need to be relatively long in order for the price difference to be large.

No salvage values of the technologies are accounted for, as stated in Assumption 10. This implies that if the modeling horizon ends before the end of the lifetime of a technology, the salvage value of the technology will not be accounted for. This may influence the investment decisions in terms of not installing new technologies in the last investment periods, but rather invest in larger capacities when the remaining time of the horizon equals the lifetime of a technology. This will especially be applicable for short modeling horizons.

Variable OM costs other than costs related to fuel is not included in the model, as stated by Assumption 11. This is reasonable because the fuel costs often constitute the majority of the variable OM costs. The remaining variable OM costs are

therefore left out of the calculations due to simplicity.

Assumption 12 states that costs associated with self-consumption of on-site heat and electricity generation, as well as heat consumed from the heat storage and electricity from the battery, are assumed to be zero, i.e. they have no direct operational costs. This is a reasonable assumption because utilizing sun as an energy source does not entail any costs. Heat consumed from the heat storage and electricity consumed from the battery are energy that are already produced and the costs related to this can therefore be assumed zero at the time of consumption.

Assumption 13 states that the neighborhood is assumed to be equipped with a central heating system. Central heating systems are flexible and is adaptable to many different heat technologies and is therefore a very provident heating solution Enova (2010). This assumption also enables the aggregated level of optimization, which does not emphasize infrastructure. Therefore, it is legitimate to assume that the neighborhood already has the infrastructure needed to distribute the energy.

We do not differentiate between domestic hot water demand and space heating demand, which Assumption 14 states. This is done for simplicity and because most of the heat technologies can meet both demands. If the demands were separated, it would require a higher number of variables, which would result in a more complex model. Thus, these demands are merged and it is assumed that all heat technologies can generate heat to cover this total demand.

Assumption 15 states that there is no minimum limit on the capacities of the technologies installed. The capacity installed of an energy technology in an investment period is defined as a continuous, non-negative variable for all the energy technologies. Considering the fact that costs often are dependent on the unit size, where larger units have lower specific costs NOK/kW than smaller units, the model runs the risk of installing very small capacities of some energy technologies. On the other hand, as this model covers an entire neighborhood, the demand is of such a magnitude that this will probably not be an issue. However, if it turns out to be a problem, a possible solution is to redefine these variables to be semi-continuous, thus forcing a minimum amount of installed capacity.

All technology efficiencies that are used as input to the model are constant, implying that there is a linear relation between energy generation and fuel consumption no matter the circumstances. This also implies that the CHP has a constant relationship between heat and electricity production. This is rendered in Assumption 16. Setting the efficiencies constant is a simplification to keep the linearity of the problem. In reality the efficiencies varies with load, and

the efficiency related to HPs, defined by the coefficient of performance (COP), is in reality heavily dependent on the ambient temperature. Note that this assumption does not include PV and ST as their efficiencies are incorporated in their respective generation parameters.

Assumption 17 addresses the efficiency of the heat storage. This technology could be modeled using several efficiencies as there are losses associated with charging, discharging and storing. In the IMEZEN, the efficiency is assumed to only include losses that occur when the heat is stored, as this represents the main loss.

For simplicity it is assumed that there is no degradation of capacity associated with the different technologies, seen in Assumption 18. This implies that all technologies will work equally well throughout their individual lifetimes. Annual fixed OM costs may be included in the investment costs and will then substantiate the reasonableness of this assumption.

Each technology is assumed to have a lifetime modeled in terms of years, stated in Assumption 19. This is a natural measure of lifetime for most technologies. However, the lifetime of batteries is more complex, but as discussed in section 5.2.3, this is also a reasonable assumption for the battery.

The electricity technologies, i.e. PV, CHP and battery, must have related inverters that can convert between AC and DC power to be able to interact with each other, the grid and to deliver power to the end users. As stated in Assumption 20 these additional equipment are assumed to have the same lifetimes as their respective technologies. In reality they usually have shorter lifetimes, but this assumption is made due to simplicity.

Assumption 21 emphasizes that the energy generating technologies do not have any associated ramping rates restricting the technologies from having large jumps and/or drops in operation. This assumption may lead to unrealistic operation of some technologies, especially referring to typical base load technologies such as CHP and ground source heat pump, which are designed to meet relatively constant demands. Since it presumably not will affect the investment decisions to a high degree, the assumption is considered reasonable.

Assumption 22 implies that the technologies can be operated at any time, without considering maximum annual full-load hours which applies to certain technologies. In reality the technologies may need to be stopped occasionally in order to perform maintenance work, among other things. This is excluded to simplify the model and is legitimate as the main focus of our model is the investments and not the operation.

As stated in Assumption 23, the CHP may generate excess heat or electricity that result in losses in favor of meeting electricity or heat demand, respectively. This assumption is made as there in some cases may be more cost beneficial to let some energy be lost, in order to meet another energy demand.

5.4 Mathematical formulation

This section provides the proposed mathematical formulation of the IMEZEN. First an overview of the different sets, indices, parameters and variables will be presented in order to give an orderly view of the different mathematical symbols. Further, the multi-horizon stochastic model will be presented. The objective function and all of the constraints will be explained in detail, while also describing the corresponding symbols explicitly in the text.

5.4.1 Sets and indices

A summary of all sets and indices is given in Table 5.3 and Table 5.4, respectively. I is defined as the set of time periods in the investment time horizon and is indexed by i . $I = \{1, 2, \dots, j\}$, where j is the number of investment time periods. All investment time periods have the same length, given in years, and each investment period consists of a number of seasons. The set of seasons is defined as $S = \{1, 2, \dots, l\}$, where l is the number of seasons, and is indexed by s . Further, there is a set of operational periods related to each season s , defined as $O_s = \{1, 2, \dots, h_s\}$, where h_s is the number of time periods in the operational time horizon in season s . An operational period is indexed by o and its length is given in hours. All operational periods have the same length, but the number of operational periods in a season s , defined as h_s , is not the same for all seasons. This is explained in section 7.1.3 in Chapter 7. As this problem is subject to operational uncertainty, there is also a set of operational scenarios included in the model. This set is defined as $\Omega = \{1, 2, \dots, m\}$ and is indexed by ω . The number of operational scenarios related to each operating time horizon is given by m .

Additionally, there are sets related to the energy technologies included in the model. Let T^H be the set of heat technologies, including solar thermal collectors, air source heat pump, ground source heat pump, electric boiler, bio boiler, gas boiler, district heating, and combined heat and power. The available power technologies, PV-panels and CHP, are collected in the set T^E . There are also two

sets denoting storage technologies, T^{SH} and T^{SE} , one for heat storage technologies and one for power storage technologies respectively. The storage technologies included are a heat accumulator tank for heat storage and a battery for electricity storage. Let T be the collection of all energy technologies, given by the union of the heat, power and storage technologies. This is defined as $T = T^H \cup T^E \cup T^{SH} \cup T^{SE}$, where all the related sets are indexed by t . Finally, F is defined as the set of energy carriers and is indexed by f .

Table 5.3: Sets

Set	Description
I	investment time periods
Ω	operational scenarios
S	seasons
O	operational time periods
T^H	heat technologies, $T^H = \{ST, ASHP, GSHP, EB, BB, GB, DH, CHP\}$
T^E	power technologies, $T^E = \{PV, CHP\}$
T^{SH}	heat storage technologies, $T^{SH} = \{HS\}$
T^{SE}	power storage technologies, $T^{SE} = \{B\}$
T	all energy technologies, $T = T^H \cup T^E \cup T^{SH} \cup T^{SE}$
F	energy carriers, $F = \{el_imp, el_exp, heat, bio, gas\}$

Table 5.4: Indices

Index	Description
i	investment time period
ω	operational scenario
s	season
o	operational time period
t	technology
f	energy carrier

5.4.2 Parameters and variables

All parameters are listed in table 5.5, defined by uppercase letters. The variables are defined by lowercase letters and are listed in table 5.6. Superscripts are used as a way of differentiating similar parameters and/or variables, while subscripts define the indices correlated to each parameter and/or variable.

Table 5.5: Parameters

Parameter	Description
C_{ti}	Total investment cost for technology t in investment period i [NOK/kW]
R	Discount factor
C^G	Total annual grid charge for the whole time horizon [NOK]
C^{DH}	Total connection charge to the district heating grid [NOK]
N	Length of an investment period [years]
K	Length of an operational period [hours]
π_ω	Probability of scenario ω
α_s	Scaling factor for the operational costs in season s
L_t	Expected lifetime of technology t [years]
$D_{i\omega s o}^H$	Heat demand of the neighborhood in period i in scenario ω in season s at time o [kWh]
$D_{i\omega s o}^E$	Electricity demand of the neighborhood in period i in scenario ω in season s at time o [kWh]
$P_{i\omega s o}^f$	Price of energy carrier $f \in \{el_imp, el_exp, heat\}$ from/to the grid in period i in scenario ω in season s at time o [NOK/kWh]
P^f	Price of energy carrier $f \in \{bio, gas\}$ [NOK/kWh]
η_t^H	Efficiency of technology $t \in T^H \cup T^{SH}$
η_t^E	Efficiency of technology $t \in T^E \cup T^{SE}$
$Q_{i\omega s o}^{ST}$	Specific solar heat generation in period i in scenario ω in season s at time o [kW/m ²]
$Y_{i\omega s o}^{PV}$	Specific PV electricity generation in period i in scenario ω in season s at time o [kW/kWp]
\bar{Q}	Maximum import from the district heating grid [kW]
\bar{Y}^{imp}	Maximum import from the electricity grid [kW]
\bar{Y}^{exp}	Maximum export to the electricity grid [kW]
\bar{V}_t	Maximum ramping rate per kWh installed capacity of technology $t \in T^{SH} \cup T^{SE}$ [kW/kWh]
\bar{A}	Maximum area of PV and ST installations [m ²]
A	Conversion factor for PV capacity [m ² /kWp]
δ^{DH}	Binary parameter, 1 if the neighborhood is connected to external district heating, 0 if not
γ	Degree of ZEN
W_f	Weighting factor for energy carrier f [gCO _{2-eq} /kWh] or [kWh _{PE} /kWh]
W^{Emb}	Weighted embodied energy [gCO _{2-eq}] or [kWh _{PE}]
W^{Ref}	Weighted energy imports with $\gamma = 0$ [gCO _{2-eq}] or [kWh _{PE}]

Table 5.6: Variables

Variable	Description
x_{ti}	Installed capacity of technology t in period i [kW]
$q_{ti\omega s o}$	Heat generated by technology $t \in T^H$ in period i in scenario ω in season s at time o [kWh]
$q_{i\omega s o}^{imp}$	Heat imported from the district heating grid in period i in scenario ω in season s at time o [kWh]
$r_{ti\omega s o}$	Resource consumed by technology $t \in T^H \setminus \{ST, DH\}$ in period i in scenario ω in season s at time o [kWh]
$s_{ti\omega s o}$	Energy stored in storage technology $t \in T^{SH} \cup T^{SE}$ in period i in scenario ω in season s at time o [kWh]
$y_{ti\omega s o}$	Electricity generated by technology $t \in T^E$ in period i in scenario ω in season s at time o [kWh]
$y_{i\omega s o}^{imp}$	Electricity imported from the grid in period i in scenario ω in season s at time o [kWh]
$y_{i\omega s o}^{exp}$	Electricity exported to the grid in period i in scenario ω in season s at time o [kWh]
$v_{i\omega s o}^+$	Electricity discharged from the battery in period i in scenario ω in season s at time o [kWh]
$v_{i\omega s o}^-$	Electricity charged to the battery in period i in scenario ω in season s at time o [kWh]

5.4.3 Multi-horizon stochastic model

This section provides a detailed explanation of the mathematical model, using the sets, indices, parameters and variables presented in the previous section. The objective function is explained, as well as each of the constraints. The full mathematical model can be found in Appendix A.

Objective function

The model minimizes total costs while meeting the electricity and heat demand of the neighborhood and fulfilling the restrictions regarding emissions imposed by the degree of ZEN, γ . The single objective function minimizes discounted investment and operational costs over the defined lifetime of the model. The defined lifetime is the same as the investment time horizon, more specifically the

number of investment periods, $|I|$, times the length of each investment period, N .

Equation (5.1) states the objective function which sums the discounted investment costs for each technology t and the total discounted operational costs.

$$\min z = \sum_{i \in I} \frac{1}{(1+R)^{(i-1) \cdot N}} \left(\sum_{t \in T} C_{ti} x_{ti} + \sum_{\omega \in \Omega} \pi_{\omega} \sum_{s \in S} \frac{1}{(1+R)^{\lfloor \frac{s-1}{|S|} \rfloor}} \alpha_s \sum_{o \in O_s} c_{i\omega so}^{totO} \right) + C^G + C^{DH} \cdot \delta^{DH} \quad (5.1)$$

The objective function sums all costs for the investment periods $i \in I$, discounted for the first year in the investment period. The discount factor is given by R , and the costs are discounted for year $(i-1) \cdot N$, where i is the investment period and N is the length of the investment periods. With $N = 5$, the costs are discounted for year 0, 5, 10, ... throughout the planning period.

The costs related to an investment period is given by two terms. The left term sums the investment cost for each technology $t \in T$. The investment cost is given by the cost of investing in one unit kW, kWh or m² of technology t in investment period i , C_{ti} , multiplied by the installed capacity of this technology in the corresponding investment period, x_{ti} .

In the right term, the sum of the operational cost, $c_{i\omega so}^{totO}$, for all periods $o \in O_s$ in season s is multiplied by a scaling factor α_s , and discounted for year $\lfloor \frac{s-1}{|S|} \rfloor$ in the investment period. $c_{i\omega so}^{totO}$ is the total operational cost in period i in scenario ω in season s at time o , and is given by Equation (5.2) explained below. With $N = 5$ as the length of the investment period, the costs are discounted for years 0, 1, 2, 3 and 4. The seasonal scaling factor, α_s , ensures that the operational costs in a season are scaled to reflect their annual costs, as each season is represented with a subset of hours. The scaled and discounted operational costs are then summed for all seasons, and multiplied by the probability of scenario ω , π_{ω} . Finally, the costs are summed for all scenarios $\omega \in \Omega$.

A grid charge, C^G , calculated as the total grid charge for all buildings in the neighborhood over the defined lifetime, is added to the discounted investment costs and the total operational costs. This grid charge is known and is given as a parameter to the model.

Finally, the connection charge to the district heating grid, C^{DH} , is also calculated

for the entire neighborhood and given as a parameter to the model. This is then added to the total costs of the neighborhood in the objective function, if the neighborhood has decided to connect to the district heating grid. This decision is given as a binary parameter to the model, defined as δ^{DH} .

The total operational costs for a operational period $o \in O_s$ in season s in scenario ω in investment period i is defined by $c_{i\omega so}^{totO}$. This is calculated, as shown in Equation (5.2), as the sum of operational costs less the operational revenue. The operational costs are given as the cost of energy imports, more specifically the price for each energy carrier, $P_{i\omega so}^f$ or P^f , multiplied by the amount of electricity imported, $y_{i\omega so}^{imp}$, the amount of heat imported from the district heating grid, $q_{i\omega so}^{imp}$ or the amount of resource consumed, $r_{ti\omega so}$. The operational revenue is given by the feed-in-tariff on electricity export, $P_{i\omega so}^{el.exp}$, multiplied by the amount of electricity exported to the grid, $y_{i\omega so}^{exp}$.

$$c_{i\omega so}^{totO} = P_{i\omega so}^{el.imp} \cdot y_{i\omega so}^{imp} + P^{bio} \cdot (r_{(CHP)i\omega so} + r_{(BB)i\omega so}) + P_{i\omega so}^{heat} \cdot q_{i\omega so}^{imp} + P^{gas} \cdot r_{(GB)i\omega so} - P_{i\omega so}^{el.exp} \cdot y_{i\omega so}^{exp} \quad (5.2)$$

The term ‘‘operating period’’ will hereafter be used when referring to an operational period o in season s in scenario ω in investment period i , given by $i\omega so$. This term is defined for all operational periods $o \in O_s$, all seasons $s \in S$, all scenarios $\omega \in \Omega$, and all investment periods $i \in I$.

Boilers and heat pumps

Equation (5.3) shows the energy balance for the boilers, and the heat pumps. The balance is defined for each heat technology $t \in T^H \setminus \{CHP, DH, ST\}$ and for every operating period $i\omega so$. It ensures that the heat generated by a technology t , $q_{ti\omega so}$, equals the amount of energy resource consumed by that technology, $r_{ti\omega so}$, multiplied by its efficiency, η_t^H . Note that the type of resource consumed differs for the technologies. The gas boiler consumes natural gas, the bio boiler consumes wood chips, and the electric boiler and heat pumps consume electricity.

$$q_{ti\omega so} - r_{ti\omega so} \cdot \eta_t^H = 0, \quad t \in T^H \setminus \{CHP, DH, ST\}, \quad (5.3)$$

$$i \in I, \omega \in \Omega, s \in S, o \in O_s$$

Equation (5.4) is the capacity constraint for the boilers and the heat pumps. The capacity constraint reflect that the heat generated by a technology t in any operating period $i\omega so$ cannot exceed the available capacity of the corresponding technology. The heat generated by heat technology t is given by $q_{ti\omega so}$. The available capacity at any point in time is denoted as the sum of the capacities installed in the investment periods prior to the current one, where the capacity installed in investment period i is defined by x_{ti} . The investment periods included in the sum are defined by a counter τ , starting from investment period $i - \frac{L_t}{N} + 1$, where L_t is the lifetime of the respective technology and N is the length of an investment period. This ensures that the available capacity only includes the installed capacities that have not yet reached the end of their lifetime. The expression $\sum_{\tau=i'}^i x_{t\tau}$ will in the following be referred to as the *available capacity* of technology t in investment period i . Note that the available capacity is multiplied by the length of an operational period, K , in order to ensure the value reflects the maximum amount of energy that can be generated during an operational period, given in kWh. This type of unit conversion will be used hereafter when necessary.

$$\begin{aligned}
 q_{ti\omega so} - K \cdot \sum_{\tau=i'}^i x_{t\tau} &\leq 0, & i' &= \max\{1, i - \left\lfloor \frac{L_t}{N} \right\rfloor + 1\}, \\
 t &\in T^H \setminus \{ST, DH, CHP\}, & & \\
 i &\in I, \omega \in \Omega, s \in S, o \in O_s & & (5.4)
 \end{aligned}$$

Combined heat and power

The CHP is modeled similar to the boilers and the heat pumps, but with one efficiency for heat generation and another for electricity generation. These energy balances are stated by Equation (5.5) and (5.6), and are defined for each operating period $i\omega so$. The balances ensure that the heat generated, $q_{CHP_{s\omega o}}$, and the electricity generated, $y_{CHP_{s\omega o}}$, is equal to or lower than the resource consumed by the CHP, $r_{i\omega so}^{CHP}$, multiplied by the corresponding efficiency, η_{CHP}^H or η_{CHP}^E . Note that the energy balances of the CHP are inequalities. The reason for this is to allow for heat or electricity loss. Also note that the variable denoting the resource consumed in an operating period is the same in both balances, thus providing a connection between them. This shows that when the CHP consumes the resource, in this case wood chips, it generates both heat and electricity.

$$q_{CHPi\omega so} - r_{i\omega so}^{CHP} \cdot \eta_{CHP}^H \leq 0, \quad i \in I, \omega \in \Omega, s \in S, o \in O_s \quad (5.5)$$

$$y_{CHPi\omega so} - r_{i\omega so}^{CHP} \cdot \eta_{CHP}^E \leq 0, \quad i \in I, \omega \in \Omega, s \in S, o \in O_s \quad (5.6)$$

The capacity constraint for the CHP is also modeled using two constraints, given by Equation (5.7) and Equation (5.8). As the CHP generates both heat and electricity, the *total* energy generation needs to be restricted by the available capacity. This is imposed by ensuring that heat or electricity generation in an operating period $i\omega so$, $q_{(CHP)i\omega so}$ and $y_{(CHP)i\omega so}$, cannot exceed the available capacity. However, the ratio between heat and electricity generation is restricted by their constant efficiencies. For this reason, the available capacity for either heat or electricity generation is defined by multiplying the available capacity of the CHP by a fraction of the efficiency for heat or electricity, η_{CHP}^H or η_{CHP}^E respectively, and the total efficiency for the CHP, $\eta_{CHP}^H + \eta_{CHP}^E$. The available capacities for heat and electricity are also multiplied by the length of an operational period, K , in order to obtain the correct unit.

$$q_{(CHP)i\omega so} - \frac{\eta_{CHP}^H}{\eta_{CHP}^H + \eta_{CHP}^E} K \cdot \sum_{\tau=i'}^i x_{(CHP)\tau} \leq 0, \quad (5.7)$$

$$i' = \max\left\{1, i - \left\lfloor \frac{L_i}{N} \right\rfloor + 1\right\}, i \in I, \omega \in \Omega, s \in S, o \in O_s$$

$$y_{(CHP)i\omega so} - \frac{\eta_{CHP}^E}{\eta_{CHP}^H + \eta_{CHP}^E} K \cdot \sum_{\tau=i'}^i x_{(CHP)\tau} \leq 0, \quad (5.8)$$

$$i' = \max\left\{1, i - \left\lfloor \frac{L_i}{N} \right\rfloor + 1\right\}, i \in I, \omega \in \Omega, s \in S, o \in O_s$$

District heating

The decision of connecting the neighborhood to an external district heating grid is given by a binary input parameter δ^{DH} , implying the decision is made beforehand. If the parameter equals one, the neighborhood has the option of importing heat from the district heating grid. The parameter value is valid for the entire planning

horizon, implying that the lifetime of the grid connection is equal to the defined lifetime for the model.

Equation (5.9) model the DH system as a heat technology with constant efficiency, defined for every operating period $i\omega so$. It ensures that the heat generated, $q_{(DH)i\omega so}$, equals the heat imported from the district heating grid, $q_{i\omega so}^{imp}$, multiplied by the corresponding efficiency, η_{DH}^H . Equation (5.10) ensures compliance with the technical restriction on the maximum amount of heat that can be imported from the grid during an operating period. This maximum amount is defined by the installed capacity of the connection to the grid, \bar{Q} , which is given as an input parameter to the model. Note that the value is multiplied by the length of an operating period, K , converting this value to the correct unit. It is also multiplied by the binary parameter, δ^{DH} , thus ensuring the maximum value of heat import is zero if the neighborhood is not connected to a district heating grid.

$$q_{(DH)i\omega so} - q_{i\omega so}^{imp} \cdot \eta_{DH}^H = 0, \quad i \in I, \omega \in \Omega, s \in S, o \in O_s \quad (5.9)$$

$$q_{(DH)i\omega so} \leq K \cdot \bar{Q} \cdot \delta^{DH}, \quad i \in I, \omega \in \Omega, s \in S, o \in O_s \quad (5.10)$$

Solar thermal collectors and photovoltaic panels

The specific solar heat generation in an operating period $i\omega so$, $Q_{i\omega so}^{ST}$, is given as an input parameter to the model. This is different from the utilized ST heat, which is a variable defining the heat generated by the solar thermal collectors, $q_{(ST)i\omega so}$. The reason for this distinction is to account for situations where the heat storage tank is full and the actual heat generated is larger than the heat demand. When this occurs, some of the actual heat generated will be lost, implying that the amount of utilized ST heat will be lower than what is generated. This is reflected in Equation (5.11), which states that the utilized heat from ST collectors can be either equal to or lower than the actual heat generation multiplied by the available capacity of the ST collectors. The specific solar heat generation is also multiplied by the length of an operational period, K , in order to obtain the correct unit.

$$q_{(ST)i\omega so} - K \cdot Q_{i\omega so}^{ST} \cdot \sum_{\tau=i'}^i x_{(ST)\tau} \leq 0, \quad i' = \max\{1, i - \left\lfloor \frac{L_{ST}}{N} \right\rfloor + 1\}, \quad (5.11)$$

$$i \in I, \omega \in \Omega, s \in S, o \in O_s$$

Similarly as for the ST collectors, there is an input parameter for PV, $Y_{i\omega so}^{PV}$, denoting the specific PV electricity generation. Equation (5.12) ensures that the variable reflecting the electricity generated by this technology, $y_{(PV)i\omega so}$, is either equal to or lower than the specific PV electricity generation multiplied by the available capacity. The specific PV electricity generation is also multiplied by the length of an operational period, K . Note that this constraint can be considered an equality in the case where there is no restrictions on the amount of electricity than can be exported to the electricity grid. However, in the model explained here, there is a restriction on the maximum amount of electricity that can be exported in an operating period $i\omega so$, given by Equation (5.15). Such a restriction imposes the possibility of a situation where the electricity storage is full, the maximum export limit is reached, and one has generated excess electricity, resulting in a loss of electricity.

$$y_{(PV)i\omega so} - K \cdot Y_{i\omega so}^{PV} \cdot \sum_{\tau=i'}^i x_{(PV)\tau} \leq 0, \quad i' = \max\{1, i - \left\lfloor \frac{L_{PV}}{N} \right\rfloor + 1\}, \quad (5.12)$$

$$i \in I, \omega \in \Omega, s \in S, o \in O_s$$

The amount of ST collectors and PV panels that can be installed is physically restricted by the size of the available area, reflected in Equation (5.13). This constraint ensures that the sum of the available capacities of PV and ST does not exceed the available area, \bar{A} . Note that, as the PV capacity is given in kWp, the available capacity of PV is multiplied by a factor A .

$$A \cdot \sum_{\tau=i'}^i x_{(PV)\tau} + \sum_{\tau=i''}^i x_{(ST)\tau} \leq \bar{A}, \quad i' = \max\{1, i - \left\lfloor \frac{L_{PV}}{N} \right\rfloor + 1\}, \quad (5.13)$$

$$i'' = \max\{1, i - \left\lfloor \frac{L_{ST}}{N} \right\rfloor + 1\}, i \in I$$

Grid constraints

Equation (5.14) and (5.15) ensure that the electricity imported, $y_{i\omega so}^{imp}$, and the electricity exported, $y_{i\omega so}^{exp}$ in each operating period $i\omega so$, cannot exceed their respective maximum values, \bar{Y}^{imp} and \bar{Y}^{exp} respectively. Note that the maximum values are multiplied by the length of an operating period, K .

$$y_{i\omega so}^{imp} \leq K \cdot \bar{Y}^{imp}, \quad i \in I, \omega \in \Omega, s \in S, o \in O_s \quad (5.14)$$

$$y_{i\omega so}^{exp} \leq K \cdot \bar{Y}^{exp}, \quad i \in I, \omega \in \Omega, s \in S, o \in O_s \quad (5.15)$$

Heat balance

For all operating periods except of those defining the first operational period in each season, the heat balance is given by Equation (5.16). It ensures that the heat demand of the neighborhood is met in each investment period $i \in I$, scenario $\omega \in \Omega$, season $s \in S$ and operational period $o \in O_s \setminus \{1\}$. The balance states that the sum of the heat generated by all heat technologies $t \in T^H$, denoted by $q_{ti\omega so}$, plus the heat stored at the beginning of the operating period, equals the heat stored at the end of the operating period, $s_{(HS)i\omega so}$, plus the heat demand of the neighborhood, $D_{i\omega so}^H$. The content of the heat storage at the beginning of an operating period is defined as the heat stored at the end of the previous operational period, $s_{(HS)i\omega s(o-1)}$, multiplied by the efficiency factor η_{HS}^H .

$$\sum_{t \in T^H} q_{ti\omega so} + \eta_{HS}^H \cdot s_{(HS)i\omega s(o-1)} - s_{(HS)i\omega so} = D_{i\omega so}^H, \quad i \in I, \omega \in \Omega, s \in S, o \in O_s \setminus \{1\} \quad (5.16)$$

Heat storage

The heat storage is assumed empty in the beginning of each season. This ensures that there is no connection between seasons, or between an operational scenario in one investment period and an operational scenario in the next investment period. Equation (5.17), defined for each investment period $i \in I$, scenario $\omega \in \Omega$, and season $s \in S$, reflects the heat balance of the first operating period in each season. As the content of the heat storage in an operating period is defined by the heat stored at the end of this period, the constraint ensures that the heat stored at the end of the first operating period in a season, $s_{(HS)i\omega s1}$, equals the sum of the heat generated by all heat technologies $t \in T^H$, $q_{ti\omega s1}$, less the heat demand of the neighborhood, $D_{i\omega s1}^H$.

$$\sum_{t \in T^H} q_{ti\omega s1} - s_{(HS)i\omega s1} = D_{i\omega s1}^H, \quad i \in I, \omega \in \Omega, s \in S \quad (5.17)$$

The heat stored in any given operating period $i\omega s o$ is limited by the available capacity of the heat storage, as defined by Equation (5.18). $s_{(HS)i\omega s o}$ is a variable representing the amount of heat stored at the end of the defined period. Note that the installed capacity of the heat storage is given in the unit of kWh.

$$s_{(HS)i\omega s o} - \sum_{\tau=i'}^p x_{(HS)\tau} \leq 0, \quad i' = \max\{1, i - \left\lfloor \frac{L_{HS}}{N} \right\rfloor + 1\}, \quad (5.18)$$

$$i \in I, \omega \in \Omega, s \in S, o \in O_s$$

The heat storage is restricted by maximum ramping constraints, reflected in Equation (5.19), (5.20) and (5.21). Equation (5.19) and (5.20) ensure that the absolute value of the difference between heat stored at the end of the operating period, $s_{(HS)i\omega s o}$, and the heat stored at the beginning of the operating period, $s_{(HS)i\omega s(o-1)}$, is less than or equal to the maximum rating, $\bar{V}_{(HS)}$. The maximum rate is given as a parameter to the model, specified as a rate per unit installed capacity, kW/kWh, and is multiplied by the installed capacity of the HS and the length of an operational period, K , to get the total amount of kWh that can be stored or extracted from the HS during an operational period. These constraints are defined for each operating period $i\omega s o$ except from the first operating period in a season.

$$\eta_{HS}^H \cdot s_{(HS)i\omega s(o-1)} - s_{(HS)i\omega s o} - \bar{V}_{(HS)} \cdot K \cdot \sum_{\tau=i'}^p x_{(HS)\tau} \leq 0, \quad (5.19)$$

$$i' = \max\{1, i - \left\lfloor \frac{L_{HS}}{N} \right\rfloor + 1\}, i \in I, \omega \in \Omega, s \in S, o \in O_s \setminus \{1\}$$

$$\eta_{HS}^H \cdot s_{(HS)i\omega s(o-1)} - s_{(HS)i\omega s o} + \bar{V}_{(HS)} \cdot K \cdot \sum_{\tau=i'}^p x_{(HS)\tau} \leq 0, \quad (5.20)$$

$$i' = \max\{1, i - \left\lfloor \frac{L_{HS}}{N} \right\rfloor + 1\}, i \in I, \omega \in \Omega, s \in S, o \in O_s \setminus \{1\}$$

Equation (5.21) ensures that the heat stored at the end of the first operating period in a season $s_{(HS)i\omega s 1}$ is less or equal to the ramping rate multiplied by the installed capacity of the HS and the length of an operational period, K .

$$s_{(HS)i\omega s1} - \bar{V}_{(HS)} \cdot K \cdot \sum_{\tau=i'}^p x_{(HS)i} \leq 0, \quad i' = \max\{1, i - \left\lfloor \frac{L_{HS}}{N} \right\rfloor + 1\}, \quad (5.21)$$

$$i \in I, \omega \in \Omega, s \in S$$

Electricity balance

The electricity balance of the neighborhood is reflected by Equation (5.22). This balance ensures that the electricity demand of the neighborhood, $D_{i\omega so}^E$, is covered in any operating period $i\omega so$. Note that the heat technologies t that consume electricity as their resource, $i \in \{EB, ASHP, GSHP\}$, increase the total electricity demand of the neighborhood. The total demand has to equal the electricity supplied by the neighborhood. The electricity supplied is given as the sum of the electricity generated by the power technologies $t \in T^E$, $y_{ti\omega so}$, added the electricity discharged from the battery, $\eta_B^E v_{i\omega so}^+$, and the electricity imported from the grid, $y_{i\omega so}^{imp}$. The electricity charged to the battery, $v_{i\omega so}^-$, and the electricity exported to the grid, $y_{i\omega so}^{exp}$, is then subtracted from the electricity supply of the neighborhood. Note that the electricity obtained from discharging the battery is the product of its efficiency, η_B^E , and the energy that is actually discharged, $v_{i\omega so}^+$.

$$\sum_{t \in T^E} y_{ti\omega so} + \eta_B^E v_{i\omega so}^+ + y_{i\omega so}^{imp} - v_{i\omega so}^- - y_{i\omega so}^{exp} - \sum_{t \in T'} r_{ti\omega so} = D_{i\omega so}^E, \quad (5.22)$$

$$I' = \{EB, ASHP, GSHP\}, i \in I, \omega \in \Omega, s \in S, o \in O_s$$

Battery constraints

The constraints explained in this section are all related to the battery, which is used as a storage for electricity. Equation (5.23) is the storage balance for the battery. This balance ensures that the state of charge, the SOC, is updated at the end of each operating period, except of the first operating period in each season, which is treated in Equation (5.24). It states that the SOC at the end of an operating period, $s_{(B)i\omega so}$, equals the SOC at the beginning of the period, $s_{(B)i\omega s(o-1)}$, added the electricity charged to the battery during the period, $v_{s\omega so}^-$, less the electricity discharged from the battery during the period, $v_{i\omega so}^+$. The electricity charged to the battery is multiplied by the conversion efficiency, η_B^E , in order to account for the efficiency loss in this process.

$$s_{(B)i\omega s o} - s_{(B)i\omega s(o-1)} - \eta_B^E v_{i\omega s o}^- + v_{i\omega s o}^+ = 0, \quad i \in I, \omega \in \Omega, s \in S, o \in O_s \setminus \{1\} \quad (5.23)$$

Similarly as for the heat storage, the SOC is assumed to be zero in the beginning of each season, and thus also each operational scenario. This is reflected by Equation (5.24), ensuring that the SOC at the end of the first operating period in a season, denoted by $s_{(B)i\omega s 1}$, has to equal the energy charged to the battery during the first operating period. The energy charged to the battery is the product of the conversion efficiency for charging the battery, η_B^E , and the electricity charged to the battery, $v_{i\omega s 1}^-$.

$$s_{(B)i\omega s 1} - \eta_B^E v_{i\omega s 1}^- = 0, \quad i \in I, \omega \in \Omega, s \in S \quad (5.24)$$

The amount of energy stored in the battery restricts what can be discharged from the battery. Equation (5.25) ensures that the electricity discharged from the battery during each operating period, denoted by $v_{i\omega s o}^+$, is less than or equal to the storage content at the end of the previous period, $s_{(B)i\omega s(o-1)}$. This constraint is not defined for the first operating period in each season.

$$v_{i\omega s o}^+ - s_{(B)i\omega s(o-1)} \leq 0, \quad i \in I, \omega \in \Omega, s \in S, o \in O_s \setminus \{1\} \quad (5.25)$$

The amount of electricity that can be discharged from the battery during the first operating period in each season is instead restricted by Equation (5.26). Since the battery is assumed empty at the beginning of each operating period in a season, the right hand side of Equation (5.25) can be substituted with zero, resulting in Equation (5.26). This implies that it is not possible to discharge electricity from the battery during the first operating period in a season.

$$v_{i\omega s 1}^+ \leq 0, \quad i \in I, \omega \in \Omega, s \in S \quad (5.26)$$

Similar to the constraint regarding maximum discharge from the battery, there is also a constraint regarding the maximum energy charged to the battery, reflected by Equation (5.27). The maximum amount of energy that can be charged to the battery during an operating period, $v_{i\omega s o}^-$, is restricted by the unused capacity of the battery. The unused capacity is equal to the sum of the installed capacities of the battery, $x_{(B)\tau}$, only including the installed capacities that have not yet reached

the end of their lifetime, less the energy that was stored in the battery at the end of the previous operating period, $s_{(B)i\omega s(o-1)}$. Note that the installed capacity of the battery in a period is given in kWh. This constraint is not defined for the first operating period in a season.

$$\eta_B^E v_{i\omega s o}^- - \sum_{\tau=s'}^i x_{(B)\tau} + s_{(B)i\omega s(o-1)} \leq 0, \quad i' = \max\{1, i - \left\lfloor \frac{L_B}{N} \right\rfloor + 1\}, \quad (5.27)$$

$$i \in I, \omega \in \Omega, s \in S, o \in O_s \setminus \{1\}$$

Equation (5.28) reflects the energy capacity constraint of the battery. It ensures that the energy stored in the battery at any point in time, $s_{(B)i\omega s o}$, is less than or equal to the installed capacity of the battery, $x_{(B)\tau}$, only including the installed capacities that have not yet reached the end of their lifetime.

$$s_{(B)i\omega s o} - \sum_{\tau=i'}^i x_{(B)\tau} \leq 0, \quad i' = \max\{1, i - \left\lfloor \frac{L_B}{N} \right\rfloor + 1\}, \quad (5.28)$$

$$i \in I, \omega \in \Omega, s \in S, o \in O_s$$

The battery is also restricted by its maximum charging and discharging power rating, reflected in Equation (5.29) and (5.30). These equations ensure that the energy discharged from the battery during an operational period, $v_{i\omega o}^+$, and the energy charged to the battery during an operational period, $v_{i\omega o}^-$ is less than or equal to the maximum power rating, $\bar{V}_{(B)}$, multiplied by the installed capacity of the battery and the length of an operational period, K , similar to the ramping constraints for the HS.

$$v_{i\omega s o}^+ - \bar{V}_{(B)} \cdot K \cdot \sum_{\tau=i'}^i x_{(B)\tau} \leq 0, \quad i' = \max\{1, i - \left\lfloor \frac{L_B}{N} \right\rfloor + 1\}, \quad (5.29)$$

$$i \in I, \omega \in \Omega, s \in S, o \in O_s$$

$$v_{i\omega s o}^- - \bar{V}_{(B)} \cdot K \cdot \sum_{\tau=i'}^i x_{(B)\tau} \leq 0, \quad i' = \max\{1, i - \left\lfloor \frac{L_B}{N} \right\rfloor + 1\}, \quad (5.30)$$

$$i \in I, \omega \in \Omega, s \in S, o \in O_s$$

ZEN constraint

Finally, as the model is developed as a single-objective problem where costs are minimized, it is necessary to add a constraint related to the fulfillment of the desired degree of ZEN. The ZEN constraint is reflected in Equation (5.31). In the left term, the total energy import in an operational period o is calculated by summing the energy import of each energy carrier, f , where each is multiplied by its corresponding weighting factor, W_f . The operational energy import is then summed for all operational periods in season s , and multiplied by the scaling factor α_s , before it is summed for all seasons $s \in S$. Finally, it is summed over all operational scenarios $\omega \in \Omega$, where each is multiplied by its probability, π_ω , and then summed for all investment periods $i \in I$. This calculation only includes the energy carriers that are either imported or exported from the neighborhood and represents the net effect. In the next term, the embodied energy is given as a parameter to the model, denoted by W^{Emb} .

$$\begin{aligned} & \sum_{i \in I} \sum_{\omega \in \Omega} \pi_\omega \sum_{s \in S} \alpha_s \sum_{o \in O_s} \left(W_{el_imp} \cdot y_{i\omega so}^{imp} - W_{el_exp} \cdot y_{i\omega so}^{exp} + W_{heat} \cdot q_{i\omega so}^{imp} \right. \\ & \left. + W_{bio} \cdot (r_{(BB)i\omega so} + r_{(CHP)i\omega so}) + W_{gas} \cdot r_{(GB)i\omega so} \right) + W^{Emb} = (1 - \gamma) \cdot W^{Ref} \end{aligned} \quad (5.31)$$

On the right hand side, W^{Ref} , is the weighted energy imports, calculated when the degree of ZEN, γ , equals zero. Thus, this parameter is determined by calculating the left hand side of Equation (5.31). This value is then used as input to the model when the ZEN constraint is imposed by requiring a degree of ZEN selected by the decision maker. This parameter has a value between zero and one, where $\gamma = 1$ indicates that the neighborhood fulfills the requirements of a ‘strictly’ ZEN by setting the right hand side of the constraint equal to zero. If $\gamma = 0$, the model will find the cost-optimal solution under the condition that the ZEN constraint is completely relaxed.

Chapter 6

Data analysis

This chapter presents a review of how the input data used when testing the IMEZEN is obtained and how this data is analyzed and pre-processed. Parameters such as the binary parameter deciding whether or not the neighborhood is connected to an external DH grid, the reference values for emission factors and the degree of ZEN are parameters that vary and will be specified in the computational study in Chapter 8 and the case study in Chapter 9. Some parameters and constraints are left out of what we later will refer to as our *base case*. These are ramping of the HS, maximum PV and ST areas and maximum electricity and DH grid constraints. This is done to see how the model performs without any maximum limits. These constraints and the applicable value of the associated parameters may be very case specific and unnecessary, and can be included if the decision maker view it as valuable and necessary. The constraints showing to be applicable to the case studied in this thesis will be applied in the case study in Chapter 9. Thus, the corresponding parameter values will be presented directly in Chapter 9, and will therefore not be specified in this chapter.

Most of the input data are obtained from Norwegian data sources and are, where possible, directly connected to the pilot project Ydalir. The chapter starts by presenting the parameters that are given as deterministic input to the model. These include financial parameters, fuel prices, emission factors, embodied energy, technological data such as costs, efficiencies and lifetimes, length of periods, as well as weighting factors of scenarios and seasons. Lastly, the operational data that are used when generating the scenarios and later used as stochastic input parameters to the model are presented. The fixed electricity grid charge will be presented along with its associated stochastic operational data. Some simplifications are made, and these and their implications will be presented and discussed in this

chapter. Where deemed necessary, justification of applicability of the obtained data will be given.

All prices and costs that are given as input to the model are in 2018 NOK and included the value added tax (VAT), unless otherwise specified. Our model is operating on an aggregated level and does for example not emphasize how much heat that are consumed by the dwellings and how much that are consumed by the school and the kindergarten. The same applies to import and export of electricity, investment in technologies and purchase of fuel. In reality, the school and kindergarten should not pay VAT, as the VAT is tax-deductable and generally not an expense for service, industry and public administration (The Norwegian Tax Administration, 2018). The dwellings should pay VAT and because of the ratio between costumers in the neighborhood that are imposed to pay VAT and the ones that are entitled to refrain from paying, the simplification to include VAT on *all* costs and incomes is made. It is also done to have a better basis for comparison when the results for the different cases are discussed in Chapter 9.

6.1 Financial data

The discount rate used in this thesis is 4 % and is the same as the one used in Sidelnikova et al. (2015). It is based on a recommendation for governmental projects with a lifetime of less than 40 years.

6.2 Fuel prices

The bio boiler and the combined heat and power technologies are based on use of dry wood chips as fuel, as forestry industry is very common in the area in and around Elverum. Eidsiva Bioenergi, which is the local district heating supplier, mainly uses wood chips residue bought from local forestry industry retailers for heat production in their plant (Dahl, 2018) and the nearby campus at Evenstad also uses local wood chips for their CHP unit (Backe, 2018). It is likely that Ydalir will make use of local resources like this to reduce costs and emissions from transport (Dahl, 2018). The gas boiler is based on consumption of liquefied natural gas delivered in tanks, while it does not exist a gas grid close to Ydalir (Dahl, 2018). Prices are given including VAT.

Wood chips

The price of wood chips used in this thesis is 0.3963 NOK/kWh, included delivery. This price is based on prices stated in the agreement between the pilot project Evenstad Campus and Rena Forst Bionenergi, which is a local supplier of wood chips (Backe, 2018). The price stated in their agreement is 312.50 NOK/ m^3 and 1875 NOK for delivery. The distance from the supplier to Ydalir is a bit shorter, and a delivery price of 1800 NOK is assumed. It is further assumed that one delivery contains 30 m^3 wood chips and an energy content of 940 kWh/ m^3 is assumed for chips of 10 % moisture (Helin, 2005). 10 % moisture is chosen because the chips used as fuel in the CHP unit at Evenstad have a required moisture < 15% (Selvig et al., 2017). Thus, the wood chips price is calculated based on this.

Natural gas

The price for natural gas in this thesis is set to 0.8125 NOK/kWh (Kverndalen, 2018). It is important to note that this is just an estimate, without taking the desired volume into account, implying that it might not necessarily be the exact price. The natural gas prices are not transparent and it is hard to find realistic prices for gas delivered in tanks, while it differs for each case and is heavily dependent on transportation costs, which again depend on the desired volume (Kverndalen, 2018).

6.3 Emission factors

The emission factors considered in this thesis are carbon factors and primary energy factors. As mentioned in Chapter 2, carbon factors describe how much CO₂-equivalent GHGs that are being emitted per unit of energy delivered, whereas primary energy factors are the ratio of all the primary energy used to deliver the energy, divided by the amount of actual delivered energy. Both emission factors are widely used and their values are fiercely discussed in the research community. The discussion of which values that are most correct to use originate in political frameworks and is out of the scope of this thesis. Values obtained from reliable references are therefore rendered in this section, without discussing the values themselves in particular. The values of these factors should therefore be considered carefully by the decision maker when performing a real case.

Carbon factors

Table 6.1 shows the CO₂ factors used in this analysis. Every country can decide which factors they want to use, making it a way of deciding what energy carriers are favoured in the specific country. This can for example be based on political decisions or on the available natural resources. The CO₂ factors listed here are based on Norwegian conditions and are obtained from Otterlei (2014) and are the same as Eidsiva Bioenergi uses for their local district heating grid in Elverum (Dahl, 2018). It is important to note that the Norwegian CO₂ factors usually have lower values than the European ones for electricity and biomass.

Table 6.1: CO₂ factors

Energy carrier	CO ₂ factor [g CO ₂ -eq/kWh]
Electricity	110
Wood chips	12
Natural gas	243
District heating ¹	14.77

¹ Calculated based on the local district heating supplier

The CO₂ factor for DH is calculated the same way as for the primary energy factor for DH, with a CO₂ factor for fossil oil equal to 289 (Otterlei, 2014) and the CO₂ factor for wood chips equal to the one listed in Table 6.1.

Primary energy factors

The primary energy factors are listed in Table 6.2. The PE factors for electricity, wood chips and natural gas are obtained from the proposed European standard values in European Committee for Standardization (2013). The PE factor for district heating is calculated based on the local district heating grid in Elverum. Eidsiva Bioenergi (Dahl, 2018) states that they use 99 % bio fuel and 1 % fossil oil for the heat production in their local grid. Thus, the PE factor for DH is calculated based on this, with a PE factor for fossil oil equal to 1.05 (European Committee for Standardization, 2013) and for wood chips equal to the one showed in Table 6.2.

Note that all PE factors listed in the table are symmetrical values. For electricity,

Table 6.2: Primary energy factors

Energy carrier	Primary energy factor [kWh _p /kWh _s]	
	Total	Non-renewable
Electricity	2.00	2.00
Wood chips	1.05	0.05
Natural gas	1.05	1.05
District heating ²	1.05	0.06

² Calculated based on the local district heating supplier

which is the only two-way energy carrier considered in this thesis, one can also divide the PE factor into symmetrical and asymmetrical values, meaning that export and import of electricity may have different PE factors in the asymmetrical case. Only symmetrical values are included here, based on the fact that energy exported to the grid will avoid an equivalent energy generation somewhere else in the grid, indicating that exported energy should have the same PE factor as imported energy from the grid (Sartori et al., 2012).

The non-renewable PE factors reflect how much of the energy carrier is based on non-renewable energy. For electricity and natural gas the total and non-renewable PE factors are equal, indicating that the primary energy used to bring the electricity to the grid is based solely on non-renewable energy. In contrast, the total PE factor for wood chips is much higher than the non-renewable one, reflecting that most of the primary energy used for the production of wood chips are based on renewable energy.

6.4 Embodied energy

The energy embodied in the materials is set to zero. Thus, the ambition level of the model is corresponding to ZEN-O; containing all operational energy consumption.

6.5 Technological data

This section will present the input parameters regarding data connected to the technologies that are included as investment alternatives in our model. First some

background on which factors that have contributed to the choice of the selected data will be provided. Further, data regarding costs and subsequently efficiencies and lifetimes will be presented and discussed.

Most of the technological data are collected from a report published by “The Norwegian Water Resources and Energy Directorate” (Sidelnikova et al., 2015), which we consider a reliable and applicable data source to our problem, as it reflects the Norwegian market. The exceptions are data used for the battery and heat storage, as no applicable values were found for these technologies in Sidelnikova et al. (2015). By using data from the same report for most technologies, a certain level of consistency is ensured, especially with regard to what is included in the investment costs, as well as the ratio between costs for the different technologies.

Each technology included in the model has a technology cost, lifetime and efficiency associated with it, that are used as input parameters to the model. For most technologies, the investment cost and in some cases also the lifetimes and efficiencies, will be highly dependent on the size of the component. We have collected two sets of technological data inputs; one representative for neighborhoods and one representative for individual residential buildings. The data applicable to buildings can be seen in Appendix B. Larger technology sizes are chosen as a basis for neighborhoods than for buildings. The sizes are selected based on the load profiles that are used to generate stochastic input to the model. Figures 6.1 and 6.2 shows duration curves for heat and electricity demand for the whole neighborhood, respectively. A duration curve depicts the demand sorted from highest to lowest and may be used to determine the share of base and peak loads.

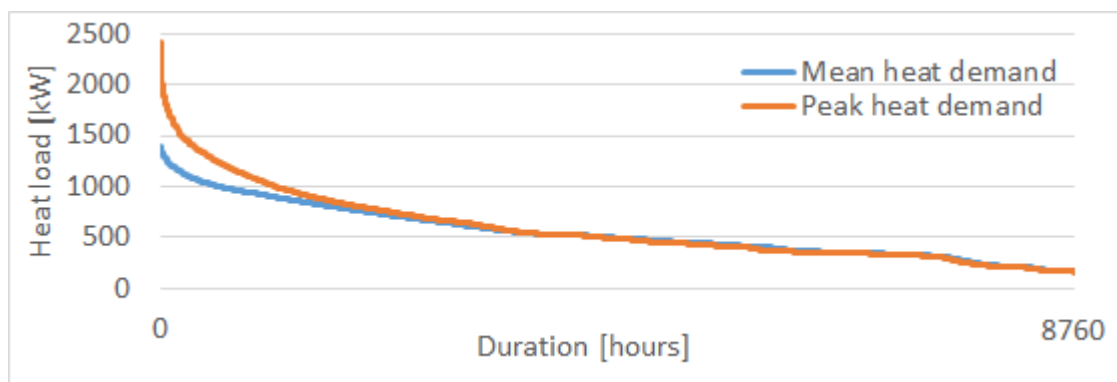


Figure 6.1: Duration curves for mean and peak heat demands, showing sorted demands from highest to lowest during one year.

Figure 6.1 includes one duration curve that represents the mean of the 15 years that are used to generate scenarios from and one duration curve for the year that contains the peak heat demand hour, being the year 2001. From the curves one can see that the base load is around 500 - 1000 kW, whereas the top loads are about 1400 kW and 2500 kW for the mean and peak load, respectively. For most technologies the available capacities are either 1000 kW or 10000 kW. As 10000 kW are a lot larger than the peak demands, heat technologies with capacities of typically 1000 kW are selected as a basis when collecting the data for the neighborhood case. To cover the top loads, larger technologies should be used, implying that technologies used for top load may have cheaper prices per kWh than reflected in this thesis.

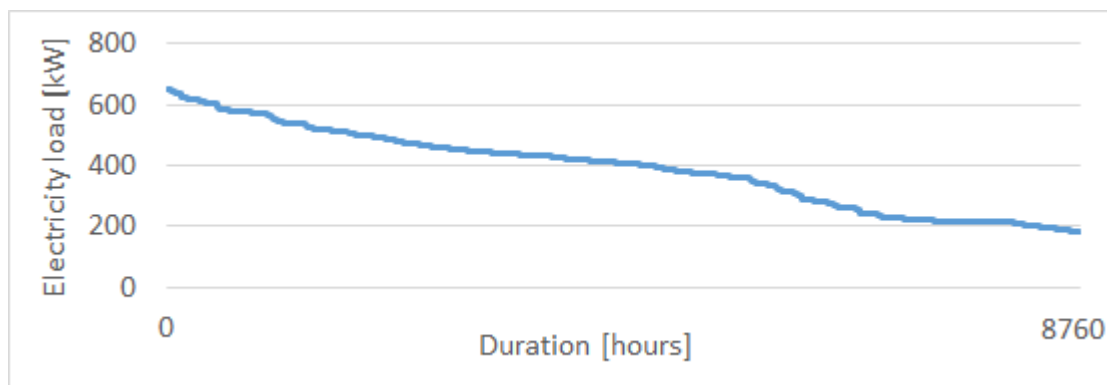


Figure 6.2: Duration curve for electricity demand, showing sorted demand from highest to lowest during one year.

Figure 6.2 shows the duration curve for the electricity load profile that are used to generate scenarios from. One can see that the base load is around 400 kW, whereas the peak load is about 650 kW. Based on this, typically sizes of 1000 kW are chosen as a basis when collecting technological data for the electricity technologies applicable to neighborhoods.

6.5.1 Technology costs

The technology costs for a neighborhood can be seen in Table 6.3. The table shows which capacity sizes that are used as a basis for the different technologies, in which unit this capacity is measured and the cost measured in NOK per unit of this unit. See footnotes for exceptions. The references of where the data are collected from are also listed in the last column.

Table 6.3: Technology costs - neighborhood size

Technology	Size	Unit	Technology cost [NOK/Unit]	Reference
EB	1000	kW	1 726.61	Sidelnikova et al. (2015)
GB	1000	kW	1 663.68	Sidelnikova et al. (2015)
BB	1000	kW	26 012.71	Sidelnikova et al. (2015)
ASHP _{a-w}	1000	kW	9 939.65	Sidelnikova et al. (2015)
GSHP _{w-w}	1000	kW	19 382.94	Sidelnikova et al. (2015)
ST	300	m ²	5 365.21	Sidelnikova et al. (2015)
DH	-	-	25 000 ³	Tonjer (2018)
CHP	10000	kW	34 519.69	Sidelnikova et al. (2015)
PV	1000	kW _p	23 599.97	Sidelnikova et al. (2015)
HS	0.5	m ³	1 021.33 ⁴	The Danish Energy Agency and Energinet (2012)
Battery	200	kWh	9 601.75	Lambert (2016)

³ [NOK/household connected to DH grid]

⁴ [NOK/kWh]

Note that all costs are given in 2018 NOK including VAT and include both equipment costs and installation costs. For all costs obtained from Sidelnikova et al. (2015), the values are originally given in 2013 NOK. The total technology costs are obtained by converting the investment costs and annual fixed OM costs (where applicable) to their corresponding values in March 2018 NOK with CPI-values gathered from Statistics Norway (2018). Then, the 2018 value of annual fixed OM costs are calculated for the entire lifetime of the technologies by using the present value of an annuity factor with the discount rate of 4 % (Investopedia, 2018d). These values are then added together and constitute the total technology costs.

The cost of the CHP is based on a size of 10 000 kW total capacity, as this was the smallest size found in Sidelnikova et al. (2015). This is larger than what is applicable to the neighborhood studied in this thesis, implying that the price might be a bit low. The cost related to PV is based on ground mounted PV panels measured in kilo watt peak power and includes inverter. The cost for DH is obtained from the contract between Ydalir and Eidsiva Bioenergi, stating that each connected household must pay a connection fee of 25 000 NOK (Tonjer, 2018). In this thesis the same connection fee is also assumed for the school and the kindergarten, making the value of this parameter represented by C^{DH} equal

to 20 050 000 NOK.

For the battery, the cost is obtained from Lambert (2016) for the Tesla Powerpack battery. This cost includes bi-directional inverter and cabling and site-support hardware. The cost is originally given in 2016 USD and is calculated to 2018 USD with CPI values from U.S. Official Inflation Data (2018*b*) and converted to 2018 NOK with the currency obtained from Norges Bank (2018*a*) April 18. 2018. Installation cost gathered from Tesla Inc. (2018*b*) is also added to the technology cost.

The cost for the heat storage is collected from The Danish Energy Agency and Energinet (2012) and is an estimated value obtained from a graphical plot. Only small or very large sizes of heat storages were found, and the price is therefore chosen to be based on a quite small heat storage, implying that this price might be a bit high when applied to this neighborhood case. The cost of the HS is originally given in 2011 EUR and is converted to 2018 NOK by calculating it to its corresponding value in 2018 EUR with CPI values from U.S. Official Inflation Data (2018*a*). Then, the currency from Norges Bank (2018*b*) April 16. 2018 is used to convert it to 2018 NOK.

6.5.2 Efficiencies and lifetimes

Efficiencies and lifetimes of the technologies are listed in Table 6.4. The lifetimes are given in years and are defined as the economic lifetimes of the technologies. This means the expected period of time during which the technologies are useful to the average owner (Investopedia, 2018*c*). The economic lifetime is often shorter than the technical lifetime, implying that the technologies might still be working after the end of their lifetime.

The efficiencies of the heat pumps are the COP-values. These values vary with the heat source temperature, which in this case is either air or ground water, and the supply temperature, which is the temperature of the accumulator tank to be heated. The values are obtained for HPs with an supply temperature of 50 °C. The efficiencies of PV and ST are not listed in the table. This is because actual PV and ST generation is given directly as input, and the efficiencies are incorporated in these parameters, as explained in subsections 6.9.5 and 6.9.4, respectively.

Note that the CHP is described with two efficiencies; one heat efficiency and one for electricity. Sidelnikova et al. (2015) suggests a total efficiency of 0.90, where the electricity share amounts 0.24. The heat efficiency is calculated by subtracting

the electricity share from the total efficiency.

Table 6.4: Efficiencies and lifetimes - neighborhood size

Technology	Efficiency	Lifetime	Reference
EB	0.98	20	Sidelnikova et al. (2015)
GB	0.92	20	Sidelnikova et al. (2015)
BB	0.86	20	Sidelnikova et al. (2015)
ASHP _{a-w}	2.45	15	Sidelnikova et al. (2015)
GSHP _{w-w}	3.1	15	Sidelnikova et al. (2015)
ST	–	25	Sidelnikova et al. (2015)
DH	1.00	100	Dahl (2018)
CHP	0.66 ⁵ / 0.24 ⁶	20	Sidelnikova et al. (2015)
PV	–	25	Sidelnikova et al. (2015)
HS	0.99	20	Lindberg, Fischer, Doorman, Korpås and Sartori (2016) and The Danish Energy Agency and Energinet (2012)
Battery	0.88	20	Tesla Inc. (2018a) and Saft Batteries (2018)

⁵ Heat efficiency

⁶ Electricity efficiency

There is assumed no loss on import of heat from the DH grid. Eidsiva Bioenergi pays for the internal losses in their grid up to the customer's facility (Dahl, 2018). We assume that no heat imported from the DH grid will be lost in the neighborhood. Since the DH grid is an external facility, we assume that the lifetime of this plant will not influence the neighborhood. To prevent this parameter from affecting the model's decisions, it is set to an arbitrary large value, in this case being 100 years.

For the Tesla Powerpack battery system, no guaranteed lifetime is specified in Tesla Inc. (2018a). The lifetime for the battery is therefore gathered from Saft Batteries (2018) which is another large producer and supplier of batteries. Lifetime predictions for the battery Intensium[®] Smart of similar size and with same type of field of application as the Tesla Powerpack is chosen to represent the lifetime of the battery in this thesis.

6.6 Length of periods

The length of an investment period is in this thesis set to 5 years, considering the possibility of the model being included as a module in EMPIRE, which also operates with five-year periods. The length of an operational period is 1 hour. This is done for simplicity and for the same reason as for investment periods.

6.7 Probability of scenarios

As a scenario tree is used as input to the model, each scenario is weighted with a factor, making sure the total contribution from all scenarios equal 1. This value is simply set to be the same for all scenarios by

$$\pi_{\omega} = \frac{1}{|\Omega|}, \quad (6.1)$$

where π_{ω} is the probability of scenario ω , and $|\Omega|$ is the number of scenarios.

6.8 Seasonal scaling factor

The seasonal scaling factor, α_s , defines the contribution from parameters and variables for a given season s to an annual figure. This is to ensure that the operational costs calculated represent a full year of operation, not considering leap years. There are two seasonal scaling factors used, one for all regular seasons and one for all extreme seasons. The concept of seasons will further be explained in section 7.1.3 in Chapter 7. Note that the inclusion of extreme seasons in each annual scenario is a way of ensuring that the energy system is capable of meeting peak demand, implying that they represent situations that rarely occurs. For this reason, the scaling factor for the extreme seasons are set to equal 1. As each extreme season consists of 48 hours, this means that the two extreme seasons in total represent 96 hours of a year. The regular seasons represent the rest of the year. The seasonal scaling factor for each of the four regular seasons is thus given by

$$\alpha_{s'} = \frac{8760 - 96}{4 * |O_{s'}|}, \quad (6.2)$$

where $O_{s'}$ is the number of hours in a regular season s' , which is 168 hours in this case. The scaling factor used for the regular season is thus approximately 12.893.

6.9 Stochastic operational data

This section provides a description of the operational data that comprises the short-term uncertainty considered in the mathematical formulation of the IMEZEN. This includes hourly profiles for the electricity and heat demand, the electricity and heat prices, and the PV and ST generation. The price and production parameters are collected as historical data series, whereas the demand profiles are predicted load profiles. The historical data is gathered from the years 2000 to 2014, as it is the range from which we were able to obtain data for all parameters, resulting in 15 different hourly profiles. It should be noted that only a single hourly profile is included for the electricity demand.

The quality of the data gathered has been analyzed and cleaned as deemed necessary before used as input for the scenario generation algorithm. Note that leap year data is disregarded by removing the 24 last data entries from each leap year, thus ensuring that all yearly hourly profiles consist of 8760 hours. The last day of the year is removed in order to maintain the correlations between consecutive hours within a year. Hence, the connection between the last hour in one year and the first hour in the next year is lost, but this has no influence as the scenario generation method always samples data within one year. The technique used for handling missing values is explained for the relevant parameters in the corresponding sections.

6.9.1 Energy demand

Hourly energy demand profiles, for both heat and electricity demand, have been provided by Lindberg (2018) using the regression model methodology as described in Lindberg (2016). Separate demand profiles are provided for each building type in Ydalir, resulting in three different demand profiles for residential units, the kindergarten, and the school. Note that all demand profiles are for passive

buildings and that the demand profiles represent average buildings, implying that the variation between different households is not reflected. As the energy demand profiles for all residential units are assumed identical, and thus perfectly correlated, an important aspect of the ZEN concept is lost. If a variety of residential energy demand profiles had been included, one would be able to take advantage of the synergies between the load profiles of the different units. This follows from the concept of portfolio theory, as diversification leads to a flattened aggregated demand where peaks from individual energy demand profiles are smoothed out (Investopedia, 2018b). It should be noted that the effect from the synergies between different building *types* are included as the IMEZEN considers the demand for the entire neighborhood, aggregating the demand for the kindergarten, the school, and the residential units. However, these synergies are probably minimal as Ydalir is mainly comprised of residential units. Thus, the gain from taking advantage of synergies between buildings is probably much higher for more diverse neighborhoods and is easily incorporated by changing the input data.

As the historical data series for heat demand and electricity demand are given in Wh/m², they are aggregated in order to reflect the size of the neighborhood at the given point in time. Thus, the heat and electricity data series given to the scenario generation algorithm as input is the total demand for the neighborhood.

Heat demand

The prediction of hourly heat demand profiles is also based on historical temperature data. For this case study, hourly temperature data for the Oslo area has been downloaded from the Norwegian Meteorological Institute's publicly available web portal⁷.

When analyzing the heat demand data series, the focus has been on the hourly profiles for residential units as they represent most of Ydalir. The daily average heat demand for a residential unit is presented in Figure 6.3. This is calculated as the average of all 15 heat demand profiles. The average temperature is also included in the figure, showing the negative correlation between the heat demand and the temperature. It can be observed that the heat demand is higher at the beginning and at the end of the year, and lower during the summer. This seasonality characteristic should therefore be accounted for by the scenario generation method.

⁷www.eKlima.no

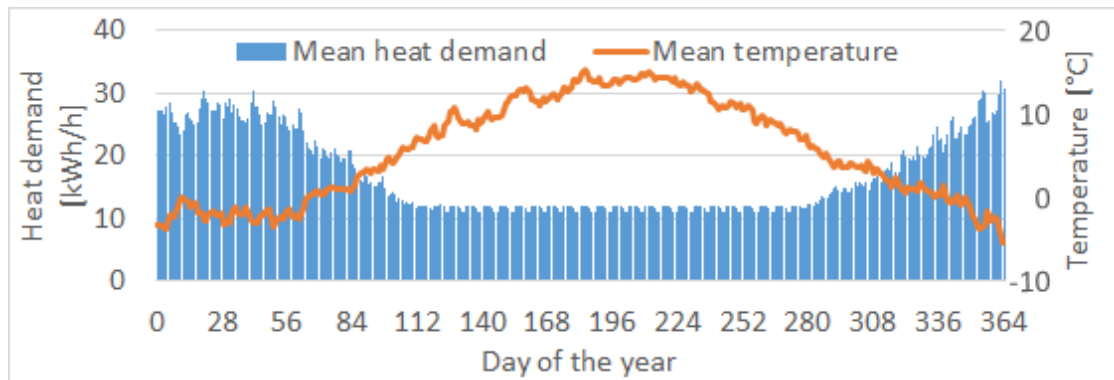


Figure 6.3: Average daily heat demand for a residential unit of 100 m²

Another aspect that should be considered is the hourly variation. This can be observed in Figure 6.4, which shows the average heat demand for each hour in the week. The general fluctuations within each day seem to follow the same pattern, where the demand is at its highest during the morning hours and at its lowest in the middle of the night. Also note that the peak demand is somewhat elevated during the weekend, represented by hours 121 to 168, compared to the weekdays. These patterns are as expected, but are important to consider when creating scenarios in order to keep the connection between consecutive hours and include both the hourly and daily variations.

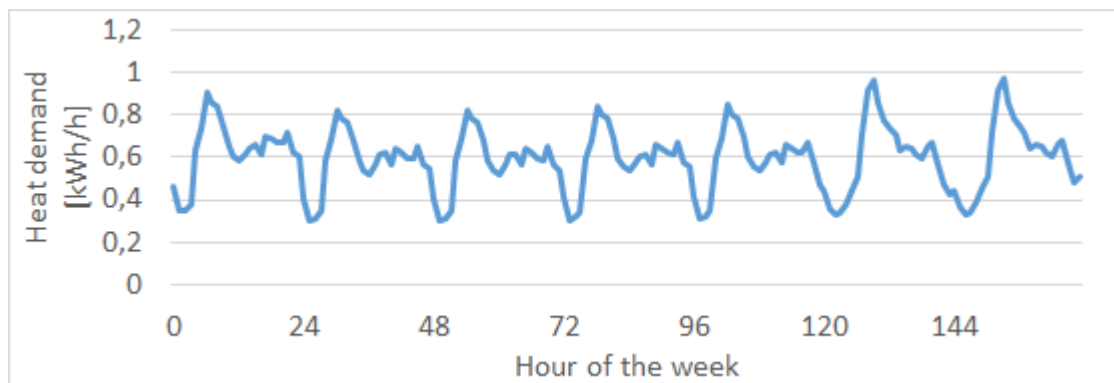


Figure 6.4: Average hourly heat demand for a residential unit of 100 m²

Electricity demand

The prediction of hourly electricity demand profiles is not based on temperature data, as is the case for the heat demand, but only on the building type and geographical position. Thus, only one hourly electricity demand profile is provided for each building type in Ydalir. This is different from the other operational data series and will be handled by the scenario generation method.

The average daily electricity demand for a residential unit is presented in Figure 6.5. As for the heat demand, there is higher demand during the winter, and lower demand during the summer. The variation is however much lower than for the heat demand, implying that the effect of seasonality is less dominant. Still, both energy demand profiles show that the seasonality must be considered by the scenario generation algorithm.

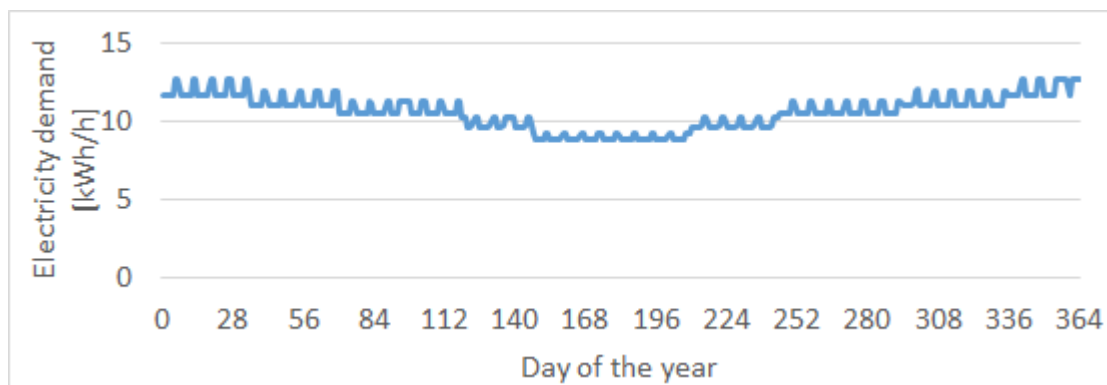


Figure 6.5: Average daily electricity demand for a residential unit of 100 m²

The hourly variation has also been analyzed for the electricity demand. This is shown in Figure 6.6. From this it is clear that the electricity demand differs from the heat demand, as the peak within a day is in the evening and not in the morning. Further, it can be observed that there is also a difference between weekdays and weekends, where the demand during the morning hours are higher in weekends than in a weekday. The peak demand in the evening is however the same, regardless of what day of the week it is. These patterns show the importance of maintaining both hourly variations in a day and daily variations during a week, similarly as for the heat demand.

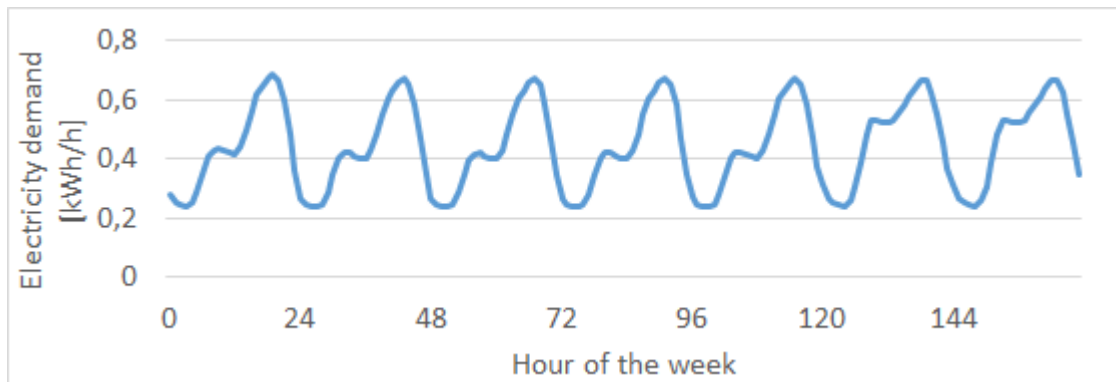


Figure 6.6: Average hourly electricity demand for a residential unit of 100 m²

6.9.2 Electricity prices

The electricity prices in Norway are divided between the grid charge that is paid to the local grid company and an electricity cost paid to the chosen company that delivers the electricity (Ånestad, 2014). In Elverum where the Ydalir project is placed, the local grid company is “Eidsiva Nett” and the local electricity company is “Eidsiva Energi”. Therefore, the grid charges are based on values obtained from Eidsiva Nett, whereas the electricity prices are based on values from Eidsiva Energi. Because most of the neighborhood will consist of dwellings and private users and since the neighborhood should be able to sell on-site generated electricity to the grid, the tariffs and agreements that are selected are the ones applicable to plus-customers and private households. A plus-customer is defined as an end user with both consumption and production behind their connection point, which is not allowed to feed in more than 100 kW at any time (Eidsiva Nett AS, 2018a). They are not required to hold a licence from The Norwegian Water Resources and Energy Directorate to produce and sell electricity (Hoff, 2018).

Electricity bought

For plus-customers the grid charges for import of electricity are the same as for regular consumers, and the grid charges are therefore taken from Tariff sheet 1.0 applicable for households (Eidsiva Nett AS, 2018b). The grid charges, including fixed charges for residential buildings, the school and the kindergarten and required energy charges applicable for all types of buildings, are presented in Table 6.5. Tariff E10 has been chosen for the dwellings, E25 for the kindergarten and E65 for

the school. Tariff E10 reflects a maximum load of 10 kW, whereas Tariff E25 and E65 reflect maximum loads of 25 and 65 kW, respectively (Hoff, 2018). From the electricity load profile in Section 6.9.1, no load for households exceeds 10 kW and the maximum loads for the kindergarten and school are around 23 and 63 kW, respectively. The tariffs are selected based on this.

Note that the energy charge is the same for all tariffs, whereas the fixed charge is what differentiates them. The payment of 0.01 NOK/kWh to Enova is really only valid for consumption registered for household purposes. The school and kindergarten would in reality be entitled to pay a fixed charge of 800 NOK/year exclusive VAT instead of the variable charge. As already mentioned simplifications are made and this is one of the simplifying assumptions. This implies that the charges representing the school and kindergarten are higher than what is actually the case in reality.

Table 6.5: Grid charges - Eidsiva Nett (Tariff E10, E25 and E65)

Charges	Price	Unit
Fixed charge dwellings	3 538	[NOK/year]
Fixed charge kindergarten	12 356	[NOK/year]
Fixed charge school	23 006	[NOK/year]
Energy charge ⁸		
Summer ⁹	0.2948	[NOK/kWh]
Winter ¹⁰	0.3073	[NOK/kWh]

⁸ Included required payments to the energy fund Enova of 0.01 NOK/kWh (excl. VAT) and consumption tax of 0.1658 NOK/kWh (excl. VAT)

⁹ Summer: April - October

¹⁰ Winter: November - March

Since Eidsiva is the local grid and electricity company, we assume that Ydalir will buy their electricity from “Eidsiva Energi”. The agreement “Innlansspot” is chosen to collect prices on electricity (Eidsiva Energi AS, 2018). These are listed in Table 6.6.

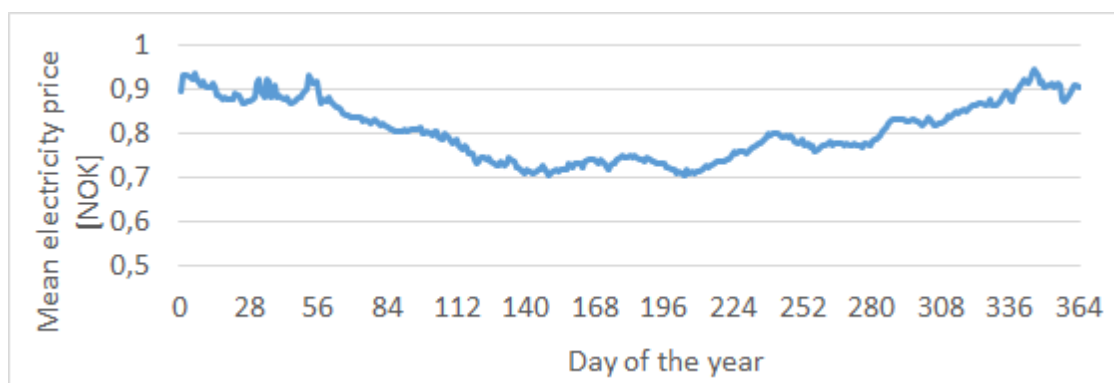
Table 6.6: Electricity prices - Eidsiva Energi (Innlansspot)

Charges	Price	Unit
Fixed charge	540	[NOK/year]
Electricity cost	Spot price	[NOK/kWh]
Energy charge ¹¹	0.045	[NOK/kWh]

¹¹ Included required el-certificate charge

The spot price is the hourly spot prices for electricity given in NOK/kWh. These have been obtained from Nord Pool via allowed access to their FTV-server (Foyen, 2018). The collected prices are the hourly electricity spot prices from years 2000 to 2014 for the Oslo-area. One hour each year were found to be missing in the data, and these hours are filled in by the average of the one previous and one following hours. The spot prices are converted to their corresponding values in March 2018 NOK with CPI-values obtained from Statistics Norway (2018) and the VAT (25 %) is added. The total price on electricity bought in a given hour is the historical spot prices in 2018 NOK, added the ENOVA-charge and energy charge paid to Eidsiva Nett and Eidsiva Energi, respectively. A plot of the total electricity prices over one year can be seen in Figure 6.7. The values are an average of prices from 2000 to 2014. The plot shows a tendency of lower prices in the summer and a gradual increase toward the winter months.

Figure 6.7: Daily mean electricity price [NOK] for one year



Further, Figure 6.8 shows how the electricity price vary throughout a week. It is not as distinct pattern throughout one week as for one year, but it may seem to be a tendency of higher prices in the mid-week. The diurnal variation is characterized by higher prices in the morning and evening, and lower in the night.

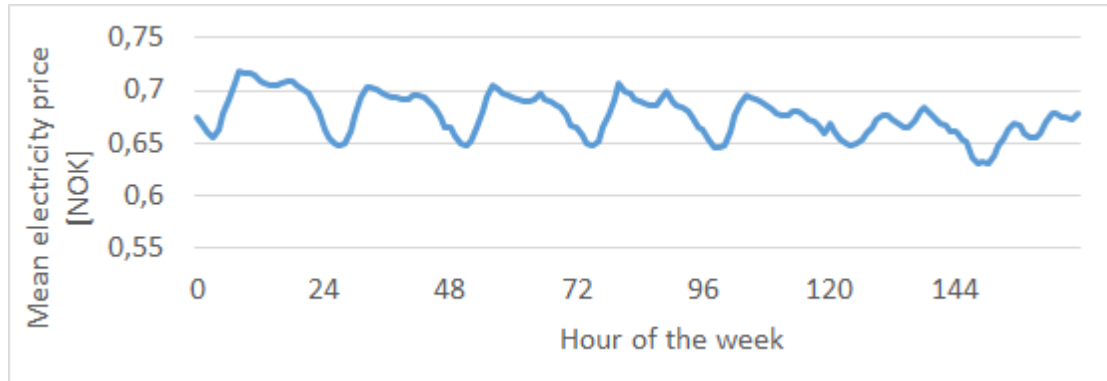


Figure 6.8: Hourly mean electricity price [NOK] for one week

These electricity price time series are used in the generation of scenarios given as stochastic input to the model. The scenario generating algorithm should therefore be developed in such way that it catches the diurnal, weekly and yearly variations caused by the spot price.

Note that the spot price is the only stochastic part of the total variable electricity price. The other charges are assumed identical for each year in the time period of year 2000 to 2014. The fixed charges are annual charges that are added together and given as deterministic input to the model, represented by the parameter C^G . This parameter adds up to be 2 865 762 NOK. Hence, this charge is also assumed to be the same each year of the time horizon.

Electricity sold

The electricity sold to the grid has an energy charge of 0.0375 NOK/kWh paid to Eidsiva Nett and an energy charge of 0.015 NOK/kWh paid to Eidsiva Energi (Hoff, 2018). The energy charge paid to Eidsiva Nett is obtained from Tariff sheet 7.1 applicable for plus-customers (Eidsiva Nett AS, 2018a). The income of exporting electricity to the grid is calculated by subtracting these energy charges from the electricity spot price. Note that these energy charges are also considered deterministic and the spot price is again the uncertain part. The price of selling

electricity will follow the same curve as electricity sold, shown in Figure 6.7.

6.9.3 DH prices

“Eidsiva Bioenergi” is the local district heating company in Elverum and there is already settled an agreement on delivery of heat to the neighborhood (Tonjer, 2018). Based on that the neighborhood mainly will consist of new residential buildings, the costs of importing heat from the grid is obtained from Tariff F4 applicable to new residential buildings (Dahl, 2018). The grid charges and the heat prices can be seen in Table 6.7 and Table 6.8, respectively. It is not possible to export heat to the grid.

Table 6.7: Grid charges - Eidsiva Bioenergi (Tariff F4)

Charges	Price	Unit
Fixed charge	0	[NOK/year]
Energy charge ¹²	0.2948	[NOK/kWh]
Down fuse effect	0.0625	[NOK/kWh]

¹² Included required el-fee

Table 6.8: Heat prices - Eidsiva Bioenergi (Tariff F4)

Charges	Price	Unit
Heat cost	Spot price	[NOK/kWh]
Energy charge	0.0375	[NOK/kWh]
ENOVA-charge	0.01	[NOK/kWh]

The total price on heat bought in a given hour is all these variable charges added together. Note that the spot price is again the part that makes up the stochastic part of the total heat price, whereas the other values are assumed to be constant over all years reaching from 2000 to 2014. Thus, the heat price will follow the same development as the total electricity price shown in the figures presented in the previous section.

6.9.4 ST heat generation

To provide ST heat generation data, the radiation on a tilted surface is needed. Equation 6.3 shows how the radiation incident on a tilted surface, S_{module} , is related to the solar radiation measured perpendicular to the sun, $S_{incident}$. α is the elevation angle and β is the tilt angle of the module measured from the horizontal plane.

$$S_{module} = S_{incident} \cdot \sin(\alpha + \beta) \quad (6.3)$$

α is again calculated from

$$\alpha = 90 - \phi + \delta, \quad (6.4)$$

where ϕ is the latitude and δ is the declination angle which is defined as

$$\delta = 23.45^\circ \cdot \left[\frac{360}{365} \cdot (284 + d) \right], \quad (6.5)$$

where d is the day of the year. The equations 6.3 - 6.5 are gathered from PV Education (2018).

$S_{incident}$ is collected from Renewables.ninja (2018). The latitude and longitude used are respectively 60.8925° and 11.5799° , representing where Ydalir is being developed. The data set used is “MERRA-2 (global)”, which is not a data set based on Europe. Thus, the climatic conditions may not be representative for Europe, but are for simplicity assumed to be approximately the same. The elevation angle, β , is assumed to be 41° , which is the same angle as used for the PV modules presented in the next section. S_{module} is calculated for the same period as the other stochastic parameters, from year 2000 to 2014.

ST heat generation for every hour is then calculated using Equation 6.6 and 6.7 from Lindberg, Doorman, Fischer, Korpås, Ånestad and Sartori (2016). First, the efficiency of a flat plate solar thermal collector is defined as

$$\eta_{ST} = c_0 - c_1 \frac{T_{collector} - T_{ambient}}{IRR_{tilt}} - c_2 \frac{(T_{collector} - T_{ambient})^2}{IRR_{tilt}}, \quad (6.6)$$

where $T_{collector}$ is the temperature of the solar thermal collector representing the output temperature, $T_{ambient}$ is the ambient temperature and IRR_{tilt} is the total irradiation on a tilted plane, earlier defined as S_{module} . The constants c_0 , c_1 and c_2 are determined by laboratory experiments, and are the same values as used in Lindberg, Doorman, Fischer, Korpås, Ånestad and Sartori (2016), equalling 0.789, 3.545 and 0.017 respectively.

$T_{collector}$ needs to be determined exogenously, and as Equation 6.6 shows, the efficiency decreases when $T_{collector}$ increases. As there is assumed no differentiation between DHW and SH demand, and ST can be utilized for both, the value of $T_{collector}$ is not intuitive. In this case $T_{collector}$ is determined to be $50^\circ C$, which is the same output temperature as for the heat pumps. This is done to ensure consistency.

ST heat generation for every hour, Q^{ST} , is then the irradiation, IRR_{tilt} , multiplied by the efficiency, η_{ST} , as stated in Equation 6.7.

$$Q^{ST} = IRR_{tilt} \cdot \eta_{ST} \quad (6.7)$$

ST heat generation, measured in $kWh/m^2_{collector}$, is then calculated for every hour from January 1. 2000 to December 31. 2014, and used as input for the scenario generation.

When analyzing the heat generation data one observes a clear seasonality and a diurnal variation. Figure 6.9 shows the daily mean heat generation from ST in one year, where one can see a greater heat generation in the middle of the summer compared to the rest of the year.

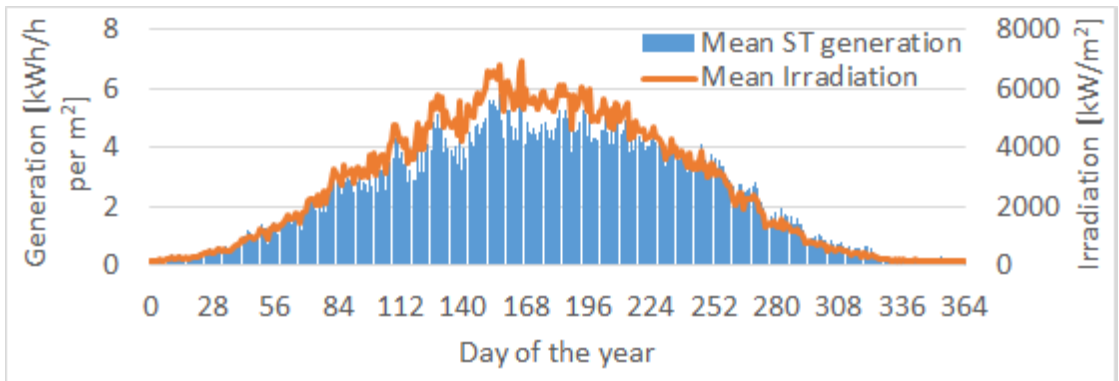


Figure 6.9: Daily mean ST generation and irradiation for one year

The diurnal variation is shown in Figure 6.10 where the hourly mean heat generation during 24 hours is presented. These patterns are as expected, as heat generation from ST is positively correlated with the irradiation from the sun. This is important to pay attention to and capture in the scenario generation process.

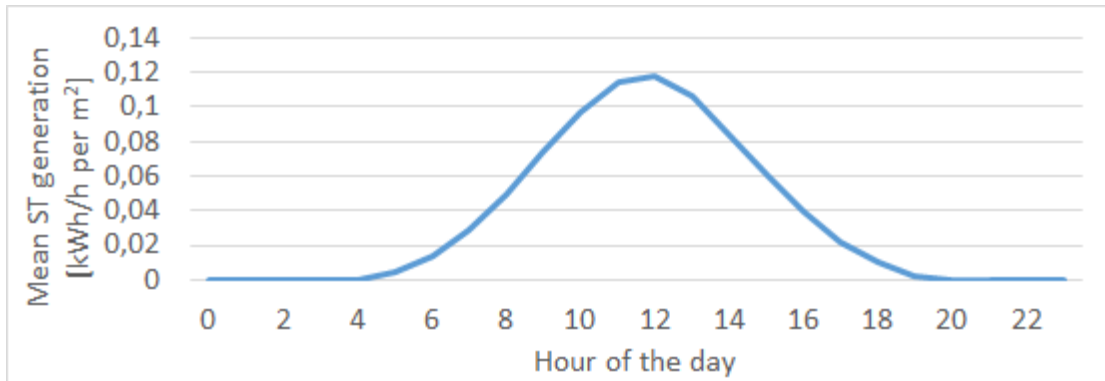


Figure 6.10: Hourly mean ST generation for one day

6.9.5 PV electricity generation

PV electricity generation is gathered from Renewables.ninja (2018), using the same values for latitude and longitude as for the ST profiles. The data set “CM-SAF SARA (Europe)” is however used, representing data gathered in Europe. System loss is set to 10%, whereas the tilt angle used is 41° and the azimuth angle 0° , as these values are seen as realistic values to represent a PV installation located in Elverum (European Commission, 2017b; Energikanalen AS, 2018). PV electricity generation is gathered for every hour from 2000 to 2014, and used as input for scenario generation, and further as a stochastic input parameters to the mathematical model.

Hourly PV generation is positively correlated with irradiation, as for ST generation, and one can therefore observe the same patterns as shown in Figure 6.9 and 6.10 for ST generation in the previous section.

Chapter 7

Scenario generation and evaluation methods

As the mathematical model presented in this thesis is stochastic, this chapter is meant to give the reader knowledge about how the stochasticity of the IMEZEN is dealt with through scenario generation, as well as evaluation methods used to analyze both the scenario generation algorithm and the value of stochasticity for the IMEZEN. An introduction to scenario generation will be given and the scenario generation algorithm developed in this thesis will be presented. Further, theory behind evaluation methods regarding the algorithm will be presented, as well as theory related to evaluation of the stochasticity. These test are further used in the computational study in Chapter 8.

7.1 Scenario generation

This section presents an introduction to scenario generation, as well as some theory on how the scenario generation method should be selected, in order to fit the respective stochastic data. Some literature regarding scenario generation is also reviewed, and lastly a discussion on which procedure that may be most applicable to our problem will be provided.

Stochastic programming relies on an adequate modeling of the uncertainties which is expressed through scenarios. This involves approximating random variables by a discrete distribution of a limited number of outcomes (Kaut and Wallace, 2007).

Note that these variables are not *decision* variables in the model, but rather input that may vary. The quality of the outcome from the optimization model is further heavily dependent on the scenario generation. As stated in Kaut (2003); a “*bad*” tree can lead to a “*bad*” solution. The term *tree* refers to a scenario tree.

Thus, scenario generation is of high importance in stochastic programming. One could even risk an infeasible computation without an approximation of distributions (Mitra, 2008). However, Høyland et al. (2003) state that scenario generation also seems to be the most challenging and time consuming in practice. The goal is to approximate in a way that provides a solution close to the true optimal solution without including too many outcomes, so the model can be solved in reasonable time (Kaut, 2006).

It is further important to find the best trade-off between a realistic and a simple mathematical model. A detailed model (with many scenarios) can result in a very complex problem, maybe even infeasible, as well as it increases the computation time. On the other hand, including few scenarios might provide a simple and insufficient image of the reality.

The main goal is to provide good solutions from the IMEZEN. There are different methods for generating scenarios, and as the quality of the generation is problem dependent, it is difficult to conclude whether a method is good or bad on a general basis (Kaut and Wallace, 2007). A high quality approximation is not equivalent to finding a statistical approximation. Kaut and Wallace (2007) state that some methods approximate distributions perfectly when the number of outcomes go to infinity, but may perform poorly with fewer outcomes. On the other hand, some methods do not guarantee convergence to the true distribution, but may still perform well for stochastic programming modeling purposes.

Some standard methods used are statistical methods, sampling and simulation approaches. Statistical methods involve determining statistical properties of a random variable such as moments to a distribution of data. Then, values of statistical properties can be used to find the best fitted theoretical distribution to a given data set, and be used to generate scenarios (Mitra, 2008). Sampling consists of sampling from either historical data or a fitted distribution, thus providing the scenario values. Simulation approaches provide scenario values by simulating an underlying stochastic process. This method uses random numbers as input to an equation, and the result, the realizations of the random variables, are then used as the scenario values. In addition to these methods, there do also exist hybrid methods which combine these standard types, e.g. by creating a mix of sampling and moment matching (Mitra, 2008).

7.1.1 Selection of method

Even though the scenario generation method is problem dependent, there are some criteria to go by when generating good scenarios. It is crucial to account for the dependencies between the random variables in the stochastic processes (Kaut, 2006). This is done by either assuming independence, or by using correlations or covariances. It is further essential to account for auto-correlations and seasonal variations within the data sets.

In Kaut (2006), it is stated that a good scenario generation should influence the solution as little as possible. In addition, the scenario based solution should converge to the *true* optimum with an increasing number of scenarios, and if fewer scenarios provide an equally good solution, the eliminated scenarios are redundant. The distance from the true distribution in the statistical sense is not as important.

Once having selected the scenario generation method, one should measure the quality of the method. Kaut and Wallace (2007) discuss how to evaluate methods and emphasize that the quality is based on the performance rather than the theoretical properties. Kaut and Wallace (2007) explain the evaluation methods *in-sample stability* and *out-of-sample stability*. These metrics are explained in section 7.2.1 below and are used to evaluate the selected scenario generation method in Chapter 8.

7.1.2 Literature regarding scenario generation

As the choice of method is problem dependent, it is interesting to investigate what methods that have been used in similar problems. The scenario generation methods in Skar et al. (2016), Seljom and Tomasgard (2015) and Arnesen and Borgen (2017) have been studied and a review of these will be given in this section.

In Skar et al. (2016) the year is divided into four seasons, while Seljom and Tomasgard (2015) and Arnesen and Borgen (2017) splits the year into twelve seasons, one for each month of the year. By dividing the year into seasons, they make sure possible seasonal effects are reflected in the scenarios. Similarly for all, the scenarios are constructed by randomly sampling sets of consecutive hours from the historical data, including one sample for each season. By using historical data, they avoid an incorrect assumption about the distribution of the stochastic process. Furthermore, since the same set of hours is sampled for all of the random variables, possible correlations between different variables are preserved. The

auto-correlation between hours *within* each profile is also kept, as each sample is a set of consecutive hours.

All of the methods rely on sampling from historical data. This is adequate under the assumption that the historical data for the random variables, in these cases weather and load data, are representative for the future. In addition, a high number of observations of weather data is often available, which is required for the direct use of historical data in scenario generation.

After a scenario tree has been constructed, the general idea in the methods studied has been to make sure the scenario tree generated fits the underlying historical data series with the use of moment matching. In Skar et al. (2016), the constructed scenario tree is simply checked to see that the sampled data profiles closely match the mean and variance of the respective underlying raw data series. In Seljom and Tomasgard (2015) several scenario trees are constructed and evaluated with moment matching, however only considering one random variable, wind data, for the evaluation. The trees are compared using a deviation measure, where the four first moments are normalized and equally weighted, and the “best fitted” tree is selected. Finally, the sampled data for the other random variable, price data, is included in the scenarios.

Arnesen and Borgen (2017) use an approach similar to Seljom and Tomasgard (2015). The main difference is that they evaluate and compare the constructed scenario trees seasonally, selecting one tree for each season, and then combining the parts from the selected trees into one final tree. They include two random variables, wind speed and irradiance, in the moment matching, while the last random variable, load demand, is included in the final scenario tree and simply checked for acceptable values of mean and variance. A final verification step is also performed, making sure the scenarios follow the same distribution as historical data.

7.1.3 Scenario generation method for the IMEZEN

This section presents and explains the scenario generation method developed during the work with what is enclosed in this thesis. The scenario generation method used for the IMEZEN includes aspects from Skar et al. (2016), Seljom and Tomasgard (2015) and Arnesen and Borgen (2017). First, the scenario generation algorithm is explained. This algorithm creates a scenario tree that represents a single year, resulting in an annual scenario sub-tree. Then, the technique used to assemble the final multi-horizon scenario tree for the IMEZEN is presented, where

the final scenario tree consists of several sub-trees.

The scenario generation algorithm

The input to the scenario generation algorithm is a set of pre-processed historical data series, one for each random variable. These are multi-annual hourly profiles for heat demand, PV generation, ST generation, electricity import prices, electricity export prices, and district heating import prices. For the electricity demand, only one hourly profile is included. The collection and pre-processing of these profiles are explained in section 6.9 in Chapter 6. An extra step of pre-processing is performed on the profiles for the heat and electricity demand. This is because the demand is dependent on which year in the time horizon of the model the scenario tree will represent as the neighborhood is expanded gradually.

The pseudo-code for the scenario generation algorithm is outlined in Algorithm 1. The method is an iterative random sampling method where the representation of one year is a collection of consecutive hours grouped into seasons to reduce the size of the scenario tree and thus the computation time. The year, more specifically each scenario, is divided into four regular seasons and two shorter peak seasons which account for extreme load situations, similar to Skar et al. (2016). In this case, each regular season is represented by 168 hours, a full week. This way we obtain auto-correlations not only between hours, but also between days, and we capture the weekly variations. The seasonal variations are also captured when the year is divided into seasons. It is however important to emphasize that this method assumes independence between the seasons. The possible correlations between the different variables are captured when choosing the same historical hours for every random variable.

For each regular season $s \in \{1, 2, 3, 4\}$, line 1 to 14, the algorithm will begin by calculating the four first moments of the historical data series, as defined by the second line. This is done separately for each random variable r , only including the values corresponding to season s . The creation of a single seasonal sub-scenario ω , line 7 to 10, is done by sampling. First, a day d' is randomly selected from the set of days in season s , denoted by D_s . The first hour of day d' , hour 00:00-01:00, is the first hour in the sample. The sample consists of $|O_s|$ consecutive hours, given by the number of operational periods in season s , in this case 168 hours. Additionally, a year k' is randomly selected from the set of years with historical data, K . Then, data is collected for each random variable r , corresponding to the sample defined. Since the historical electricity demand only has one hourly profile, the data sampled for this random variable will only be defined by the set of hours

and not the randomly selected year.

This process is repeated until a pre-defined number of seasonal sub-scenarios, $|\Omega|$, has been generated. The set of seasonal sub-scenarios thus represents one seasonal scenario sub-tree, u . In line 12, the four first moments is calculated for the seasonal sub-tree u for each random variable r , where each calculated moment m is given by $moment_{urm}^{tree}$. In line 13, the deviation in statistical moments between the seasonal scenario sub-tree u and the underlying historical data is calculated by

$$deviation_u = \sum_{r \in R} \sum_{m \in M} \left| \frac{moment_{rm}^{hist} - moment_{urm}^{tree}}{moment_{rm}^{hist}} \right|, \quad (7.1)$$

where R is the set of random variables, $M = \{1, 2, 3, 4\}$ is the set representing the four first moments, and $moment_{rm}^{hist}$ is the historical moment m calculated for random variable r . Note that the deviation for each moment m and random variable r is normalized, and that the total deviation for the seasonal scenario sub-tree, $deviation_u$, is the sum of all normalized deviations.

After a pre-defined number of seasonal sub-trees, $|U|$, have been generated, the tree with the lowest deviation, u'_s , is selected as the seasonal scenario sub-tree representing season s . In line 17, after selecting the “best fitted” tree for every regular season, the selected seasonal scenario sub-trees are merged into one scenario tree. Assuming independence between seasons, the seasonal scenario sub-trees are merged randomly, meaning each sub-scenario in one seasonal sub-tree is connected to a randomly chosen sub-scenario from another seasonal sub-tree. Finally, two extreme seasons, $s \in \{5, 6\}$, are added to each scenario in the merged scenario tree, where each extreme season consists of 48 hours. The idea behind including extreme seasons is to ensure that the energy system is capable of meeting peak demand.

The process of adding the first extreme season, based on peak heat demand, is defined by lines 21 to 24. In line 21, a year k' is randomly selected from the set of years with historical data, K . Then, the hour with the maximum heat demand is selected from the hourly profile for year k' . The sample representing this extreme scenario is from this defined as an interval of hours, with the maximum hour h' placed in the middle of the sample. The length of the interval is defined by $|O_s|$, the number of operational periods in the first extreme season. Data for each random variable r is then included in scenario ω .

Algorithm 1 Scenario generation algorithm

```

1: Input: Pre-processed historical data series for each random variable  $r$ 
2: Output: A scenario tree matching the underlying historical data
3: for all regular seasons  $s \in \{1, 2, 3, 4\}$  do
4:   Calculate the four first moments of the historical data for each random
   variable  $r$ 
5:   for all seasonal scenario sub-trees  $u \in U$  do
6:     for all seasonal sub-scenarios  $\omega \in \Omega$  do
7:       Select a random day  $d'$  from  $D_s$ 
8:       Create a sample of  $|O_s|$  consecutive hours, starting from the first hour
       of day  $d'$ 
9:       Select a random year  $k'$  from  $K$ 
10:      Populate sub-scenario  $\omega$  with sample data for each random variable  $r$ 
11:     end for
12:     Calculate the four first moments of seasonal scenario sub-tree  $u$  for each
     random variable  $r$ 
13:     Calculate the deviation from the historical data using moment matching
14:   end for
15:   Select the seasonal scenario sub-tree  $u'_s$  from  $U$  with the least deviation
16: end for
17: Merge the seasonal scenario sub-trees,  $u'_s$ , selected for each season  $s$ , into one
   scenario tree
18: for all scenarios  $\omega \in \Omega$  do
19:   for all extreme seasons  $s \in \{5, 6\}$  do
20:     if  $s = 5$  then
21:       Select a random year  $k'$  from  $K$ 
22:       Select maximum hour  $h'$  from historical heat demand data of year  $k'$ 
23:       Create a sample from interval  $[h' - (|O_s|/2), h' + (|O_s|/2) - 1]$ 
24:       Populate scenario  $\omega$  with sample data for each random variable  $r$ 
25:     else
26:       Find all maximum hours from historical electricity demand data
27:       Select a random hour  $h'$  from list of maximum hours
28:       Create a sample from interval  $[h' - (|O_s|/2), h' + (|O_s|/2) - 1]$ 
29:       Select a random year  $k'$  from  $K$ 
30:       Populate scenario  $\omega$  with sample data for each random variable  $r$ 
31:     end if
32:   end for
33: end for

```

The second extreme season is based on peak electricity demand. As the historical electricity demand only has one hourly profile, the sampling is somewhat different from the method used for the first extreme season. After analyzing the electricity demand, the cyclic nature of the hourly profile was revealed, resulting in the discovery that a number of hours had the maximum value. For this reason, the process of creating the second extreme season, line 26 to 30, begins by finding all the hours having the maximum electricity demand. From this, a hour h' is randomly selected. This hour is then placed in the middle of the sample interval, similar to the execution in line 23. Before adding data for each random variable r to scenario ω , a year k' is randomly selected as the historical year from which the data is collected.

Note that the moments are calculated across all hours and sub-scenarios within a season. An alternative way is the method used in (Arnesen and Borgen, 2017), where moments are calculated separately for *each* hour across all scenarios within a season.

Assembling the multi-horizon scenario tree

This subsection aims to discuss and justify the technique used for assembling the multi-horizon scenario tree for the IMEZEN, considering what might be most applicable to the model and the stochastic input data used in this thesis.

In Skar et al. (2016) and Arnesen and Borgen (2017), the same scenario tree is used for all investment periods in the entire time horizon of the model, which basically implies that all years are represented by the same set of scenarios. This has recently been changed in EMPIRE, by instead creating a different representative annual scenario tree for each investment period, meaning that only the five years within the same investment period are assumed represented by the same set of scenarios. An argument for choosing this approach could be that in the case of the IMEZEN being used as a module in EMPIRE, applying the same level of granularity would be sufficient.

On the other hand, an important aspect of the IMEZEN is the inclusion of the gradual development of a neighborhood. E.g. in the case of Ydalir, the area is developed incrementally, building new houses every year throughout the development period, and thus increasing the electricity and heat demand annually. Thus, if a representative annual scenario tree for each investment period was to be used for the case of Ydalir, the annual size increments of the neighborhood could not be included.

In order to include the development aspect, a different annual scenario sub-tree can be created for each year in the investment period. The scenario tree representing an investment period would then consist of five different annual scenario sub-trees, one for each year in the investment period. This would essentially increase the number of operational periods in an investment period scenario, as this scenario would consist of the operational periods in five different years, instead of repeating the same operational periods five times. In order to make the model more realistic and relevant for decision makers, including a larger variation of operational periods and incorporating annual developments is important. At the same time, this choice will not exclude the possibility of using the IMEZEN as a module in EMPIRE, provided that the run time is kept under a certain level.

The technique selected for assembling the multi-horizon scenario tree for the IMEZEN consists of creating a different scenario tree for each investment period. These investment period scenario trees are created by generating a annual scenario sub-tree, using the scenario generation algorithm presented, for each of the five years in the investment period. Then, the annual scenario sub-trees are merged together into one investment period scenario tree. When merging together the annual scenario sub-trees, each scenario in one annual sub-tree is connected to a randomly chosen scenario from another annual sub-tree. This is done randomly in order to make sure none non-existing dependencies are imposed on the relationship between years, hence assuming there are no correlation between years. E.g. if a scenario for one year has very high electricity prices, the electricity prices in the following year are uncorrelated. This is similar to the approach used in the scenario generation algorithm when creating a annual scenario sub-tree by merging together seasonal sub-trees. Finally, when a scenario tree has been created for all investment periods, the assembled multi-horizon scenario tree is used as input to the IMEZEN.

7.2 Evaluation of the scenario generation method

This section will provide different evaluation methods that may be performed to identify the stability of the scenario generation algorithm and the value of modeling stochastic rather than deterministic. First, two stability tests will be explained, followed by some short theory of the expected value of perfect information and the value of the stochastic solution.

7.2.1 Stability of the algorithm

This subsection presents in-sample and out of sample stability testing. The main goal of scenario generation is to procure a small optimality gap. The ideal method to evaluate the scenario generation method is thus to test the optimality gap and by this test if the scenario-based solution is optimal and not suboptimal (Kaut and Wallace, 2007).

If we define the true random vector as $\tilde{\xi}$ and the random scenario tree as $\hat{\xi}$, then the error of approximating the random vector $\tilde{\xi}$ by $\hat{\xi}$ is defined by

$$e(\mathbf{F}, \hat{\mathbf{F}}) = \dots = \mathbf{F}(\hat{\mathbf{x}}^*) - z^* \quad (7.2)$$

where \mathbf{F} is the true objective function, $\hat{\mathbf{x}}^*$ is the optimal solution of the approximated problem, and z^* is the objective value of the true problem.

However, it is often difficult or impossible to test this property as it requires solving the optimization problem with the *true* random vector. As this is not possible in most practical problems other weaker requirements such as *stability* is used to evaluate the quality of the scenarios.

Kaut and Wallace (2007) state that when evaluating scenario generation methods, the focus should be on whether the method provides stable solutions rather than how well it approximates the underlying stochastic process. Further, it is presented two requirements that are used to test if the generation method is stable; *In-sample Stability* and *Out-of-sample Stability*.

In-sample stability

In-sample stability requires that regardless of which scenario tree used, generated by the same data and with the same setting, the objective value of the stochastic problem stays approximately the same. Without in-sample stability the results are random and we can not verify the quality of the results.

In practice, this stability test is done by generating k scenario trees $\hat{\xi}_k$ provided by the same scenario algorithm with the same input and settings. For each $\hat{\xi}_k$ the optimization problem is solved and the optimal solution \hat{x}_k^* is obtained. The stability requirement is then

$$\hat{\mathbf{F}}_k(\hat{\mathbf{x}}_k^*) \approx \hat{\mathbf{F}}_l(\hat{\mathbf{x}}_l^*) \quad (7.3)$$

where $\hat{\mathbf{F}}$ is the approximated problem.

Out-of-sample stability

Out-of-sample stability requires that the real performance of the solution is not dependent on which scenario tree that is used. In other words, when solving the stochastic programming problem with different scenario trees, $\hat{\xi}_k^*$, generated from a random vector, $\tilde{\xi}$, one should get approximately the same value as the value of the true objective function:

$$\mathbf{F}(\hat{\mathbf{x}}_k^*) \approx \mathbf{F}(\hat{\mathbf{x}}_l^*) \quad (7.4)$$

However, when using this definition of out-of-sample stability, the true objective function $\mathbf{F}(x)$ needs to be evaluated, and as mentioned earlier, this is often impossible in practical problems. Thus, when testing for out-of-sample stability, one would use a weaker form of this requirement using the approximated problem $\hat{\mathbf{F}}$.

If we have two scenario trees $\hat{\xi}_k$ and $\hat{\xi}_l$ and their respective optimal solutions $\hat{\mathbf{x}}_k^*$ and $\hat{\mathbf{x}}_l^*$, then a stable method will meet the requirements

$$\hat{\mathbf{F}}_k(\hat{\mathbf{x}}_k^*) \approx \hat{\mathbf{F}}_k(\hat{\mathbf{x}}_l^*) \quad (7.5)$$

$$\hat{\mathbf{F}}_l(\hat{\mathbf{x}}_l^*) \approx \hat{\mathbf{F}}_l(\hat{\mathbf{x}}_k^*) \quad (7.6)$$

and finally

$$\hat{\mathbf{F}}_k(\hat{\mathbf{x}}_l^*) \approx \hat{\mathbf{F}}_l(\hat{\mathbf{x}}_k^*) \quad (7.7)$$

This means that the objective function stays approximately stable when we use a different sample than was used for finding the solution.

In practice, the stability test is done by generating k scenario trees $\hat{\xi}_k$, then solving the problem with each one of them, and obtaining optimal solutions $\hat{\mathbf{x}}_k^*$ for $k = 1 \dots k$, and finally, using Requirement 7.7 to evaluate stability.

Kaut and Wallace (2007) focus on the importance of both in-sample and out-of-sample stability. They state that stability tests should always be run, starting with the in-sample test and then running some out-of-sample tests, if feasible. Note that having in-sample stability without out-of-sample stability would mean that the real performance of the solution is dependent on the scenario tree used. Having out-of-sample stability means that the real performance of the optimal first-stage solution is stable and does not depend on the scenario tree used, but without also having in-sample stability one would not know how good the solutions really are.

7.3 Value of stochasticity

This subsection presents how one can evaluate the value of stochastic modeling. When modeling we strive to include the important aspects of the problem, and leave out the ones that are considered less important. Most real problems are affected by randomness, but if one choose to include this randomness in the model, it will lead to a model much more computationally challenging to solve than their deterministic counterpart (Kall and Wallace, 2003). Based on this, it is valuable to discuss if the randomness is one of the less important aspects in our problem, i.e. determine whether the more simpler versions provide solution near optimality or if they are incorrect. The real value of solving more difficult programs can be found through the *expected value of perfect information* (EVPI) and the *value of the stochastic solution* (VSS) (Birge and Louveaux, 2011).

EVPI

EVPI gives the maximum amount the decision maker is willing to pay for a complete information about the future (Birge and Louveaux, 2011), and is defined as the difference between the *wait-and-see solution* (WS) and the *recourse problem* (RP) solution:

$$EVPI = RP - WS \tag{7.8}$$

RP is the objective value of the stochastic problem, and WS is the expected value when solving all scenarios as independent deterministic problems (Birge and Louveaux, 2011).

VSS

VSS gives the expected value of planning with uncertainties compared to the deterministic counterpart (Birge and Louveaux, 2011), and is defined as the difference between the *expected result of using the expected value solution* (EEV) and the RP:

$$VSS = EEV - RP \quad (7.9)$$

The expected value solution is obtain from solving the *expected value problem* (EV), which is the problem where all random variables in the stochastic program are replaced with their expected values.

Alternative measures of the quality of the deterministic solution

The *VSS* is often used to show how important it is to use a stochastic model. However, if the model has hard constraints, one will often find that the *VSS* is ∞ . This happens if the problem becomes infeasible when calculating the expected cost of the deterministic solution. At the same time, the expected cost of using the deterministic solution can be arbitrarily bad with the use of soft constraints by setting high penalties (Wallace, 2011). In these situations one will not really know whether the deterministic solution provides useful information for the stochastic setting. For this reason, some alternative measures are included, as defined in Maggioni and Wallace (2012).

First, a measure of the structure of the deterministic solution is introduced, denoted as *Test B* in Maggioni and Wallace (2012). This measures the *loss of using the skeleton solution* (LUSS), and is defined as the difference between the *expected skeleton solution value* (ESSV) and the RP:

$$LUSS = ESSV - RP \quad (7.10)$$

The *ESSV* is obtained by fixing all first stage variables which are at zero, or at the lower bound, in the expected value solution and then solving the stochastic program.

Secondly, a measure of the upgradeability of the deterministic solution is introduced, denoted as *Test C* in Maggioni and Wallace (2012). This measures

the *loss of upgrading the deterministic solution* (LUDS), and is defined by the difference between the *expected input value* (EIV) and the *RP*:

$$LUDS = EIV - RP \quad (7.11)$$

The *EIV* is obtained by considering the expected value solution as a starting point for the stochastic model, only allowing it to be upgraded, thus testing if the solution is upgradeable.

Chapter 8

Computational study

This chapter provides an evaluation of the performance of the IMEZEN and the scenario generation algorithm proposed in this thesis. First, the hardware and software used when running the model is described, as well as the solver settings applied. Then, the results from the stability testing and the value of stochasticity will be presented and analyzed.

The *base case* used in this computational study is solved using the IMEZEN as formulated in section 5.4 in Chapter 5. Recall that ramping of the HS, maximum PV and ST areas and maximum electricity and DH grid constraints are not included in the base case. The base case is further defined by a degree of 100 % ZEN and the use of carbon emission factors. The level of ZEN used is ZEN-O, excluding weighted embodied energy in materials. In addition, the neighborhood is connected to a DH grid and the investment time horizon is set to 30 years. From the stability test results, an applicable number of scenarios will be selected and be part of the base case further used in this thesis.

The choice of using carbon emission factors is made on the basis that these are the most widely used factors in Norway and because their values are gathered from local references. The degree of 100 % ZEN is chosen since this is the desired goal. The length of the time horizon is selected on the basis of the planning horizon in EMPIRE, which is until 2050. Also, the length of the time horizon will include both the development period of Ydalir, as well as a period of 15 years after the neighborhood is completed. The other input parameters are described in Chapter 6. Test cases that deviates from the base case will be specified.

8.1 Hardware and software

This computational study has been performed on an Intel ®Core™i7-7700 CPU processor at 3.60 GHz and 32 GB RAM with operating system Windows 10 Education 64-bit. The software used is FICO ®Optimizer Suite with Xpress-IVE Version 1.24.18 64-bit, Xpress Mosel version 4.6.0 and Xpress optimizer version 31.01.09.

8.2 Solver settings

Initial testing showed that the computation time of the IMEZEN was highly dependent on the algorithm used when solving the linear program in Xpress. The default setting is that the selection of the algorithm will be automatically determined by the Optimizer, which is often sufficient for most users of commercial optimization software. However, in large problems, as is the case for the IMEZEN, it can be a lot to gain from customizing the solution procedure.

The selection of algorithms for solving the linear program in Xpress consists of *dual simplex*, *primal simplex*, and *Newton barrier*. In order to determine the best algorithm to be used for the IMEZEN, some simple tests were performed on three different instances all using three scenarios, defined by the degree of ZEN applied. The results from these tests is shown in Table 8.1.

Table 8.1: Computation time using different algorithms in Xpress, given in minutes

ZEN degree	Dual simplex	Primal simplex	Newton barrier
0 %	125	28	3
50 %	3385	2728	18
100 %	7194	2306	27

It is clear from the results presented that there is a substantial gain in computation time when applying the Newton barrier algorithm, especially when the degree of ZEN is larger than 0 %. Therefore, this solver setting is used throughout this computational study and in the case study in Chapter 9.

8.3 Stability tests of the IMEZEN

The stability testing is a way of validating the scenario generation method. As the stability of the scenario generation method is problem dependent, the tests will only reveal the stability of the problem instance that is being tested. For the IMEZEN, a problem instance depends on a number of parameters. Changes in these parameters will change the optimal solution, and, as the tests consider the stability of the optimal solution, these changes can potentially have an impact on the stability. This implies that one can only trust that the problem instances that have been tested for stability actually produce stable results. Performing stability tests on all problem instances would be extremely time consuming and is not part of the scope for this master's thesis. For this reason, the stability tests will only be performed on a subset of the possible problem instances, focusing on the base case. Still, the more problem instances that prove to provide stable results, the more the scenario generation method can be trusted.

Another important aspect to consider is the number of scenarios included in the scenario tree. A high number of scenarios results in a large tree, thus increasing the computation time when running the optimization model as well as the stability tests. For this reason, the stability tests will be performed using scenario trees with an increasing number of scenarios. The results will then be evaluated to determine the number of scenarios that should be used for other parts of this computational study, considering which level of stability and computation time is satisfactory.

8.3.1 In-sample stability

In this section, the results from the in-sample stability testing of a number of relevant problem instances are presented. The focus is on instances defined by the base case, but with varying values of the ZEN degree. The tests are performed using an increasing number of scenarios. Note that the number of scenarios equals the number of scenarios in each investment period, and that a different scenario tree is generated for every investment period.

All problem instances tested are listed in Table 8.2. For each combination of a problem instance and a specified number of scenarios, ten full scenario trees are created using the scenario generation method explained in Chapter 7. Then, for each combination, the IMEZEN is solved ten times, one time for each scenario tree generated. The objective value is recorded each time, and for each set of ten runs, the coefficient of variation (CV) is calculated as the ratio of the standard deviation

to the mean (Investopedia, 2018a). The CV is used as it provides a measure of the degree of variation between the results from the different scenario trees, and can be used to compare this variability across the different sets. Thus, by evaluating the CV value, one can determine if $\hat{\mathbf{F}}_k(\hat{\mathbf{x}}_k^*) \approx \hat{\mathbf{F}}_l(\hat{\mathbf{x}}_l^*)$. Note that the fixed costs have been excluded from the objective function in these tests as they are the same for all combinations and would decrease the CV value erroneously if included.

Table 8.2: Problem instances tested for in-sample stability

Instance	Emission factor	ZEN degree	# of scenarios
Instance 1	-	0 %	1, 2, 3, 4, 5
Instance 2	Carbon	50 %	1, 2, 3, 4, 5
Instance 3	Carbon	100 %	1, 2, 3, 4, 5

The results from the in-sample stability testing is presented in Figure 8.1. The combinations with two scenarios have slightly higher CV values compared to other combinations for Instance 1 and 2, but all CV values calculated are below 2 %. This illustrates that the objective value variation is quite small in general. For Instance 2 and 3, the CV value is even below 1 % for all combinations having three or more scenarios. Thus, for all combinations tested, we conclude that there is in-sample stability in the objective function.

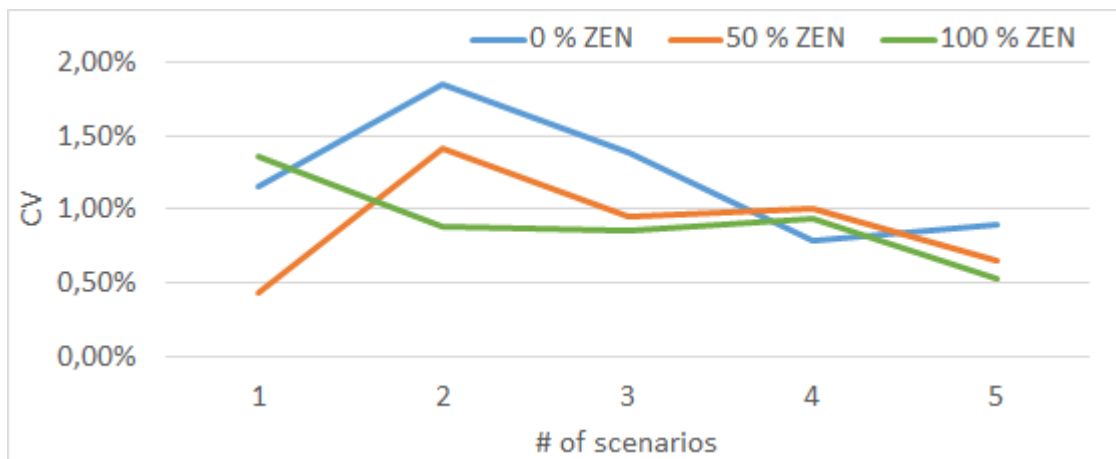


Figure 8.1: Average coefficient of variation [%] for all problem instance combinations

Note that the stability is also calculated for the case with a single scenario. This is valid as a scenario is created for each investment period, meaning the full scenario tree for the whole time horizon in fact consists of the same number of scenarios as there are investment periods. Thus, as the time horizon used is 30 years, which is equivalent to six investment periods, the combinations with a single scenario are actually solved with six different scenarios, one for each investment period.

Also note that, as most stochastic programming problems have a flat objective function (Kaut and Wallace, 2007), these results do not indicate in-sample stability of the *solutions*. A simple investigation of the first-stage solutions suggest that the composition of the energy technologies invested in are close to identical for different combinations of the same problem instance, but there is some variation in the size of the capacities installed in the different investment periods. Thus, a high level of out-of-sample stability can be expected, but this is not guaranteed.

The computation time will also be taken into account when deciding the number of scenarios that should be used for later evaluations. Figure 8.2 plots the average computation time, in minutes, for all problem instances, with the number of scenarios on the x-axis. For Instance 1, the computation time is almost the same for all combinations, explained by the fact that the ZEN constraint is not applied and this has a great impact on the computation time. For the other instances, the computation time increases with an increasing number of scenarios. The computational time ranges from around 1-2 minutes for a single scenario, to almost 90 minutes for five scenarios. This illustrates the great impact a small increase in the number of scenarios has on the computation time.

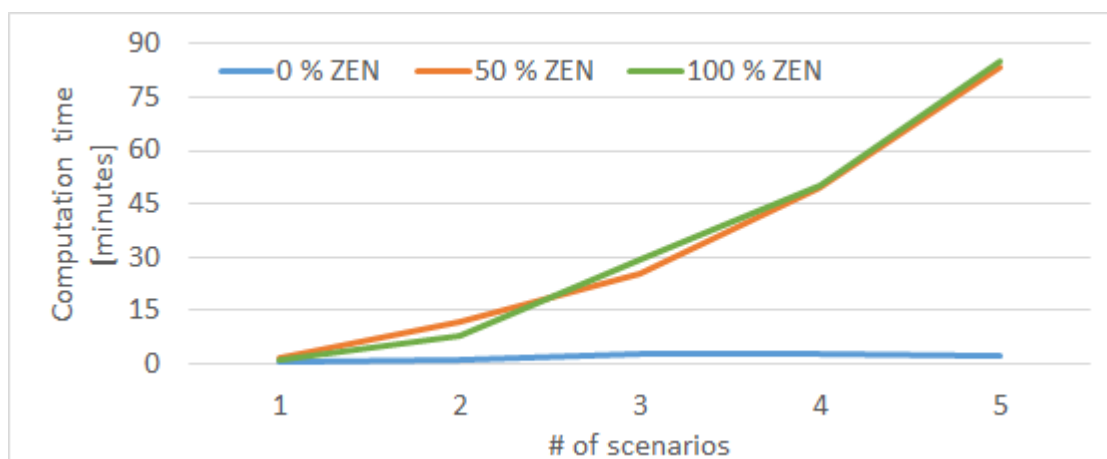


Figure 8.2: Average computation time [minutes] for all problem instance combinations

The in-sample stability testing indicates that the scenario generation method provides a satisfactory level of in-sample stability for all the combinations tested. This suggests that the number of scenarios does not impact the in-sample stability significantly. However, there are other reasons for why one would want to use a higher number of scenarios even if it increases the computation time. When investigating the average objective values for each combination, there is an observable tendency where the combinations with a low number of scenarios has lower objective values, especially the case with a single scenario. One might think that they provide better solutions, but in reality they are probably optimistic and underestimate the objective value. This is similar to what happens for deterministic problems (in the case of convex minimization), which always underestimate the actual expected cost (Birge and Louveaux, 2011). The observed tendency can be seen in Figure 8.3, where the the number of scenarios are represented on the x-axis and the y-axis is the objective value deviation from the average. The deviation is calculated as the average objective value for ten runs of the same combination, divided by the average of all 50 runs of the same problem instance. From this it is clear that the average objective values for each problem instance seem to stabilize when the number of scenarios used are three or more. This can indicate that three scenarios might be a good choice as it also is in-sample stable and the computation time is acceptable.

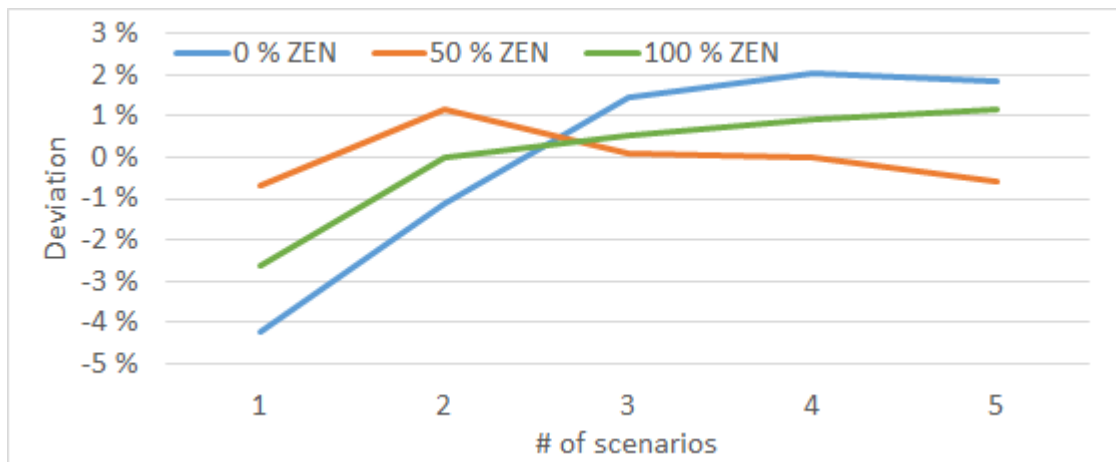


Figure 8.3: Average objective value deviation from problem instance average for each combination

8.3.2 Out-of-sample stability

After determining that the scenario generation method is in-sample stable, the next step is to evaluate its out-of-sample stability. The general idea behind the out-of-sample stability is to test a solution on a different scenario tree than the one used to find it, thus testing the real performance of the solution. The out-of-sample tests have been performed on all the same combinations of instances, number of scenarios, and scenario trees as the ones tested for in-sample stability. However, as the base case in this thesis is the problem instance with a ZEN degree of 100 %, only the results related to this instance will be presented and discussed.

In section 7.2.1 in Chapter 7, three requirements an out-of-sample stable method should meet are presented. The main requirement, $\hat{\mathbf{F}}_k(\hat{\mathbf{x}}_k^*) \approx \hat{\mathbf{F}}_l(\hat{\mathbf{x}}_k^*)$, requires one to perform pairwise tests on different scenario trees. Considering that we have created 50 scenario trees for each problem instance, this would require performing 1225^1 pairwise tests for each problem instance if all combinations are to be tested. As an alternative testing method, we have instead created a large reference tree with 100 scenarios on which all solutions will be tested, only considering the requirement given by $\hat{\mathbf{F}}_k(\hat{\mathbf{x}}_k^*) \approx \hat{\mathbf{F}}_l(\hat{\mathbf{x}}_k^*)$. The reference tree, l , is built using the same scenario generation method, generating 100 scenarios for each of the six investment periods. Then, for each combination and scenario tree k tested for in-sample stability, the first-stage solution, $\hat{\mathbf{x}}_k^*$, is used as fixed input for the reference tree, and the objective value, $\hat{\mathbf{F}}_l(\hat{\mathbf{x}}_k^*)$, is recorded. In order to determine whether the requirement is met, the relative difference between the objective values is calculated for each k as defined by Equation (8.1). The relative difference is given by the absolute deviation between the objective values divided by the average objective value.

$$\frac{|\hat{\mathbf{F}}_k(\hat{\mathbf{x}}_k^*) - \hat{\mathbf{F}}_l(\hat{\mathbf{x}}_k^*)|}{(\hat{\mathbf{F}}_k(\hat{\mathbf{x}}_k^*) + \hat{\mathbf{F}}_l(\hat{\mathbf{x}}_k^*))/2} \quad (8.1)$$

Then, for each combination tested for in-sample stability, the average relative difference of all the ten scenario trees tested is calculated. In addition, the objective values obtained by each solution on the reference tree, $\hat{\mathbf{F}}_l(\hat{\mathbf{x}}_k^*)$, is evaluated as a measure on the performance of the different combinations. The results for the combinations related to problem instances with a ZEN degree of 100 % are presented in Figure 8.4, where the x-axis shows the number of scenarios and the y-axis shows the relative difference. A secondary y-axis is also included, showing

¹ $\frac{50 \cdot (50-1)}{2}$

the average objective value obtained on the reference tree. It can be observed that both the relative difference and the average objective value decrease when the number of scenarios increase. This shows that the combinations with a high number of scenarios are more stable and perform better on the reference tree. However, the differences in both stability and objective value are very small for all combinations with more than a single scenario, indicating that they are all out-of-sample stable. It should be noted that the results for the other problem instances are a bit different, but that the stability measure is below 2.50 % for all combinations with two or more scenarios.

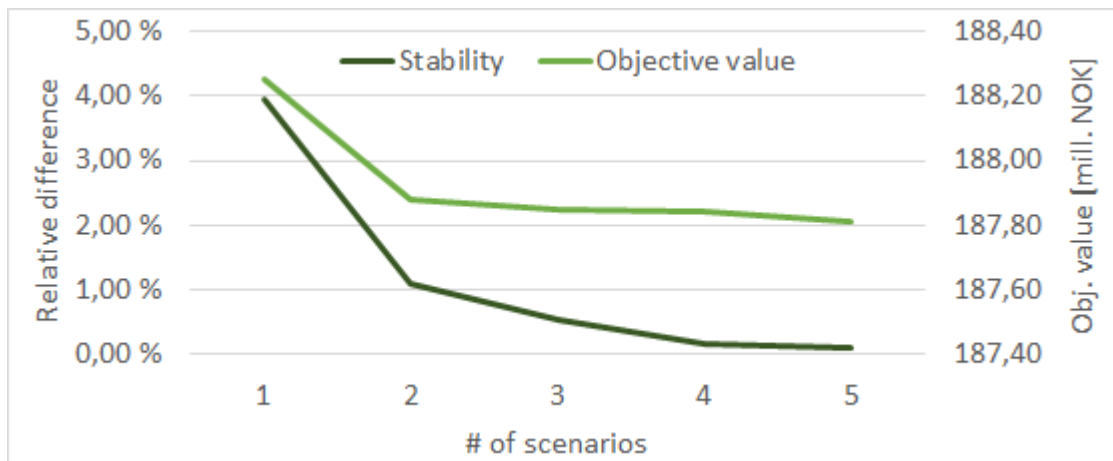


Figure 8.4: Relative difference using Equation 8.1 for all combinations with a ZEN degree of 100 %, as well as the objective value obtained on the reference tree

Considering the results from both in-sample and out-of-sample stability testing, there is no clear candidate with respect to the number of scenarios to use for later analysis in this computational study. Taking only the out-of-sample tests into account, the combinations with a single scenario are dismissed as candidates as they are significantly less stable than the other combinations. With regard to the other combinations, they have quite similar performances on both the in-sample and out-of-sample tests. However, the combinations using two scenarios did perform slightly worse than the others in the in-sample tests. For this reason, we have decided to use three scenarios for the remaining parts of this computational study. This is valid for the problem instances tested as there is extremely little to gain in stability performance from increasing the number of scenarios. Also, a computation time of about 30 minutes for the problem instances including the ZEN constraint is acceptable.

After deciding to use three scenarios, a set of supplementary out-of-sample tests have been completed. These tests are pairwise tests, included to make sure that

the results obtained in later analysis are not influenced by the scenario tree used. The tests are performed by taking the first-stage solution obtained from using one scenario tree, and then using this as fixed input when solving the problem for another scenario tree, and vice versa. The objective values obtained for each pair are recorded and their similarity evaluated. The tests are only performed on a subset of all possible pairs as the goal is simply to verify the out-of-sample stability results from using the reference tree. The relative difference is calculated for the five pairs tested and for all the three requirements related to the out-of-sample stability. The results for the problem instance with a ZEN degree of 100 % are shown in Table 8.3, only including the average values for the pairs tested. Note that the relative differences for all requirements are very low, implying a high level of stability. The results for the other problem instances are not presented, but it should be noted that these were satisfactory as well.

Table 8.3: Out-of-sample stability results from pairwise testing using 3 scenarios

ZEN degree	$\hat{\mathbf{F}}_k(\hat{\mathbf{x}}_k^*) \approx \hat{\mathbf{F}}_k(\hat{\mathbf{x}}_l^*)$	$\hat{\mathbf{F}}_l(\hat{\mathbf{x}}_l^*) \approx \hat{\mathbf{F}}_l(\hat{\mathbf{x}}_k^*)$	$\hat{\mathbf{F}}_k(\hat{\mathbf{x}}_l^*) \approx \hat{\mathbf{F}}_l(\hat{\mathbf{x}}_k^*)$
100 %	0.08 %	0.07 %	1.03 %

Hereafter, there will always be used scenario trees with three scenarios, also when testing or analyzing other problem instances. As mentioned, performing stability tests on all problem instances used would be extremely time consuming. Therefore, we assume that, as the scenario generation method has been tested on several different problem instances and combinations and proved to be very stable, this will probably also be the case for other problem instances.

8.4 Value of the IMEZEN

In this section the value of stochasticity related to the IMEZEN will be tested. The tests are related to the theory presented in section 7.3 in Chapter 7.

8.4.1 EVPI

The structure of the multi-horizon model assumes independence between the investment periods, and therefore no connection between scenarios in consecutive periods. However, the process of obtaining the WS involves solving all scenarios

as independent deterministic problems, which further implies that the simplicity of the structure is eliminated, as all possible combinations of scenarios in the multi-horizon model have to be tested. Thus, in this case, calculating the WS indicates solving 3^6 (729) independent problems. This is extensive work, and may also be computationally demanding.

In light of this complexity, one could also discuss the *relevance* of the $EVPI$ for the IMEZEN. In practice, one can say that the $EVPI$ provides a value of how much a better forecasting technology is worth when solving the problem. For the IMEZEN, this would require forecasting the spot price, weather conditions, and the heat and electricity demand. Here, one can argue that particularly the weather conditions, which are used as a basis for several stochastic parameters, are subject to an external uncertainty that is hard to eliminate regardless of the forecasting method.

Considering the limited opportunities for perfect information as well as the complexity of obtaining the WS , we have decided not to analyze the $EVPI$ in this thesis. Instead, other measures have been investigated and discussed to a larger extent.

8.4.2 VSS

The VSS of the IMEZEN is calculated for three different problem instances, differentiated by the degree of ZEN used. The instances are otherwise equal to the base case. One scenario tree is used for all tests as the scenario generation method proved to be satisfactory stable for these problem instances. The scenario tree used is generated with three scenarios in each of the six investment periods. Note that the fixed costs have been excluded from the objective function in these tests as they are the same for all instances and we want to evaluate the difference in the variable costs.

When calculating the EEV , one first has to obtain the solution from solving the EV problem. In order to solve the EV problem, all random variables have to be replaced by their expected values. Recall that the scenarios in the stochastic problem are created to represent one investment period consisting of five years, where each year consists of four regular seasons with 168 operational hours each and two extreme seasons with 48 operational hours each. As the structure of the IMEZEN is based on the assumption of seasonal variation, this should also be considered when calculating the expected values. However, a representation of the extreme seasons is not included as extreme values in themselves are not

representative expected values. Instead, the expected value of each of the 168 operational hours in each of the four regular seasons are calculated, resulting in 672 ($168 \cdot 4$) expected values representing one year in the investment period. In order to also include the development aspect of the IMEZEN, the expected values are calculated for every year of the development period, reflecting the expected annual increase in heat and electricity demand from the increase in the size of the neighborhood. The results for the three instances tested are presented in Table 8.4.

Table 8.4: VSS for the IMEZEN, calculated for three problem instances

ZEN degree	EEV	RP	VSS	Δ
0 %	67 900 602	67 535 284	365 319	-0.54 %
50 %	Infeasible	89 814 408	N/A	N/A
100 %	Infeasible	186 230 641	N/A	N/A

For each instance, the table lists the ZEN degree used, the *EEV* obtained, the *RP*, the *VSS*, and the change in the objective value when going from the *EEV* to the *RP*. The *RP* obtained for the instance with a ZEN degree of 0 % shows a relatively small improvement of 0.54 %. This is not very surprising when considering that the scenarios generated are based on moment matching with historical data, which is similar to the idea behind the calculation of the expected values of the random parameters. The extreme seasons are however not reflected in the expected values, an aspect that potentially can lead to an undersized or inflexible solution. This might be the main reason for the improvement, but as the extreme seasons are weighted with a small value in the objective solution, it does not affect the *EEV* negatively to a large extent. An undersized or inflexible energy system is therefore not expected to perform very badly in the case where one only has to cover demand, as one always has the possibility of importing both heat and electricity from the respective grids at an acceptable cost. But, in situations where the ZEN constraint is applied, we expect that the impact from having an undersized or inflexible system will be greater. For the problem instances tested with a ZEN degree of 50 % and 100 %, the *EEV* could not be calculated as the problems were infeasible. As mentioned in section 7.3 in Chapter 7, this is typical for stochastic problems that have a hard constraint, which is the case for the IMEZEN. One might say that the corresponding *VSS* for these instances thus is ∞ , but this does not provide any real information about the quality of the deterministic solution.

In order to evaluate the *VSS*, the ZEN constraint is transformed into a soft constraint (as explained in section 5.2 in Chapter 5), and the penalty cost is set to

a high value. This reflects that not fulfilling the ZEN constraint should be a last resort and not a realistic option. The value is arbitrarily set to 1 NOK/g_{CO₂-eq}, only making sure that the *RP* does not change its optimal solution and objective value. The results from using the IMEZEN with a soft ZEN constraint for the three instances tested are presented in Table 8.5.

Table 8.5: VSS for the IMEZEN with penalty, calculated for three problem instances

ZEN goal	EEV	Penalty	Achieved	VSS	Δ
0 %	67 900 602	-	0.00 %	365 319	-0.54 %
50 %	128 472 035	35 296 463	47.26 %	38 657 627	-30.09 %
100 %	242 010 699	63 394 546	95.07 %	55 780 059	-23.05 %

The *RP* is not included in the table as this is the same as listed in Table 8.4. Instead, the penalty cost from solving the *EEV* is listed, as well as the ZEN degree achieved. The *EEV* of the first instance is the same as previously because the penalty is only related to the ZEN constraint, which is not imposed for this instance. For the other two instances it is interesting to observe the ZEN degree achieved by the deterministic solution in the stochastic setting. This can provide some information with regard to how large a buffer one should include when solving the *EV*, if one wants to avoid solving the stochastic problem. In this case, a buffer of about 5 % seems reasonable in order to account for its tendency to underestimate. This is however specific for these problem instances and not guaranteed to work for other instances. Note that the improvement obtained by using the *RP* is quite high, about 30 % and 23 %, but that the interpretation of these values are closely related to the choice of penalty cost. As mentioned in section 7.3 in Chapter 7, one can make the *VSS* take an arbitrarily high value by setting a high penalty cost. As the penalty cost in this case is not intended to reflect the reality, the concrete *VSS* is not discussed. However, in cases where the ZEN constraint in reality should be fulfilled, meaning the actual penalty cost is high, these results strongly suggest that the *VSS* is high and thus is worth the effort of solving the stochastic problem.

The results presented suggest that the *VSS* is high, but, as mentioned in section 7.3 in Chapter 7, this does not tell us a lot about the quality of the deterministic solution or *why* the *VSS* is high. Therefore, the *LUSS* and *LUDS* will be calculated and discussed.

8.4.3 LUSS

This is a measure of the *loss of using the skeleton solution*, providing an evaluation of what the deterministic solution does wrong. The *LUSS* has been calculated for the same three instances as the ones used for the *VSS*, also using the same scenario tree, and the results are presented in Table 8.6. The *RP* is the same as before and is not included in the table, but its computation time is listed. Note that the computation time listed for the *ESSV* is the total computation time for solving both the *EV* problem and the *ESSV*.

Table 8.6: LUSS for the IMEZEN, calculated for three problem instances

ZEN degree	ESSV	LUSS	Δ	ESSV [sec]	RP [sec]
0 %	67 535 339	54.97	0.00 %	44	185
50 %	89 814 408	0.00	0.00 %	691	1 029
100 %	186 230 641	0.00	0.00 %	1 0120	1 590

From the table it is observed that the *LUSS* is zero or close to zero for all three instances tested. This indicates that the choice of variables in the deterministic solution is good, but that their values are wrong. In this case this means that the technologies chosen in the deterministic solution are the same as those chosen in the *RP*, but that the capacities installed in different periods are different. The reason why the *LUSS* is above zero for the first instance is that the stochastic problem installs a very small gas boiler in one investment period while it is not included in the deterministic solution, making the resulting *ESSV* barely above the *RP*. These results are only tested on a subset of the possible problem instances, but they imply that the structure of the deterministic solution can be very useful. An alternative to solving the IMEZEN to obtain the optimal solution could therefore be to solve the deterministic problem to find which technologies should be included, and then solve the stochastic problem to decide the capacities that should be installed of the technologies in the different investment periods. This is the reason why the computation time for these two alternatives has been included in Table 8.6, showing that one can save some time and still obtain an optimal solution by using the structure of the deterministic solution. It should however be noted that the computation time listed for the *ESSV* is only a sum of the computation time used to solve both problems, and some overhead might be expected related to the process of reusing the solution from the deterministic problem. But, it might be an alternative to consider using the skeleton solution in cases where a more complex problem is solved. This can be applicable to situations where it is necessary to include some of the constraints left out from the base case. An

example is the inclusion of the maximum limit of the area available for PV and ST. This increases the complexity of the problem, but is only necessary in some cases. This is however not investigated further.

8.4.4 LUDS

This is a measure of the *loss of upgrading the deterministic solution*, providing an evaluation of the upgradeability of the deterministic solution. The *LUDS* has been calculated for the same three instances as the ones used for the *VSS* and the *LUSS*, also using the same scenario tree, and the results are presented in Table 8.7. The *RP* is the same as before and is not included in the table.

Table 8.7: LUDS for the IMEZEN, calculated for three problem instances

ZEN degree	EIV	LUDS	Δ
0 %	67 819 816	284 532	-0.42 %
50 %	91 969 556	2 155 149	-2.34 %
100 %	186 668 480	437 839	-0.23 %

For all instances tested we have that $0 < LUDS < VSS$, implying that the deterministic solution is partially upgradeable. This means that the solution is upgraded from the deterministic solution, but it is not as good as the *RP*. The upgrade does not result in an optimal solution, but it will provide feasible solutions, which is an important improvement from the deterministic solution. But, as the *VSS* for two of the instances were not obtained due to infeasibility, it is difficult to evaluate the value of the upgrade. It should be noted that the computation times are not listed, but that they are comparable to the case of the *ESSV*.

Still, as the *LUDS* for all instances tested are relatively low, it can be interesting to discuss the possibility of using the deterministic solution as a lower bound for the stochastic solution. This will not be investigated in this thesis, but is only mentioned as an interesting aspect.

Chapter 9

Case study – Ydalir

In this chapter, a case study on the pilot project Ydalir is performed, in addition to a practical analysis of the model to verify its applicability to other real cases. First, the case study will be performed for the base case, as well as the other included emission factors. Subsequently, a practical analysis will follow, where the model's sensitivity with regard to changes in certain parameters will be identified. The model will also be tested for different types of neighborhoods, where the availability of different technologies will be restricted in one or another way. Lastly, the value of thinking ZEN rather than ZEB will be evaluated, by testing the model for both a ZEN and a neighborhood consisting of independent ZEBs. The characteristic of the chapter is that results followed by corresponding discussions will be presented continuously within the different sections.

9.1 The base case

In this section, the base case is tested. First, results from testing the base case with different degrees of ZEN will be presented, and the main tendency of the investment decisions will be discussed. Further, results showing the operational behaviour will also be discussed.

Figure 9.1 shows the sum of installed capacities of the different technologies over the entire investment time horizon, for an increasing degree of ZEN. The objective values representing the total costs are also plotted, using the secondary y-axis of the graph. Note that the installed capacity of the heat storage is given in kWh.

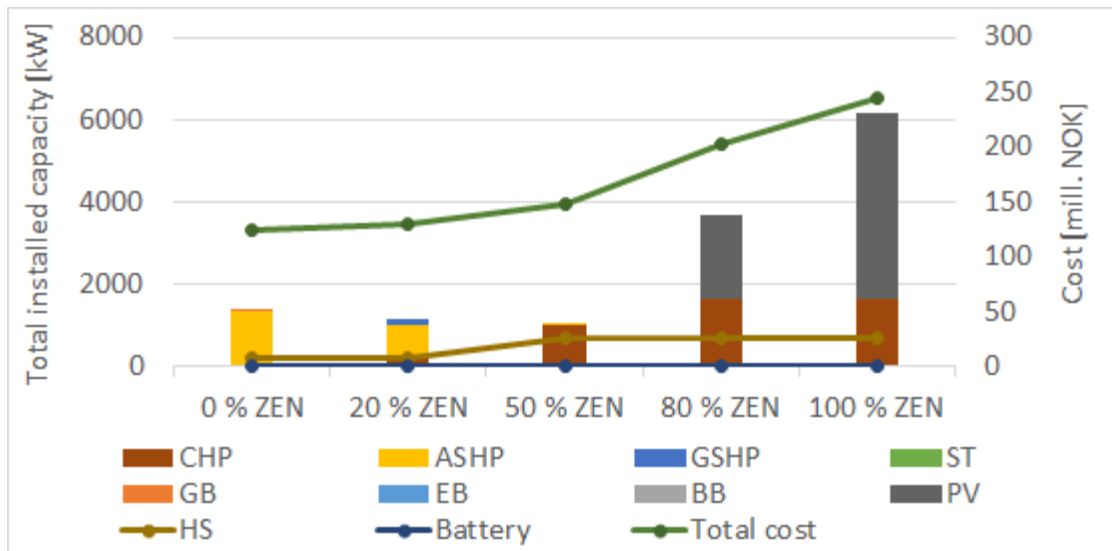


Figure 9.1: Total installed capacities and costs for increasing degree of ZEN, using carbon factors

For 0 % ZEN, ASHP and small amounts of GB are installed. Further, one can observe a tendency where a higher degree of ZEN leads to higher installed capacities of CHP and PV. A small amount of GSHP is also installed for 20 % ZEN.

This result seems logical as the heat pump has a high efficiency and thus generates heat at a relatively low cost, only consuming a small amount of electricity. However, as the value of the carbon factor for electricity is high, the investment decision shifts toward a more environmental friendly solution as the degree of ZEN increases, replacing the use of the heat pump as heat technology with the CHP. The CHP has a high investment cost, but is preferred as it consumes wood chips, which has a lower weighting than electricity.

Figure 9.1 also shows that the installed capacity of the HS is relatively stable for 0 - 20 % ZEN, increases between 20 % and 50 % ZEN, and then stabilizes again from 50 % ZEN. This coincides with larger investments in the CHP, and it is clear that bio fuel becomes the most dominant resource in the energy system when the degree of ZEN increases.

Another observation that can be seen in Figure 9.1 is that the total costs have a relatively linear increase from 0 - 50 % ZEN, and also from 50 - 100 % ZEN, whereas the slope is much steeper for the latter. This is as expected as an increase

in the degree of ZEN will reduce the solution space, implying that the objective value will either stay the same or increase. However, as the slope becomes steeper, the relative cost of increasing the degree of ZEN becomes higher. Thus, the willingness to pay for a higher degree of ZEN is an important aspect that needs to be considered when applying the IMEZEN.

It is also interesting to investigate how the electricity demand and heat demand are covered. Figure 9.2 shows the annual energy generation and energy imports, calculated as an average of the five years reaching from year 20 to 25 for scenario 1. This period is chosen because it illustrates the total demand of the neighborhood with the operational behaviour stabilized, as it is after the development period has been completed. The heat and electricity demand are included in the figure as areas in the background to show how these are covered by on-site generation and import of energy. Note that the electricity demand does not include the electric demand related to the operation of the heat pumps. Also note that only the technologies invested in are included in this graph.

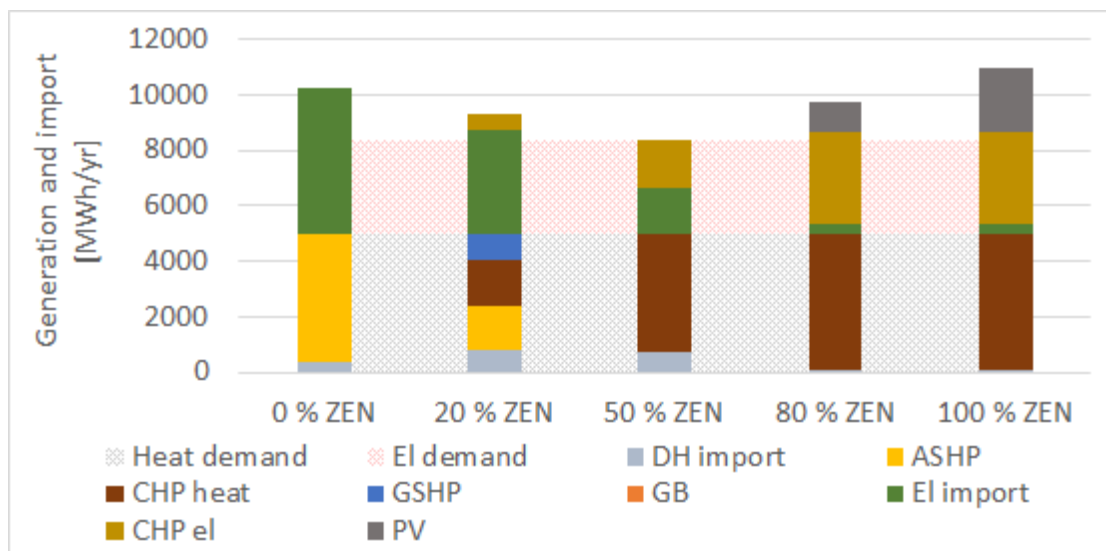


Figure 9.2: Average annual demand covered by on-site energy generation and import, using carbon factors

For the case of 0 % ZEN, it can be observed that the heat demand is mostly covered by the ASHP. In addition, some of the heat demand is covered by importing heat from the DH grid and by the GB (not visible on the graph). The electricity demand is covered by importing electricity from the grid. For higher degrees of ZEN, the amount of electricity imported decreases, whereas the heat import first increases

before it decreases again. The decrease in energy imports is replaced by on-site energy production from the CHP and PV, making the neighborhood more and more self-sufficient as the degree of ZEN increases.

For 80 % and 100 % ZEN, one can see that the electricity supplied to the neighborhood exceeds the electricity demand. The reason for this is that some of the electricity generated on-site is exported to the grid in order to compensate for emissions. This explains the large increase in PV capacity and some of the increase in CHP capacity that can be seen in Figure 9.1. Note that for 0 % ZEN and 20 % ZEN the electricity supplied that exceeds the electricity demand is not exported but used as a resource by the heat pumps in order to generate heat.

The IMEZEN makes its investment decisions by simultaneously optimizing the operational decisions. Thus, it is also interesting to study the operation. Figure 9.3 - 9.6 show how the model performs on the operational level. The degree of ZEN used is 100 %, representing the base case.

Figure 9.3 shows how the electricity demand (red line) is covered by electricity generation and electricity import (stacked areas) for a representative week in a winter season. This shows that the electricity demand is covered in all hours. The CHP acts as a base load technology, generating a constant amount of energy throughout the season. This is reasonable as wood chips are low at cost and have a low carbon factor. Electricity imported from the grid and electricity generated from the PV installations are used as top load technologies to cover peak loads. As expected, the figure also shows that electricity is exported to the grid when there is overproduction from the CHP and PV installations (blue line).

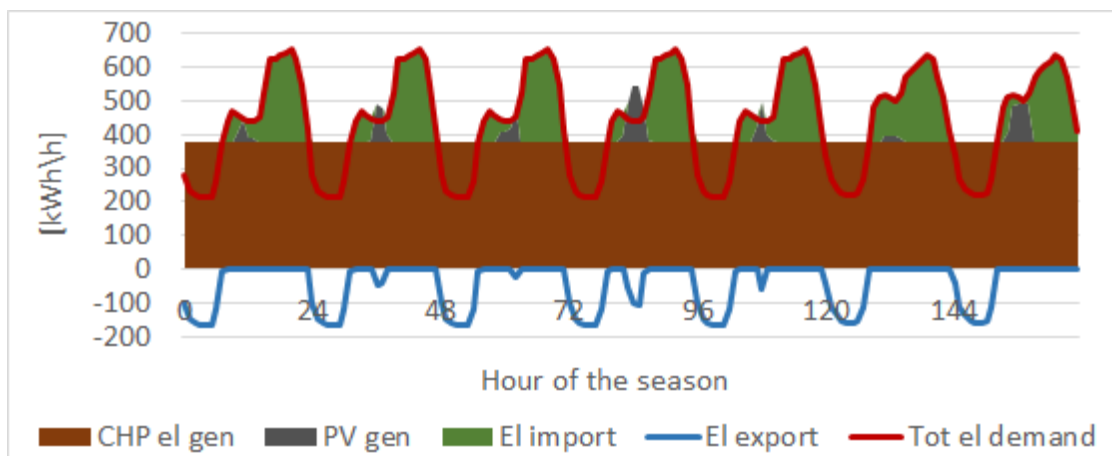


Figure 9.3: Electricity balance for a representative week in season 1

Figure 9.4 shows how the heat demand (black line) is covered by heat generation, heat import and heat from storage (stacked areas), for a representative week in a winter season. As for the electricity, the CHP is used as a base load technology and generates heat constantly throughout the season. When the heat generation exceeds the heat demand, the excess heat is stored. This is seen by the yellow line in the figure. Further, when the heat generation from the CHP alone is insufficient to cover heat demand, heat from the DH grid and the heat storage are used. This indicates that DH and heat storage are used as top load technologies. Again, this seems reasonable as the CHP consumes wood chips. In the extreme seasons, the operational behaviour is similar to the behaviour in the winter season. These results are therefore not included.

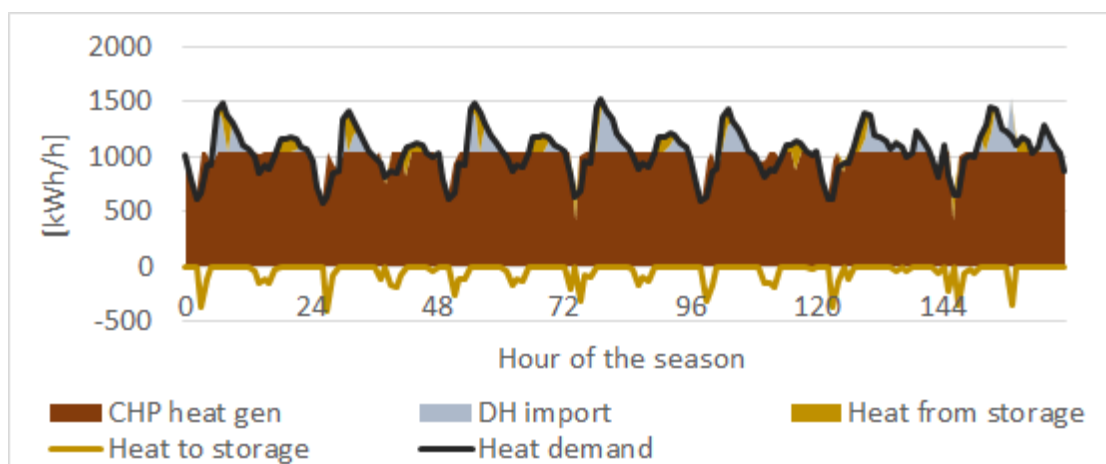


Figure 9.4: Heat balance for a representative week in season 1

In the summer season, the demand is low relative to the rest of the year. Figure 9.5 shows how the electricity demand is covered for a representative week in the summer. One can see that the base load technology still is the CHP. However, the top load technology in this case is PV, and there is almost no electricity imported from the grid. This is reasonable as the PV generation is much higher in the summer, and one manages without importing any electricity most of the time. During the night, when there is no PV generation, the CHP covers the demand alone as it is lower at this time. The figure also shows that excess electricity is exported to the grid, which is to be expected.

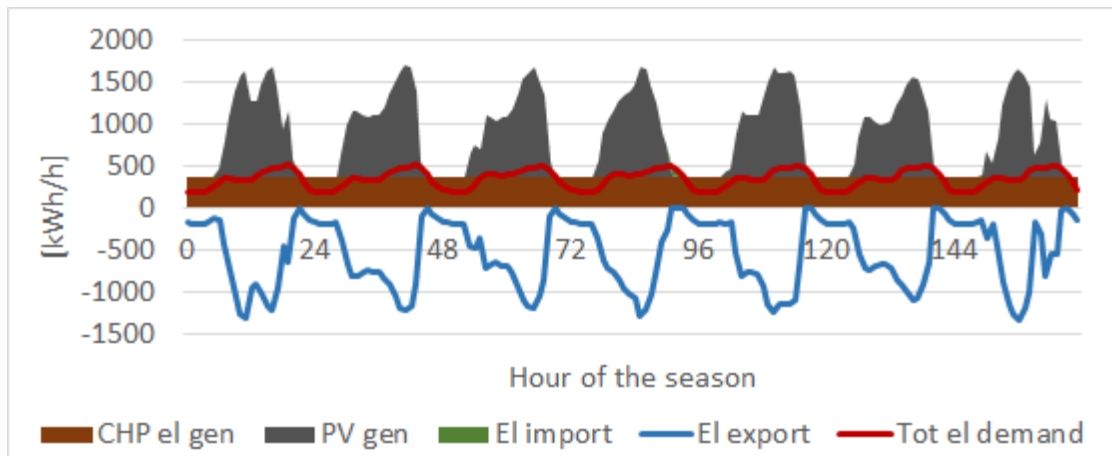


Figure 9.5: Electricity balance for a representative week in season 3

Figure 9.6 shows how the heat demand is covered for a representative week in the summer season. Here, one can observe that as the heat demand is much lower in the summer compared to the winter season, all demand is covered by the CHP.

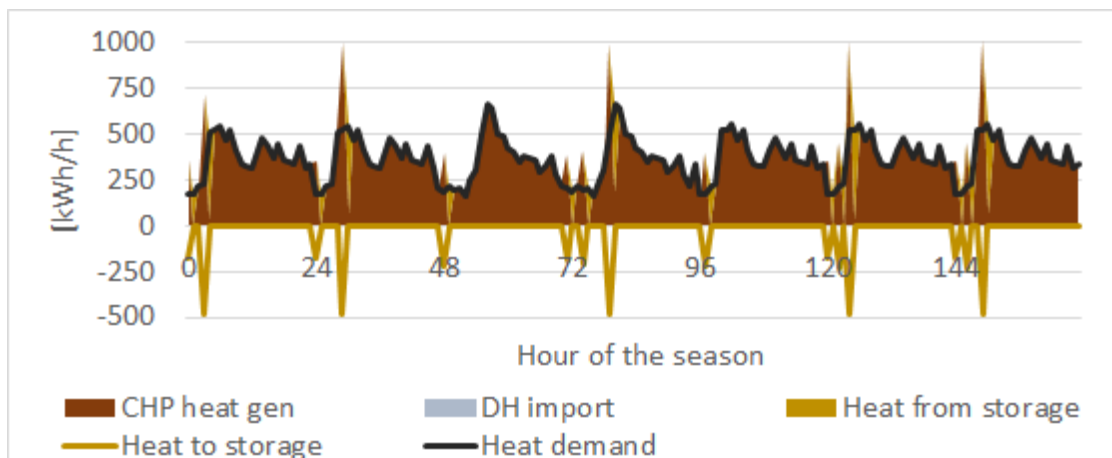


Figure 9.6: Heat balance for a representative week in season 3

Figure 9.5 shows that the electricity generated by the CHP is constant in the summer season, implying that the heat generated is also constant. However, some of the heat generated is unused, explaining why it does not appear to be constant in Figure 9.6. This means that loss of heat occurs in all hours where the excess heat is not stored. This suggests that the operation of the CHP is mainly driven by the need for electricity, and that it is more beneficial from a cost perspective

to incur heat loss in order to cover the electricity demand. This is reasonable as electricity imported from the grid has a higher carbon factor than wood chips, and thus, when the degree of ZEN is 100 %, on-site production of electricity is preferred.

The operation of the HS seems unnecessary during some hours in the summer season, as heat is stored and then later used, even though the CHP overproduces heat at all times. This does not affect the optimal solution since there are no costs related to the use of the HS. This happens as it is indifferent whether there is constantly a heat loss from the CHP or whether there is less heat loss in some hours when heat is stored, and then more heat loss in other hours as the heat stored is used.

Table 9.1 shows the investment decisions, reflecting the distribution of the installed capacities over the six investment periods. Note that only the technologies installed are included in the table.

Table 9.1: Installed capacities of the included technologies in each investment period

Technology	Investment period					
	1	2	3	4	5	6
CHP	203.30	211.59	987.95	221.67	–	–
PV	–	4 522.42	–	–	–	–
HS	217.96	182.85	303.18	–	–	–

From the table one can see that the CHP is installed in investment period 1, 2, 3, and 4, with a larger capacity being installed in investment period 3. This investment pattern may be related to the lifetime of the CHP, which is 20 years. It can be observed that the largest capacity is installed when there is 20 years left of the optimizing horizon. This is a reasonable decision when considering that the model does not account for salvage values of the technologies. Thus, in order to utilize the installed capacity of the technology, it is profitable to invest when the remaining time horizon is equal to the lifetime of the technology. However, one can see that a small capacity of CHP is installed in investment period 4, when the remaining time horizon is shorter than the lifetime of the CHP. The CHP capacity installed in investment period 1 has at this time only five years left of its lifetime, indicating there might be necessary to re-invest in this technology. Still, the decision to invest in period 4 is probably due to a combination of reasons,

including the need for re-investment and the desire to maximize the utilization of the technologies, but also considering that the present value is lower for investment costs placed further into the future. Note that no technologies are installed in the two last investment periods. This is reasonable as the utilization of the installed technology capacities in these periods would be low. One can see the same pattern for the other technologies as well. Especially the PV investment, as the entire capacity is installed in one investment period, which presumably is related to its lifetime of 25 years.

The development period, which lasts three investment periods, is also reflected in the investment decisions. This is observed as, for the CHP and HS, investments are made throughout the development period, gradually increasing the total capacity of these technologies as the size of the neighborhood also increases. This is to be expected when considering the discounting of future costs and the fact that there is no need to install in units that will not be utilized right away.

9.2 Different emission factors

In this section an evaluation of the effect from using different emission factors is included. This evaluation is performed by testing the IMEZEN with both total PE factors and non-renewable PE factors. These results will be analyzed using the same degrees of ZEN as when testing the base case. The focus will in this section be on the investment decisions. A comparison of using all the different emission factors will be provided. Note that 0 % ZEN is equivalent for all emission factors.

9.2.1 Total PE factors

Figure 9.7 shows the total capacity of the installed technologies and the related cost from using total PE factors, and has the same characteristics as Figure 9.1, which was explained for the case with carbon factors. Note that the installed units for 0 % ZEN are the same regardless of the weighting factors applied.

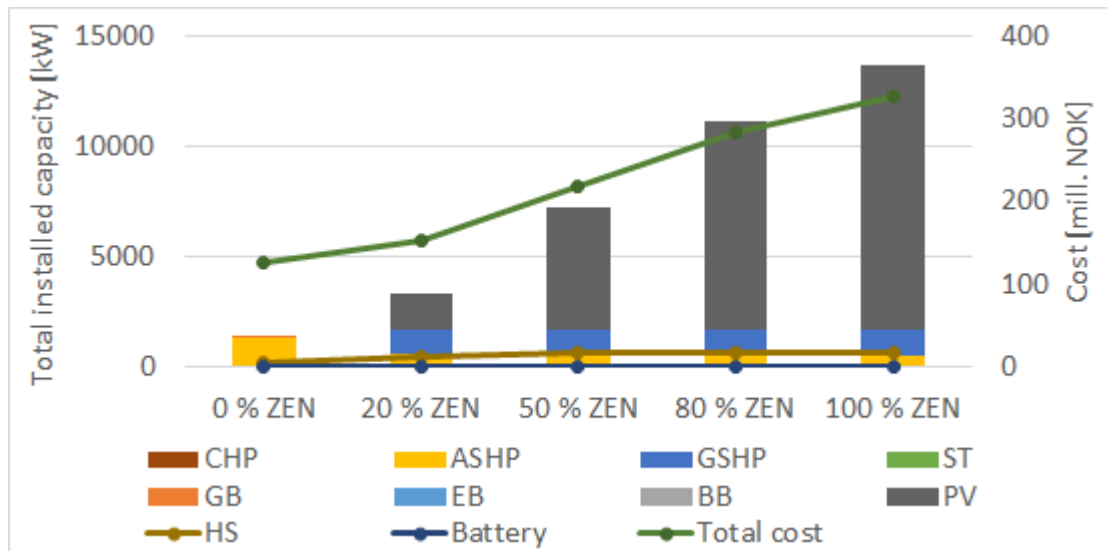


Figure 9.7: Total installed capacities and costs for increasing degree of ZEN, using total PE factors

The figure shows that the technologies installed are ASHP, GSHP, HS, and PV. The investment in GSHP, ASHP and HS seems to stabilize from 20 % ZEN, whereas the installation of PV has a relatively linear increase relative to the degree of ZEN. One can also see that the total costs have an increase similar to the installed PV capacity. Thus, the large investments in PV explains the increase in total costs, implying that accomplishing the goal of 100 % ZEN is quite expensive.

Figure 9.8 shows the average annual on-site energy generation and import, calculated for the same years and same scenario as for carbon factors. This graph also depicts the same as Figure 9.2, which was explained for carbon factors. A big difference from the base case, where carbon factors are used, is that there is no investment in the CHP technology. This is sensible when considering that the total PE factor of bio fuel does not favor this energy carrier in the same way as carbon factors. In fact, the total PE factor is the same for wood chips, gas and heat import, while it is higher for electricity. This also impacts the amount of heat imported from the DH grid, as this energy carrier is not as favourable as when using carbon factors. It can be observed that investments in heat pumps are made instead, even though they consume electricity, and that electricity is also imported from the grid. This can be explained by the fact electricity is not as unfavorable as when applying the carbon factors. Also, this is the preferred energy system composition for 0 % ZEN, implying that it is the best choice from a cost perspective.

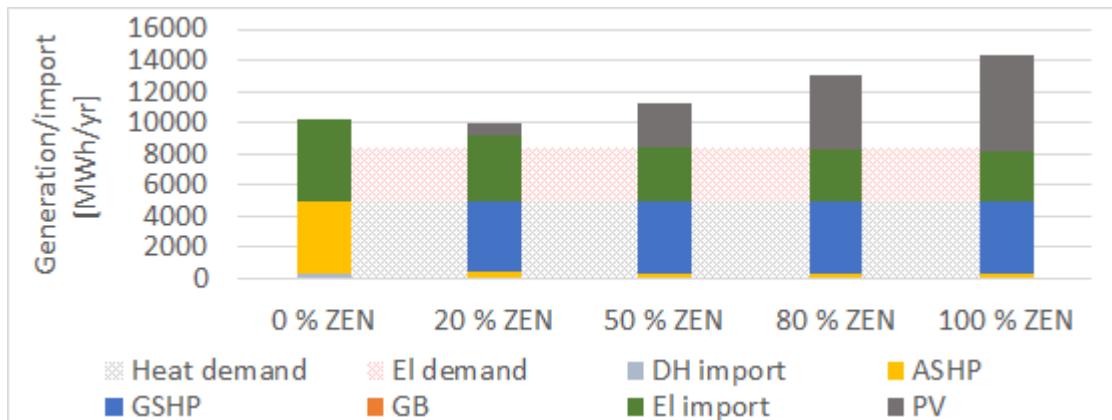


Figure 9.8: Average annual demand covered by on-site energy generation and import, using total PE factors

However, contrary to the case with 0 % ZEN, the GSHP is preferred over the ASHP for higher degrees of ZEN. Although the investment cost of the ground source heat pump is greater than for the air source heat pump, it has a higher COP value which presumably makes up for this. Thus, due to the required fulfillment of the ZEN degree, the ground source heat pump is preferred because it is able to generate more electricity than the air source heat pump from the same amount of electricity.

One can also see from Figure 9.7 that the PV capacity installed is much higher compared to the investments made in the base case. This is to be expected when the heat technologies installed consume electricity, which increases the need for compensation of emissions, and thus the need for exporting electricity. As there is no limit on the maximum amount of electricity exports, all excess electricity generated by PV is exported, as seen in Figure 9.8. As PV is a emission free producer of electricity, the investments made in this technology are huge. In this case, one may consider restricting the investment in PV by including a limit on the area that can be used for PV installments and/or a limit on the export of electricity within an hour. This will ensure a more realistic solution, although there is a possibility of the problem becoming infeasible if the restrictions are too tight. A short discussion regarding this issue will follow in section 9.3.4.

9.2.2 Non-renewable PE factors

Figure 9.9 shows the total capacity of the installed technologies and the total costs when using non-renewable PE factors. It has the same characteristics as Figure

9.1, which was explained for the case with carbon factors, and Figure 9.7, which was presented for the case with total PE factors. Note that the installed units for 0 % ZEN are the same regardless of the weighting factors applied.

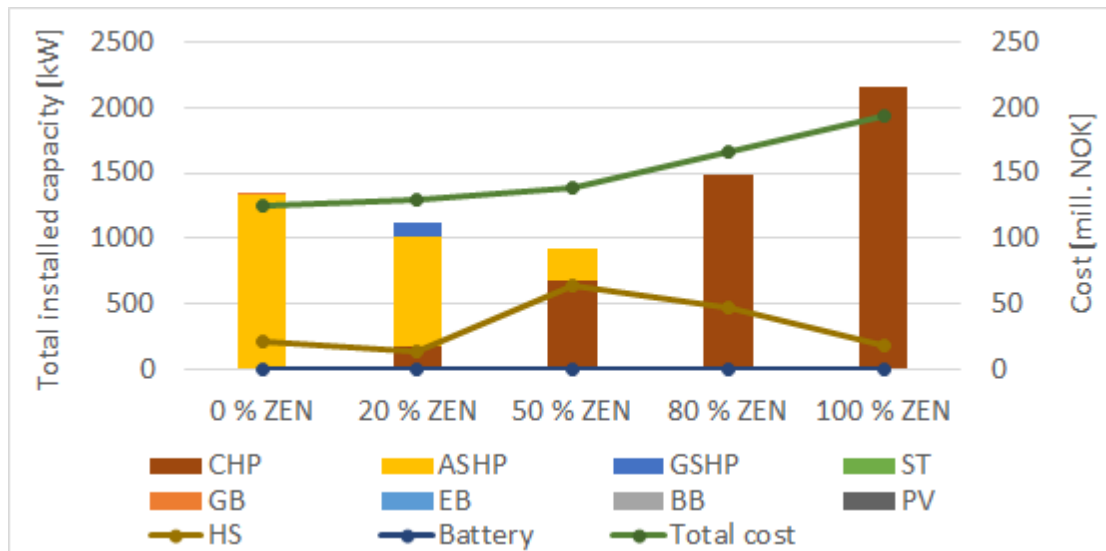


Figure 9.9: Total installed capacities and costs for increasing degree of ZEN, using non-renewable PE factors

From the graph one can see that, as the ZEN degree increases, the investment in heat pumps decreases and the investment in CHP increases quite linearly. For 20 % ZEN, GSHP is also installed. Note that, similar to the carbon factors, bio fuel is favored by the non-renewable PE factors. This is reflected through the extensive investments in CHP for high degrees of ZEN.

Figure 9.10 shows the average annual on-site energy generation and import, calculated for the same years and same scenario as for the other emission factors. This graph depicts the same as Figure 9.2 and Figure 9.8 does for the carbon and total PE factors, respectively.

From this figure one can see that the import of electricity is reduced when the ZEN degree increases. For 100 % ZEN, the CHP is almost able to cover the total electricity demand by itself. Import of electricity is presumably only used to cover the peak loads in the extreme seasons and during the winter season. It can also be observed that the utilization of the connected DH grid is very low for high ZEN degrees, contrary to the increase in heat import seen from 0 - 50 %. It is reasonable that heat is imported from the DH grid to cover the peak loads in the cases where

the installed capacity of the CHP is low. As the installed capacity of the CHP increases, more heat is generated on-site. A higher percentage of the peak loads are thus covered by the CHP, meaning the need for heat import decreases.

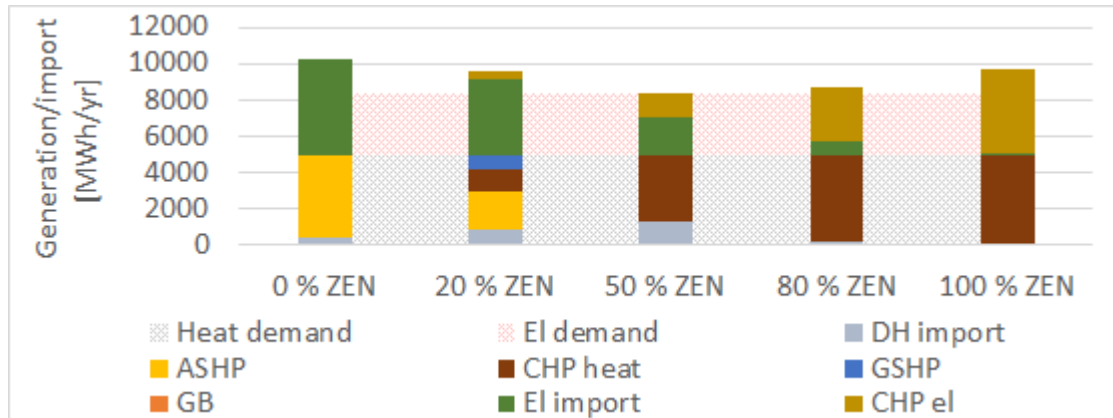


Figure 9.10: Average annual demand covered by on-site energy generation and import, using non-renewable PE factors

From Figure 9.9 one can see that the heat storage investment culminates around 50 % ZEN. From 20 - 50 % ZEN, the increase is similar to the increase seen when using the other weighting factors, and from 50 - 100 % there is a decrease in the installed capacity of HS. This is the same development as for the heat import from the DH grid seen in Figure 9.10, and may be explained by the increase in CHP capacity. As the CHP generates electricity in excess of the demand in order to export electricity, thus compensating for emissions, a large amount of heat is also generated. Hence, the heat generated by the CHP often exceeds the heat demand. This indicates that the need for storing heat decreases, as the operation of the CHP, driven by the need for electricity, ensures that the heat demand is covered most of the time.

9.2.3 Effect of the emission factors

This case study has shown that the IMEZEN is very sensitive to the emission factors used, and that the definition of 100 % ZEN is dependent on these factors. Figure 9.11 shows the total installed capacities and the total costs for the case of 100 % ZEN when using the three different emission factors.

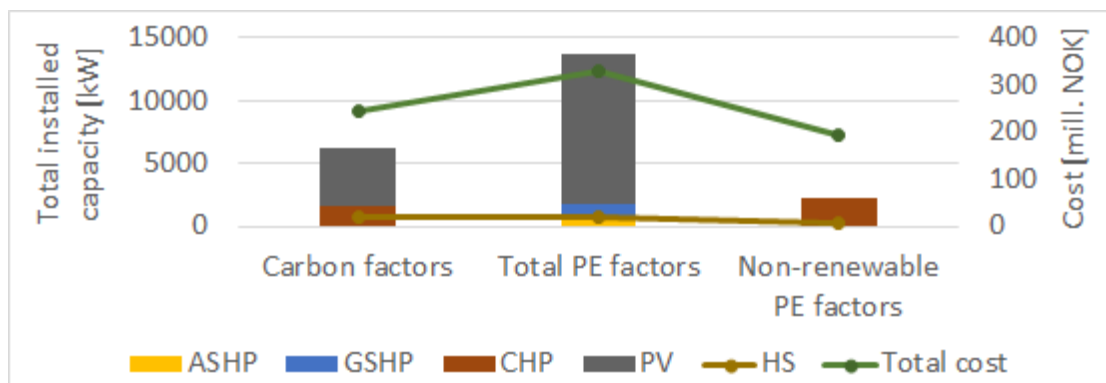


Figure 9.11: Total installed capacities and total costs for 100 % ZEN, using different emission factors

The figure shows the difference in the composition of technologies selected when applying the different emission factors. For both carbon factors and non-renewable PE factors the investment in CHP is large, which can be seen in relation to their favoring of bio fuel. This is especially prominent for the non-renewable PE-factors, as the CHP is the only energy generating technology installed. As mentioned before, the high ZEN degree results in an operation of the CHP with over-production of heat, incurring large amounts of heat loss.

The figure also shows the immense PV investment that occurs when using the total PE factors. In this case the PV is used to produce electricity that can be exported in order to achieve the goal of 100 % ZEN. Additionally, due to the fact that the installed heat technologies consume electricity and because the electricity demand is covered by importing electricity when there is no PV production, an even larger amount of PV is installed.

When applying the carbon factors, which is the base case, one can see that the technologies installed are a combination of the technologies selected when using total PE factors and non-renewable PE factors. Here, both the CHP and PV is used to cover the electricity demand and to export electricity in order to achieve the goal of 100 % ZEN, in addition to the CHP being used to cover the heat demand.

The figure also provides a clear view of how the installed capacity of PV drives the total costs. PV has only an associated investment cost, and does not have any variable costs related to its operation. Still, as the investment cost is relatively high, this has a large influence on the total costs. It is clear that the case where total PE-factors are used is the one with the highest cost. These results imply

that the selection of which emission factors to use has a large impact on the optimal decisions and the corresponding objective value. Therefore, it is important to emphasize that the values of these factors should be studied carefully before running the IMEZEN. Also, as these values are of political interest, which values are considered to be the most “correct” might depend on the region or country in question.

9.3 Practical analysis

In this section a practical analysis is performed, identifying the sensitivity of the IMEZEN to changes in certain parameters. The analysis mainly focuses on how the changes affect the investment decisions, as the IMEZEN is an investment model. However, the operational behaviour will be commented where deemed necessary. First, the sensitivity to an increase in the bio fuel price will be identified. Further, it will be tested how the IMEZEN reacts to changes in the investment cost of the battery, as well as its reaction to restricting the electricity export. Finally, tests using maximum limits on PV and ST areas, as well as maximum ramping of the HS, are performed. The base case will be used throughout this practical analysis, only changing the parameters that are being evaluated, unless otherwise specified.

9.3.1 Increased bio fuel price

The bio fuel price used in this thesis is based on local resources. As stated in Enova (2010), a disadvantage of bio fuel is that there is a lack of access to it, dependent on geographical locations, and that there is a limited production nationwide. Also, transportation costs constitute a large amount of the fuel costs, which implies that wood chips is more expensive for neighborhoods placed far from a supplier. Therefore, it might be interesting to study how the model will behave when optimizing a similar neighborhood, but without having wood chips available as a *local resource*. A short analysis will follow.

When increasing the bio fuel price, the amount of CHP installed decreases and shifts towards larger investments in PV. Also, the energy imports, of both heat and electricity, becomes more extensive. When the bio fuel price is doubled, investments in ground source heat pump are also made. The invested capacity in heat storage first increases, before it decreases when the installed capacities of heat generating technologies decrease, and the heat import from the DH grid

becomes more prominent.

The initial increase in heat storage is assumed related to the fact that the operation of the CHP becomes more expensive with higher fuel costs. Thus, the desire to utilize the excess heat generated by the CHP and reduce the heat loss, results in more heat being stored for later use. When the bio fuel price is further increased, the investment in CHP decreases, thus reducing the excess heat production and the need for storage. The reduction in the installed CHP capacity is a natural reaction to the increased bio fuel price as its low fuel costs was one of the main reasons for the selection of this technology in the base case.

9.3.2 Reduced battery price

The price of the battery is the technology cost that is expected to decrease the most in the future. Because of this, it would be interesting to see how much the price has to decrease in order for the IMEZEN to invest in this technology. This evaluation is performed by solving the IMEZEN for different values of the investment cost. The price of the battery was gradually decreased until an investment in this technology was made.

The results from these tests revealed that the battery price has to decrease with as much as 99.4 % before the battery is included in the energy system. Note that even with this price reduction only an unrealistically small capacity is installed, and the battery price should therefore decrease even more in order for the IMEZEN to invest in a more realistic capacity size. However, this implies that an extremely large decrease in the battery price is required. It is important to point out that these results depend on the other input parameters used, and that other results may be obtained for a different neighborhood.

Another aspect to consider is the case where large capacities of PV is installed and there is a limit on the maximum electricity that can be exported at the same time. In this case, the battery may be of interest, enabling one to generate PV, store the excess electricity, and then export the energy stored steadily in order to achieve the ZEN goal. The percentage of which the battery price has to decrease will therefore presumably be highly dependent on the export limit set. This is a valid assumption as the operation of the PV installments is very inflexible because it depends on the solar irradiation, thus having a storage provides flexibility as excess electricity produced can be stored for later use or export. Therefore, a test to see how the IMEZEN reacts when there is a maximum limit on the electricity export is also performed.

9.3.3 Maximum export of electricity

The maximum export limit is in this evaluation set equal to the maximum demand in the historical load profile for the entire neighborhood, specifically 650.67 kW. The export of electricity is regulated by tariff sheet 7.1 for plus-customers, and this states that a connected unit cannot exceed the maximum power limit of 100 kW at any point in time (Eidsiva Nett AS, 2018a). Note that this value is related to political restrictions and may undergo changes in the future. However, this limit is very high if we consider it as a limit for a single building and aggregate it for the entire neighborhood, and very low if we assume only one connection point between the grid and the neighborhood. Therefore, the export limit is instead based on the electricity load profile. This is reasonable because it is likely that the power capacity of the installed connection points to the electricity grid will reflect the expected demand.

Results showing the change in investment behaviour when including the maximum limit on electricity export is presented in Figure 9.12. The figure shows the total installed capacities and the total costs. Note that only the technologies that are invested in are included in the figure. When solving the IMEZEN the base case values are used, i.e. also the original battery price.

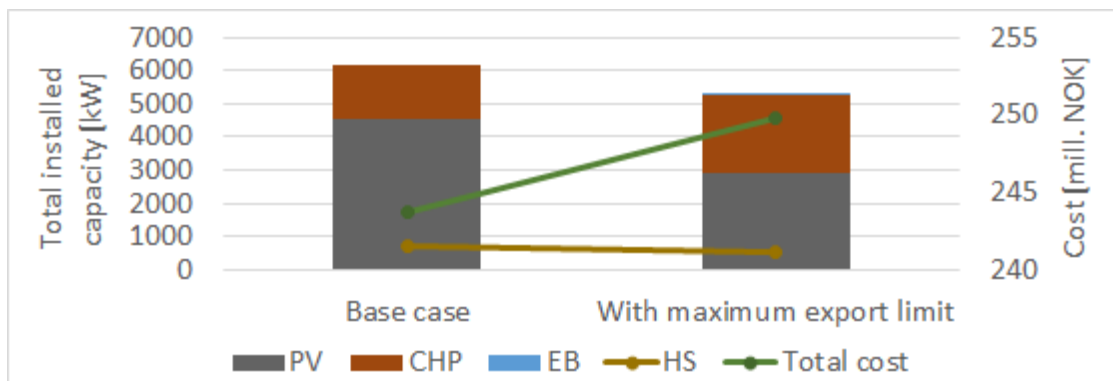


Figure 9.12: Total installed capacities and total costs with and without maximum electricity export limit

The graph shows that the installed capacity of PV is almost halved when applying the maximum export limit, whereas the investment in CHP is increased. A small capacity of the electric boiler is also installed, which might be due to situations where the export limit is reached and there is still excess electricity. Then, the excess electricity can be utilized by the electric boiler to generate heat, instead of

for example importing heat from the DH grid. Utilization of on-site produced electricity incurs no emissions or costs, and will therefore be favored over for example heat import.

We have also included a test aiming to identify how much the battery price has to decrease before it is included as an investment, when the maximum limit on electricity export is applied. These tests are performed the same way as described in the previous section. The results show that the battery price would have to decrease with 81.07 %, before the battery was installed. This confirms our assumption that the battery would be of a higher interest when it is not possible to export unlimited amounts of electricity.

9.3.4 Maximum PV and ST areas

The installment of the PV and ST technologies may physically depend on the actual available area that can be covered by PV panels and ST collectors. Ydalir is a 300 000 m² large area, where buildings constitute around 86 500 m². If one assume angled roofs and that about 70 % of the south facing sides may be covered, this implies there is 30 275 m² available roof space for PV and ST (Gupta, 2012). One can also look at the possibility of having a small free-standing ground mounted PV and ST park. By assuming that around 150 000 m² of the area will be used for other facilities, like green areas, infrastructures and other municipal areas, it leaves about 60 000 m² for a park. Since the installed capacity of PV is given in kWp, we estimate that 1 kWp PV corresponds to 10 m² (Gupta, 2012). Considering that the total PV installed in the base case is less than 6000 kWp, and no ST is installed, this would require an area of approximately 60 000 m². Thus, we have chosen to use the limit calculated from the available roof space, 30 275 m², in order to test how this affects the optimal solution of the base case.

When applying the maximum area limit, the entire area is utilized for PV installments. The installed capacity is thus lower than in the base case. At the same time, more CHP and less heat storage are installed. The increase in the CHP capacity installed is probably a compensation for the decrease in electricity generation from PV. Since the CHP consumes wood chips, which has an associated carbon factor, it is necessary to export even more electricity in order to compensate for this. Also, as a higher CHP capacity is installed for the sake of electricity production, the amount of excess heat produced increases. This implies that the need for a short-term heat storage decreases, because there is enough heat produced to cover the demand most of the time.

An evaluation from including a maximum PV and ST area limit for the case using total PE factors is also performed. The reason for this is that the investment in PV installments was extremely high when these factors were used, as described in section 9.2.1 above. As stated, in these type of situations it might be necessary to limit the PV installments, as the optimal solution proposed is very area demanding. The maximum limit is in this case set to 60 000 m², based on the discussion above. When this limit was applied, the problem became infeasible, implying that it was not possible to reach a degree of 100 % ZEN without installing more than 60 000 m² of PV-panels. This verifies earlier statements regarding the fact that reaching the goal of 100 % ZEN may in some cases be impossible to accomplish.

9.3.5 Maximum HS ramping

The rate at which a heat storage can operate is hard to determine. It depends on many factors, and will in this evaluation simply be tested for arbitrary values to see how this affects the investment decisions. The maximum ramping capability of the heat storage is first set to 0.2 kW/kWh, meaning that the storage can be fully charged within five hours. The same applies to the discharge rate. The results showed that the limit does not affect the investment decisions to a large extent. It somewhat influences the operational behaviour, but these changes are minor. When the limit is set to 0.05 kW/kWh, implying that the heat storage can be fully charged or discharged within 20 hours, it has a large influence on the investments as it does not install HS at all.

As seen in the analysis of the base case, the operation of the heat storage is short-term. This is expected since the heat storage is restricted in terms of being forced to be empty at the beginning of each season. As each season is represented by a single week, this implies that the storage components must be empty at the beginning of each week, not allowing long-term usage of the heat storage. A decreased ramping parameter implies a more long-term operation of the heat storage. Since the formulation of the IMEZEN does not allow for long-term storing of heat, it is reasonable that the heat storage is left out of the investments as this parameter decreases. Note that the over-estimated price of the heat storage used in this thesis may impact the sensibility to changes in this parameter.

Considering that the value of this rate is hard to determine, as well as the fact that the inclusion of a ramping rate will increase the complexity of the IMEZEN, this operational issue is not investigated further. This is also because the main focus of the IMEZEN is the investment decisions, and not the operational aspect.

9.4 Different types of neighborhoods

It is important to establish whether the model developed is applicable to different types of neighborhoods, and not only for the case study presented in this thesis. Therefore, different changes in technology types and available resources are done, to show how the model reacts to these changes. First, a case where the CHP technology is based on gas fuel instead of bio fuel is tested followed by a case where bio fuel is not available at all. Further, a comparison between only having local heat generation and only using a district heating grid is presented.

9.4.1 Restricted access to bio fuel

In the Ydalir case, investments in CHP and the use of bio fuel are dominating when using both carbon factors and non-renewable PE factors. However, combustion of bio products causes local particle pollution and emissions of soot (Enova, 2010), which might be a problem when using large amounts of bio fuel in urban areas. Another disadvantage of using bio fuel is the imbalance in availability across the country (Enova, 2010). This especially applies to bio pellets and wood chips. Based on this, it is interesting to investigate the optimal investments in a neighborhood where the CHP is based on gas instead of wood chips, as well as a neighborhood where bio fuel is not an option at all.

In the first case the CHP is remodeled to consume gas instead of wood chips. The price and efficiencies of the CHP is assumed the same as before. In reality, a CHP based on gas is cheaper, and may also have a different ratio between the efficiencies (higher electricity share and lower heat share) (Sidelnikova et al., 2015). A simplification is made in this evaluation and this is thus not considered.

In the latter case, the CHP still consumes gas, but the bio boiler is no longer included as an investment alternative. Figure 9.13 shows the results from the two cases, along with results from the base case.

For the first case considered, it is cost-effective to continue using bio fuel, rather investing in the bio boiler instead of the CHP. The decrease in the use of bio fuel can be observed in Figure 9.14, which shows the import of heat and electricity, the export of electricity, and the consumption of bio fuel in all three cases. The cost of wood chips is thus sufficiently low for the model to invest in a more expensive technology. One can also see an increase in the installed PV capacity in Figure 9.13, compensating for the reduction in on-site electricity production. Further, the

heat storage capacity is reduced. This is probably due to the reduction in local heat generation, and thus a decline in the amount of excess heat. As mentioned earlier, operating the CHP leads to heat loss during the summer season when the heat demand is low. Thus, a reduction in the installed CHP capacity results in a reduction of the heat loss. However, as the CHP is not installed at all, an increase in heat import from the district heating grid is necessary, as seen in Figure 9.14. Heat import from the grid is still used as top load technology.

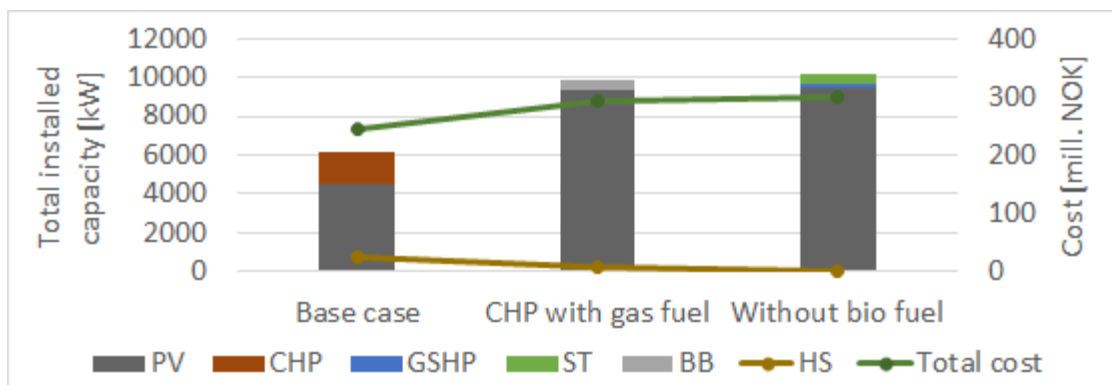


Figure 9.13: Total installed capacities and costs for the base case, CHP with gas, and without bio fuel

When excluding bio fuel completely, investments in ST and a small investment in GSHP are preferred, as seen in Figure 9.13. The heat storage capacity is here close to zero, which is reasonable as the heat generation from ST is concentrated in the summer season, and a short term storage is thus not beneficial. The investment in PV is slightly higher in this case compared to the previous case. This may be due to the fact that the heat pumps consume electricity and, as the ZEN degree is 100 %, it will therefore be beneficial to generate this electricity on-site instead of importing electricity from the grid.

The objective value increases significantly when going from the base case to either of the other cases, as seen in Figure 9.13. This shows that when the access to bio fuel is restricted, the investment in power technologies shift towards PV installments, which increases the total costs as we have seen in earlier evaluations.

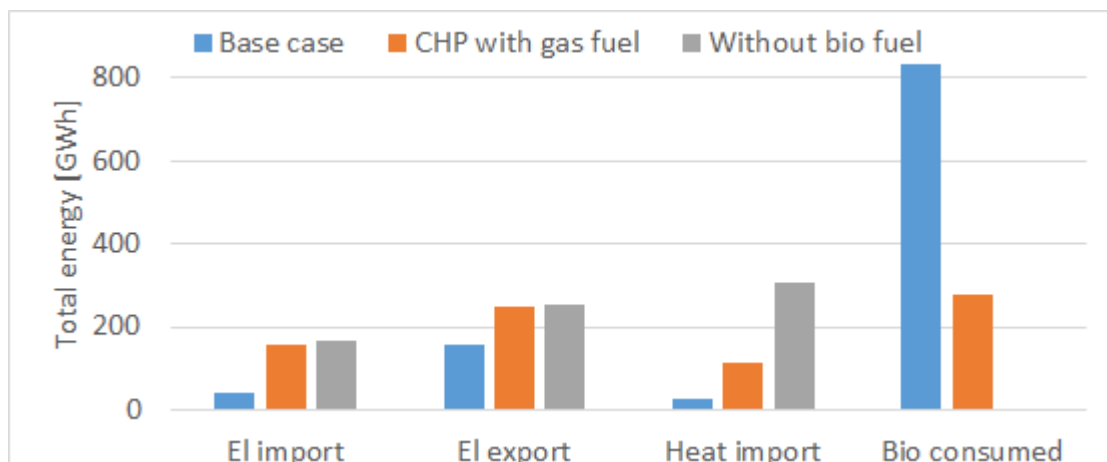


Figure 9.14: Total energy imports and exports and consumption for the base case, CHP with gas and without bio fuel

9.4.2 Local vs. district heat generation

In a neighborhood, one often chooses to utilize heat from either a local *or* an external facility. For the pilot project Ydalir it is already established an agreement to be connected to the external district heating grid which is present in Elverum, but local heat technologies within the neighborhood are still considered as potential investments. This is reflected in the case study performed above, where both local heat generation and the DH grid is included in order to retain the flexibility in the choice of investments. This is done as a combination of these might be beneficial.

In the base case, heat import from the DH grid is only used as a top load technology. This might imply that it is not beneficial for the neighborhood to be connected to the DH grid at all. The connection fee is included in the objective function as a fixed sunk cost, and does not affect the optimal solution. In addition, some neighborhoods do not have the possibility of connecting to an external DH grid. It is therefore interesting to investigate how the optimal solution changes when the DH grid is not a part of the energy system. The fixed connection charges for the DH grid are in this case excluded from the objective function. Then, the objective values, and thus the profitability of being connected to the grid, can be evaluated.

As one often chooses either local heat generation or connecting to an external DH grid, the case where heat import from the grid is the only available source of heat is also considered. In this case, all other heat technologies are excluded and cannot be a part of the solution. Note that heat storage is still included as an option.

The profitability of these two cases will be compared to the base case.

Figure 9.15 shows the objective values and the capacities for the installed technologies in the base case, the case without DH grid, and the case where DH is the only option.

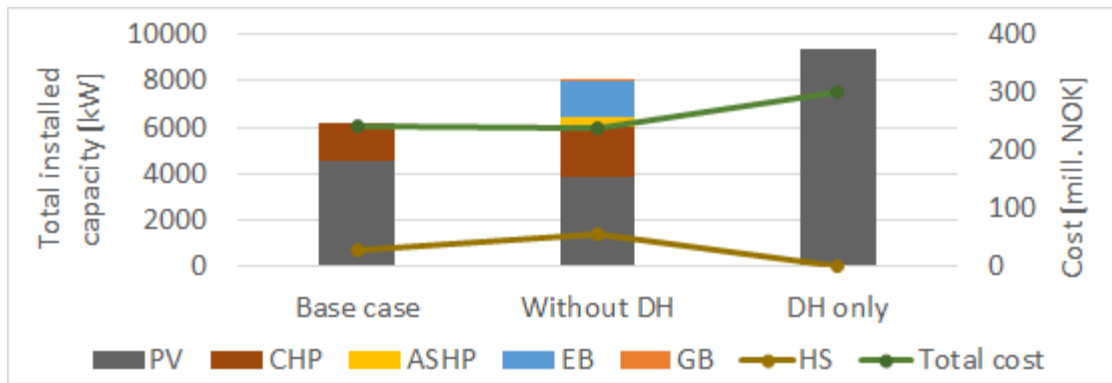


Figure 9.15: Total installed capacities and costs for the base case, without DH and for DH only

For the case of DH only, when excluding all local heat technologies, heat import is obviously the only heat source used. The other changes in investments are seen in the amount of PV capacity installed, which is increased by 10.7 % from the base case. This is presumably to compensate for the decline in electricity generation from the exclusion of the CHP. In addition, the large increase in PV is explained by the fact that the neighborhood has to achieve a degree of 100 % ZEN, and heat import has a higher carbon factor than local heat generation based on bio fuel. The increase in heat import is illustrated in Figure 9.16, which shows the changes from the base case regarding heat import and electricity, export of electricity and bio fuel consumption. It is clear that there is an increase in both heat and electricity import compared to the base case, which both require compensation through an increase in PV capacity and thus electricity export.

On the other hand, in the case where the DH grid is excluded, several other technologies are included in the energy system, illustrated by Figure ???. EB, ASHP, and a small amount of GB are all included as top load technologies, used to cover peak loads, since heat import is no longer an option. With regard to PV, the opposite from the case with DH only is observed, as the installed PV capacity is decreased. This is a consequence of the change in top load heat technologies, as the heat imported is replaced by an increase in the CHP capacity, which consumes bio fuel, and the ASHP and EB, both using on-site generated

electricity to produce heat. Figure 9.16 shows that the emissions from energy imports require less compensation as there is a decrease in both electricity import and heat import, and this is not offset by the increase in the bio consumed as bio has a lower carbon factor. Thus, there is less need for PV installments and electricity export.

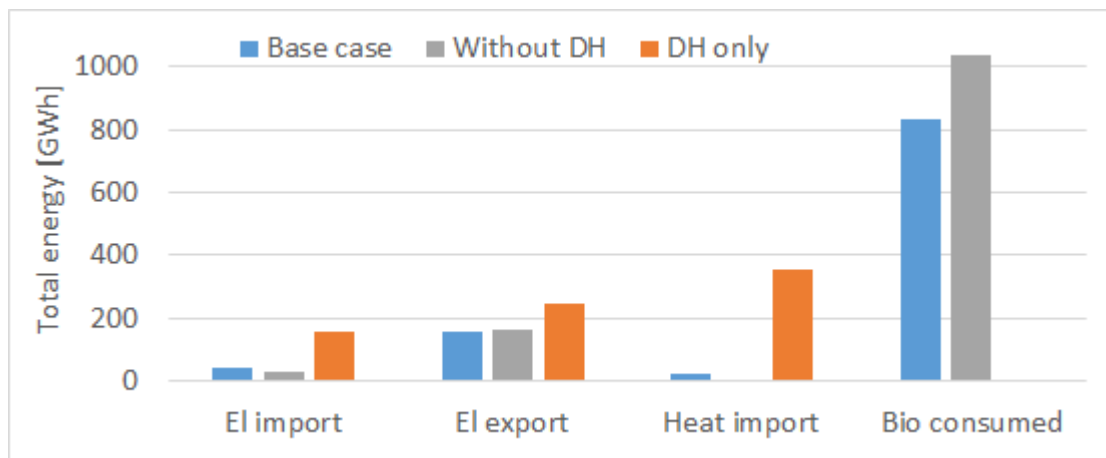


Figure 9.16: Total energy imports and exports and consumption for the base case, without DH and for DH only

An interesting finding is that, even though the case without DH invests in a higher number of technologies, the objective value is lower than for the base case. The cost decreases by 1.8 % and indicates that, in the case of Ydalir, it is more cost-effective not being connected to Eidsiva's DH grid. However, this difference in costs is not huge, and one also needs to consider the potential benefits from having an external DH grid available, which may increase the reliability of the energy system. It is also clear that a combination of local heat generation and DH generation is the second best choice, whereas the use of DH only is the most costly choice with an increase of 22.9 % from the base case. Finally, it should be noted that all input data naturally have a great impact on these results, and should be considered carefully before drawing any concluding remarks concerning whether or not this really is the case for Ydalir.

9.5 ZEN vs. ZEB

The focus of this computational study has been to investigate different aspects of the IMEZEN. However, there has not been any emphasis on the value of the IMEZEN relative to the concept of ZEBs. This would require more extensive research, but a simple analysis is provided in this section.

As the IMEZEN considers the neighborhood as a single unit with all demand aggregated, the same model can be applied to a building by only changing the input data. The load profiles for the heat and electricity demand need to reflect the demand for a building, and all input data related to the technologies should reflect the smaller technology sizes needed for a single building. The technology data gathered to represent the building technologies may be seen in Appendix B. Also note that the CHP is not included as a technology when solving the model for a building, as this technology is based on large-scale units.

In order to compare the two concepts, we need to solve the model separately for a single residential unit, a kindergarten and a school, which are the components included in Ydalir. Then, the results obtained from solving the model for a residential unit need to be scaled up by the number of residential units in the entire neighborhood. This is valid as the load profiles are assumed to be the same for all residential units in the neighborhood. In addition, the scaling needs to consider the development of the neighborhood as not all residential units are built the first year. In reality this would require solving the model once for each year in the development period, as one will only be able to scale up the solutions for the units built at the same time. However, as the load profiles are assumed identical, we can aggregate the demand for all residential units, solving the model as a ZEN consisting of only residential units. Note that this would not be valid in the case where the residential units have different load profiles. The model is also solved separately for the kindergarten and the school as they have different load profiles. Finally, the objective values for all components are added together and compared to the objective value obtained from solving the IMEZEN. The results are presented in Table 9.2, where the last row shows the difference in objective values. Note that the fixed costs have been excluded from the total objective values in this table in order to emphasize the difference in variable costs, and that the fixed costs are the same for both concepts.

It can be observed that the value of the ZEN concept is extremely high, saving more than 100 mill. NOK compared to the case of aggregated ZEBs. However, this is not a completely realistic number as the infrastructure of the neighborhood is not

considered in the IMEZEN, thus excluding all costs related to the infrastructure. On the other hand, the synergies between the different energy demand profiles is expected to have a positive impact on the total costs of a ZEN, but this aspect is only captured to a very small degree in the data, as explained in Chapter 6. Therefore, one could expect the value of ZEN to be even higher by including this aspect. This implies that the high value of the ZEN is almost exclusively related to the difference in technology costs when compared to the case with aggregated ZEBs. This is to be expected, but it is interesting to consider how this influences the investment decisions.

Table 9.2: Objective values for a ZEN and for the case of aggregated ZEBs

–	Residential	Kinder	School	Total
ZEN	–	–	–	186 000 000
Agg. ZEBs	274 475 417	7 629 718	20 753 141	302 858 275
Δ	–	–	–	-116 858 275

Table 9.3 lists the total amount of installed capacities from solving the model for the two cases. The ZEN invests in three technologies; CHP, PV and HS, while all of the ZEBs invest in a combination of PV and BB. It should be noted that the size of the BB installed in each ZEB is unrealistically small. This happens because there is no minimum limit imposed. However, when solving the ZEB models without the BB, the only compensation comes from an extremely small increase in the capacity of the PV installed. Thus, in reality one would probably only install PV in the ZEB cases and cover the heat demand by import of heat from the DH grid.

Table 9.3: Total installed capacities of technologies for a ZEN and for the case of aggregated ZEBs

Technology	ZEN	Agg. ZEBs
BB	0 kW	360 kW
CHP	1 625 kW	0 kW
PV	4 521 kWp	9 324 kWp
HS	682 kWh	0 kWh

An interesting observation is that the total amount of PV installed is almost doubled for the aggregated ZEB case compared to the ZEN. As discussed in section 9.3.4, there are physical restrictions on the available area in reality that imply that the ZEB solution is infeasible in practice. This shows that the concept of ZEN might even be necessary to achieve the environmental ambitions, at least at an acceptable cost, as it can reduce the PV installed by more than 50 % with the inclusion of CHP for on-site production of both heat and electricity.

With a higher degree of on-site production, the ZEN solution also reduces the strain on the grid significantly. This is illustrated by Figure 9.17, showing the total energy imports and exports for the whole time horizon of 30 years for both cases. The total electricity imports are reduced by almost 75 % when going from the case of aggregated ZEBs to the ZEN case, the heat imports are reduced by around 85 %, and the electricity exports are reduced by more than 35 %. Thus, the strain on the grid can be reduced immensely by applying the concept of ZENs.

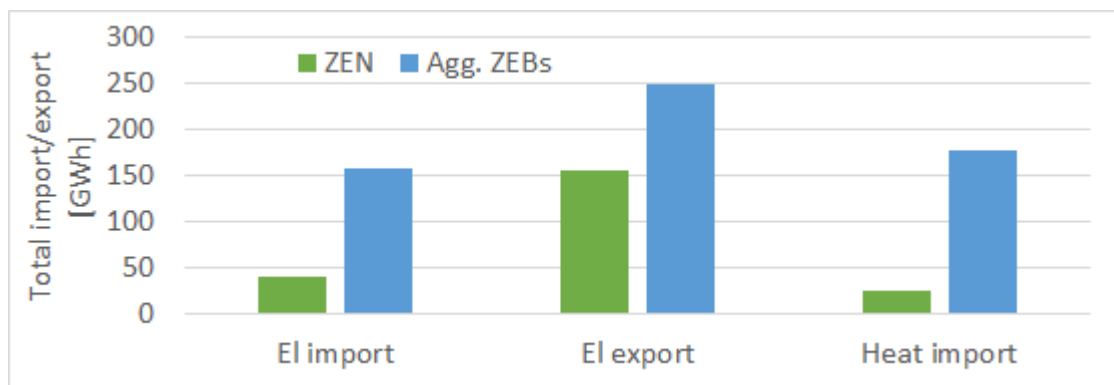


Figure 9.17: Total energy imports and exports for a ZEN and for the case of aggregated ZEBs

Chapter 10

Concluding remarks

In this thesis we have developed the IMEZEN, a single-objective two-stage stochastic multi-horizon optimization model for investment planning of energy systems in ZENs. The model optimizes both long-term investments and short-term operational dynamics over the whole time horizon, while taking into account the short-term operational uncertainties.

The proposed model includes a high number of technologies; electric boiler, gas boiler, bio boiler, air source heat pump, ground source heat pump, combined heat and power, solar thermal collectors, photovoltaic panels, district heating, heat storage and battery. Emphasis should especially be put on the inclusion of storage components for both heat and electricity as this enables load shifting and a certain degree of demand side flexibility. Export of electricity is also enabled by imposing feed-in-tariffs.

For stochastic programs considering both strategic investment decisions and operational decisions, the number of scenarios increases exponentially with the number of investment periods. When applying a long time horizon, these multi-stage stochastic problems quickly become intractable for commercial solvers. To resolve this issue, the multi-horizon information structure is applied, reducing the number of scenarios significantly and transforming the multi-stage stochastic problem to a multiple two-stage stochastic problem. This has proved to be applicable to the IMEZEN.

This thesis also provides a scenario generation method developed for the IMEZEN, supplying the model with a representation of the random variables related to the operational dynamics. The method is based on a combination of sampling from

historical data and moment matching. It has been extensively tested for different problem instances, validating its high stability for a number of these instances. This testing showed that the IMEZEN has an acceptable computation time, which is about 30 minutes. In addition, the IMEZEN has been evaluated with regard to the value of its stochasticity. The results showed that the stochastic problem is valuable in the context of avoiding infeasibility, but also that the deterministic skeleton solution is of high quality.

A comprehensive case study on the pilot project Ydalir has also been performed. The main focus has been to evaluate the base case, providing a thorough analysis of both the investment decisions and the operational aspect. From this evaluation we conclude that the preferred technologies when using carbon factors as weighting factors for emissions are PV and CHP. The effect from using other emission factors has also been observed. This showed that there is a great increase in both PV installments and costs when applying the total PE factors, as well as the CHP was replaced by heat pumps. When applying the non-renewable PE factors, only CHP was installed, and the total costs were similar to the base case. From this it can be concluded that the choice of emission factors determine the energy system composition as well as the total related costs. A practical analysis related to the base case is also completed, where one of the main findings is that the battery is only included in the energy system after a extremely large price reduction.

Finally, a study of different types of neighborhoods is included. This proves that the IMEZEN is applicable to a variety of different neighborhoods, and that it can be useful for decision makers in ZENs, as it provides a set of investment decisions regarding the technologies that should be included in the energy system, as well as the specific capacity sizes of each technology. This also implies that the IMEZEN may be incorporated as a module into EMPIRE, as it is able to represent a number of different neighborhoods.

Some shortcomings has also been identified during the work with this thesis. Primarily, only a small variation in building types and energy demand profiles were gathered in the data analysis and thus included in the aggregated demand profiles for the neighborhood. Because of this we were not able to evaluate the possible advantages from utilizing the synergies between different buildings and demand profiles. However, a short analysis of the comparison between the concept of ZEN and the concept of ZEB is presented, concluding that there is a great value in applying the concept of ZEN. Secondly, salvage values related to the technologies installed are not included in the IMEZEN. This influences the optimal solution, especially with regards to when the investments are made, and is therefore considered as a weakness of the model.

An important contribution from this thesis is the extensive study performed regarding the ZEN concept, as there does not exist many optimization studies regarding this research area. In conclusion, both the IMEZEN and the corresponding scenario generation method have proved to provide reasonable results in reasonable time.

Chapter 11

Future research

During the work with the proposed IMEZEN presented in this Master's Thesis, we have recognized several aspects of the problem which advantageously can be studied to a larger extent. There are three main directions which we find interesting to pursue; strategic uncertainty, demand side flexibility and additional technologies.

Exploiting the potential of the multi-horizon information structure may be investigated by including uncertainty on the strategic level. The question of whether the strategic uncertainty will provide any value to the model, despite a higher complexity, is interesting to study. The prediction of future load data is especially of interest in this context. The load data used in this thesis have been subject to short-term uncertainty, whereas the long-term development of demands are not considered. Even though the energy industry aims toward a low carbon society and demands are expected to decrease with the introduction of ZENs, one can also argue that electricity demand might increase due to a gradual increase in charging of electric vehicles, new types of electric demand for heating purposes, and the use of power demanding appliances. This implies a larger power variability and less predictability of the demand. The impact of including such long-term developments would be interesting to consider.

The assumptions of constant long-term prices and costs are also interesting to view in terms of strategic uncertainty. Long-term prices are related to future changes in the price of different energy carriers, whereas long-term costs are related to the development of future investment costs of the technologies. The growing uncertainty in demand also causes increasing uncertainty related to market prices of energy carriers. In addition, some technologies, i.e. especially battery, PV and

ST, are expected to have a significant decrease in price. Including these aspects in the model could therefore also be of interest.

The changes in electricity systems and markets all over the world involve an increased value of the flexibility in energy systems. As electricity demand is expected to increase, higher peak loads are also expected to occur. Demand side flexibility is a future-oriented feature, which the energy systems become more and more able to deliver as advanced infrastructures, distributed storage technologies, and intelligent information and communications technologies are introduced as parts of the energy system solutions.

Including peak load tariffs on import of electricity may also enforce a certain degree of flexibility on the demand side and cause load relief of the electricity grid by smoothing out the peaks. It would also be interesting to reflect the synergies between load profiles of the individual buildings, a possible flexibility arising from the ZEN concept, which is not considered to a large extent in this thesis. In reality, inclusion of these aspects are expected as technology and policy measures change, and will presumably lead to smoother peak loads and ease the strain on the grid. As this is one of the main purposes of introducing ZENs and smart energy systems, the inclusion of these aspects would be a beneficial improvement of the model in order for it to become a useful decision tool in the future.

Including additional technologies would also be an interesting direction to pursue. Power from especially wind, but also waves and tidal, could be incorporated as alternative energy sources. Further, as the introduction of ZENs lead to extensive use of RESs, which are characterized by intermittent uncontrolled energy generation, the inclusion of advanced storage and distribution technologies are of high relevance. This may also lead to a higher degree of the desired load shifting. Firstly, seasonal storage may be an important addition to the model. Further, it may be interesting to investigate the opportunities of including hydrogen technology. A larger neighborhood may benefit from hydrogen production from excess electricity, by later providing electricity from stored hydrogen when there is an electricity deficit. Supercapacitors are also an emerging energy storage technology that might be relevant to include in a model for a future energy system.

Bibliography

- Alharbi, H. (2015), ‘Optimal planning and scheduling of battery energy storage systems for isolated microgrids’. Available at: https://uwspace.uwaterloo.ca/bitstream/handle/10012/9320/Alharbi_Hisham.pdf?sequence=1.
- Arnesen, K. E. and Borgen, S. T. (2016), ‘A stochastic programming approach to optimal component sizing for the strategic microgrid design problem’.
- Arnesen, K. E. S. and Borgen, S. T. (2017), ‘A Multi-Horizon Stochastic Programming Approach to Optimal Component Sizing for The Strategic Microgrid Design Problem’. Available at: <http://hdl.handle.net/11250/2470453>.
- Backe, S. (2018), Private Communication. FME ZEN.
- Baer, D. and Andresen, I. (2017), Mapping of the pilot projects within the Center for Zero Emission Neighbourhoods in Smart Cities. [Unpublished].
- Bakken, B. H., Skjelbred, H. I. and Wolfgang, O. (2007), ‘eTransport: Investment planning in energy supply systems with multiple energy carriers’, *Energy* **32**(9), 1676 – 1689. Available at: <http://www.sciencedirect.com/science/article/pii/S0360544207000175>.
- Beus, L., Eldrup, C. and Hammersbøen, I. (2018), Expansion Planning for Energy Systems in ZENs: A Multi-horizon Stochastic Model for Cost Optimization of Technology Investments and Operation, Technical report. Unpublished project report at NTNU.
- Birge, J. R. and Louveaux, F. (2011), ‘Introduction to Stochastic Programming’. Available at: <https://link.springer.com/content/pdf/10.1007%2F978-1-4614-0237-4.pdf>.
- Boilers Guide (2018), ‘Boilers Guide: Working Principle’. Available at: <http://www.boilers.guide/working-principle/> [Accessed: 27/01/18].

- Bruckner, T., Groscurth, H.-M. and Kümmel, R. (1997), ‘Competition and synergy between energy technologies in municipal energy systems’, *Energy* **22**(10), 1005 – 1014. Available at: <http://www.sciencedirect.com/science/article/pii/S0360544297000376>.
- Cano, E. L., Moguerza, J. M., Ermolieva, T. and Ermoliev, Y. (2014), ‘Energy efficiency and risk management in public buildings: Strategic model for robust planning’, *Computational Management Science* **11**(1), 25–44. Available at: <https://doi.org/10.1007/s10287-013-0177-3>.
- Chou, A. (2016), ‘What’s Biomass Pellet and Bio-pellets Species’.
- Curry, C. (2017), ‘Lithium-ion Battery Costs and Market’. Available at: <https://data.bloomberglp.com/bnef/sites/14/2017/07/BNEF-Lithium-ion-battery-costs-and-market.pdf>.
- Dahl, O. T. (2018), Private Communication. Eidsiva Bioenergi AS.
- Defourny, B., Ernst, D. and Wehenkel, L. (2011), ‘Multistage Stochastic Programming: A Scenario Tree Based Approach to Planning under Uncertainty’, *Decision theory models for applications in artificial intelligence: concepts and solutions* pp. 97–147.
- Delaille, A., Lemaire, E., Malbranche, P. and Mattera, F. (2008), ‘Assessment of Storage Ageing in Different Types of PV Systems: Technical and Economical Aspects’.
- der Voort, E. V. (1982), ‘The EFOM 12C energy supply model within the EC modelling system’, *Omega* **10**(5), 507 – 523. Available at: <http://www.sciencedirect.com/science/article/pii/030504838290007X>.
- Dinker, A., Agarwal, M. and Agarwal, G. (2017), ‘Heat storage materials, geometry and applications: A review’, *Journal of the Energy Institute* **90**(1), 1 – 11. Available at: <http://www.sciencedirect.com/science/article/pii/S1743967115301215>.
- Dokka, T. H., Kristjansdottir, T. F., Time, B., Mellegård, S. E., Haase, M. and Tønnesen, J. (2013), ‘A zero emission concept analysis of an office building’, *SINTEF Academic Press*.
- Eidsiva Energi AS (2018), ‘InnlandsSpot’. Available at : <https://www.eidsivaenergi.no/stromavtaler/innlandsspot/> [Accessed: 07/05/2018].

- Eidsiva Nett AS (2018a), 'Priser for plusskunder'. Available at : https://www.eidsivanett.no/globalassets/dokumenter/priser/priser_plusskunder.pdf [Accessed: 07/05/2018].
- Eidsiva Nett AS (2018b), 'Priser for privatkunder 2018'. Available at: <https://www.eidsivanett.no/globalassets/dokumenter/priser/priser-for-privatkunder-2018.pdf> [Accessed: 06/05/18].
- Elverum Vekst AS (2017), 'Ydalir masterplan del 1 - versjon 2'. Available at: <https://www.ydalirbydel.no/wp-content/uploads/2017/12/Ydalir-Masterplan.pdf>.
- Energikanalen AS (2018), 'Temaside: Solenergi'. Available at: <http://www.energikanalen.no/temaside-solenergi.aspx> [Accessed: 07/05/2018].
- Energy Saving Trust (2018a), 'Air source heat pumps'. Available at: <http://www.energysavingtrust.org.uk/renewable-energy/heat/air-source-heat-pumps> [Accessed: 31/01/18].
- Energy Saving Trust (2018b), 'Ground source heat pumps'. Available at: <http://www.energysavingtrust.org.uk/renewable-energy/heat/ground-source-heat-pumps> [Accessed: 31/01/18].
- Enova (2010), Kompetansekompedium for varmeanlegg 2011, Technical report. Available at: https://m.rornorge.no/getfile.php/136720/Dokumenter/L%C3%A6reb%C3%B8ker/Kompedium_varmeanlegg_SISTE.pdf.
- European Commission (2016), 'Accelerating clean energy in buildings'. Available at: http://eur-lex.europa.eu/resource.html?uri=cellar:fa6ea15b-b7b0-11e6-9e3c-01aa75ed71a1.0001.02/DOC_2&format=PDF.
- European Commission (2017a), 'Buildings'. Available at: <https://ec.europa.eu/energy/en/topics/energy-efficiency/buildings> [Accessed: 23/01/18].
- European Commission (2017b), 'PHOTOVOLTAIC GEOGRAPHICAL INFORMATION SYSTEM'. Available at: <http://re.jrc.ec.europa.eu/pvgis/apps4/pvest.php#> [Accessed: 25/05/2018].
- European Committee for Standardization (2013), Energy performance of buildings - Overarching standard EPBD, Technical report. DRAFT prEN 15603.
- European Parliament (2010), 'Directive 2010/31/EU of the European Parliament and of the Council of 19 May 2010 on the energy performance of buildings', *Official Journal of the European Union*. Available at: http://www.buildup.eu/sites/default/files/content/EPBD2010_31_EN.pdf.

- Ferrara, M., Fabrizio, E., Virgone, J. and Filippi, M. (2014), 'A simulation-based optimization method for cost-optimal analysis of nearly Zero Energy Buildings', *Energy and Buildings* **84**(Supplement C), 442 – 457. Available at: <http://www.sciencedirect.com/science/article/pii/S0378778814006732>.
- Fosso, O. B. and Gustavsen, A. (2016), 'From Zero Emission Buildings (ZEBs) to Zero Emission Neighbourhoods (ZENs)'. Available at: <http://eua.be/Libraries/uni-set/olav-b-fosso.pdf?sfvrsn=0>.
- Foyn, J. (2018), Private Communication. Nord Pool AS.
- Gavric, M. (2016), 'Optimal placement and sizing of battery energy storage using the genetic algorithm'. Available at: <http://hdl.handle.net/11250/2433738>.
- Geidl, M. and Andersson, G. (2005), A modeling and optimization approach for multiple energy carrier power flow, in '2005 IEEE Russia Power Tech', pp. 1–7.
- Grohnheit, P. E. (1991), 'Economic interpretation of the EFOM model', *Energy Economics* **13**(2), 143 – 152. Available at: <http://www.sciencedirect.com/science/article/pii/0140988391900474>.
- Gupta, N. (2012), '5 things to consider before you plan for a rooftop PV plant'. Available at: <http://www.sustainabilityoutlook.in/content/5-things-consider-you-plan-rooftop-pv-plant> [Accessed: 02/06/2018].
- Hamdy, M., Hasan, A. and Siren, K. (2013), 'A multi-stage optimization method for cost-optimal and nearly-zero-energy building solutions in line with the EPBD-recast 2010', *Energy and Buildings* **56**(Supplement C), 189 – 203. Available at: <http://www.sciencedirect.com/science/article/pii/S0378778812004276>.
- Hamdy, M., Nguyen, A.-T. and Hensen, J. L. (2016), 'A performance comparison of multi-objective optimization algorithms for solving nearly-zero-energy-building design problems', *Energy and Buildings* **121**(Supplement C), 57 – 71. Available at: <http://www.sciencedirect.com/science/article/pii/S0378778816301724>.
- Helin, M. (2005), 'Wood as a fuel and drying of wood chips'. Available at: http://www.karelia.fi/bioenergia/nwh/woodfuel_production_technology/woodfuel/material/Helin_2005_Drying_of_wood_chips.pdf.
- Hellemo, L., Midthun, K., Tomasgard, A. and Werner, A. (2013), 'Multi-stage Stochastic Programming for Natural Gas Infrastructure Design with a Production Perspective', *Stochastic Programming : Applications in Finance, Energy, Planning and Logistics* pp. 259 – 288.

- Henning, D. (1997), ‘MODEST—An energy-system optimisation model applicable to local utilities and countries’, *Energy* **22**(12), 1135 – 1150. Available at: <http://www.sciencedirect.com/science/article/pii/S0360544297000522>.
- Hoff, E. (2018), Private Communication. Eidsiva Nett AS.
- Huws, H. and Jankovic, L. (2014), ‘A method for zero carbon design using multi-objective optimisation’, *1st Conference on Zero Carbon Buildings in Birmingham*. Available at: http://www.ljubomirjankovic.com/papers/p1129_final.pdf.
- Høyland, K., Kaut, M. and Wallace, S. (2003), ‘A Heuristic for Moment-Matching Scenario Generation’, *Computational Optimization and Applications* **24**(2), 169–185.
- Investopedia (2018a), ‘Coefficient of variation (cv)’. Available at: <https://www.investopedia.com/terms/c/coefficientofvariation.asp> [Accessed: 01/06/18].
- Investopedia (2018b), ‘Diversification’. Available at: <https://www.investopedia.com/terms/d/diversification.asp> [Accessed: 14/06/18].
- Investopedia (2018c), ‘Economic life’. Available at: <https://www.investopedia.com/terms/e/economic-life.asp> [Accessed: 08/05/18].
- Investopedia (2018d), ‘Present value of an annuity’. Available at: <https://www.investopedia.com/terms/p/present-value-annuity.asp> [Accessed: 10/06/2018].
- IRENA (2017), Electricity Storage and Renewables: Costs and Markets to 2030, Technical report. Available at: <http://irena.org/publications/2017/Oct/Electricity-storage-and-renewables-costs-and-markets>.
- Kall, P. and Wallace, S. (1994), *Stochastic Programming*, Vol. 46.
- Kall, P. and Wallace, S. W. (2003), ‘Stochastic Programming’. Available at: <https://www.stoprog.org/sites/default/files/files/manujw.pdf>.
- Kalogirou, S. A. (2004), ‘Solar thermal collectors and applications’, *Progress in Energy and Combustion Science* **30**(3), 231 – 295. Available at: <http://www.sciencedirect.com/science/article/pii/S0360128504000103>.
- Kaut, M. (2003), ‘Scenario tree generation for stochastic programming: Cases from finance’, p. 2. Available at: https://brage.bibsys.no/xmlui/bitstream/handle/11250/258115/122673_FULLTEXT01.pdf?sequence=1.

- Kaut, M. (2006), ‘Scenario Generation for Stochastic Programming. A Practical Introduction’.
- Kaut, M., Midthun, K. T., Werner, A. S., Tomasgard, A., Hellemo, L. and Fodstad, M. (2014), ‘Multi-horizon stochastic programming’, *Computational Management Science* **11**(1–2), 179–193. Special Issue: Computational Techniques in Management Science.
- Kaut, M. and Wallace, S. W. (2007), ‘Evaluation of Scenario-Generation Methods for Stochastic Programming’, *Pacific Journal of Optimization* **3**(2), 257–271. Available at: <https://pdfs.semanticscholar.org/c19c/2858e1fec32215411fe9eef686bfc29a1a01.pdf>.
- Korpås, M., Midtgård, O.-M. and Ranaweera, I. (2017), ‘Distributed control scheme for residential battery energy storage units coupled with pv systems’, *Renewable Energy* **113**, 1099 – 1110. Available at: <http://www.sciencedirect.com/science/article/pii/S0960148117305888>.
- Kverndalen, J. Å. (2018), Private Communication. Air Liquide Skagerak.
- L. Higle, J. (2005), ‘Stochastic Programming: Optimization When Uncertainty Matters’.
- Lambert, F. (2016), ‘Tesla quietly reduced the price of the Powerpack by 5% and its commercial inverter by 19%’. Available at: <https://electrek.co/2016/09/09/tesla-quietly-reduced-the-price-of-the-powerpack-by-5-and-its-commercial-inverter-by-19/> [Accessed: 12/05/2018].
- Lindberg, K. B. (2016), Impact of Zero Energy Buildings on the Power System. A study of load profiles, demand side management and system investments, PhD thesis.
- Lindberg, K. B. (2018), Private Communication. Department of Electric Power Engineering, NTNU.
- Lindberg, K. B., Doorman, G., Fischer, D., Korpås, M., Ånestad, A. and Sartori, I. (2016), ‘Methodology for optimal energy system design of Zero Energy Buildings using mixed-integer linear programming’, *Energy and Buildings* **127**(Supplement C), 194 – 205. Available at: <http://www.sciencedirect.com/science/article/pii/S037877881630408X>.
- Lindberg, K. B., Fischer, D., Doorman, G., Korpås, M. and Sartori, I. (2016), ‘Cost-optimal energy system design in Zero Energy Buildings with resulting

- grid impact: A case study of a German multi-family house', *Energy and Buildings*. Available at: <http://www.sciencedirect.com/science/article/pii/S0378778816304327>.
- Loulou, R., Goldstein, G., Kanudia, A., Lettila, A. and Remme, U. (2016), 'Documentation for the TIMES Model, PART 1', *Energy Technology Systems Analysis Programme*. Available at: https://iea-etsap.org/docs/Documentation_for_the_TIMES_Model-Part-I_July-2016.pdf.
- Loulou, R., Goldstein, G. and Noble, K. (2004), 'Documentation for the MARKAL Family of Models', *Energy Technology Systems Analysis Programme*. Available at: https://iea-etsap.org/Mrk1Doc-I_StdMARKAL.pdf.
- Lu, Y., Wang, S., Zhao, Y. and Yan, C. (2015), 'Renewable energy system optimization of low/zero energy buildings using single-objective and multi-objective optimization methods', *Energy and Buildings* **89**(Supplement C), 61 – 75. Available at: <http://www.sciencedirect.com/science/article/pii/S0378778814010834>.
- López Jaimes, A., Zapotecas-Martínez, S. and A Coello Coello, C. (2011), 'An introduction to multiobjective optimization techniques'.
- Maggioni, F. and Wallace, S. (2012), 'Analyzing the quality of the expected value solution in stochastic programming', **200**(1), 37–54.
- Marszal, A., Heiselberg, P., Bourrelle, J., Musall, E., Voss, K., Sartori, I. and Napolitano, A. (2011), 'Zero Energy Building – A review of definitions and calculation methodologies', *Energy and Buildings* **43**(4), 971 – 979. Available at: <http://www.sciencedirect.com/science/article/pii/S0378778810004639>.
- Messner, S. and Strubegger, M. (1995), 'User's Guide for MESSAGE III', *International Institute for Applied Systems Analysis*. Available at: <http://pure.iiasa.ac.at/4527/1/WP-95-069.pdf>.
- Milan, C., Bojesen, C. and Nielsen, M. P. (2012), 'A cost optimization model for 100% renewable residential energy supply systems', *Energy* **48**(1), 118 – 127. Available at: <http://www.sciencedirect.com/science/article/pii/S0360544212004148>.
- Mitra, S. (2008), Scenario generation for stochastic programming, Technical report.

- NASA Science (2018), ‘How do Photovoltaics work?’. Available at: <https://science.nasa.gov/science-news/science-at-nasa/2002/solarcells> [Accessed: 27/01/18].
- Natural Resources Canada (2017), ‘What Is a Heat Pump and How Does It Work?’. Available at: <http://www.nrcan.gc.ca/energy/publications/efficiency/heating-heat-pump/6827> [Accessed: 31/01/18].
- Norges Bank (2018a), ‘Valutakurs for amerikanske dollar (USD)’. Available at: <https://www.norges-bank.no/Statistikk/Valutakurser/valuta/USD> [Accessed: 18/04/2018].
- Norges Bank (2018b), ‘Valutakurs for euro (EUR)’. Available at: <https://www.norges-bank.no/Statistikk/Valutakurser/valuta/EUR> [Accessed: 16/04/2018].
- Noris, F., Musall, E., Salom, J., Berggren, B., Jensen, S. O., Lindberg, K. and Sartori, I. (2014), ‘Implications of weighting factors on technology preference in net zero energy buildings’, *Energy and Buildings* **82**, 250 – 262. Available at: <http://www.sciencedirect.com/science/article/pii/S0378778814005386>.
- Office of Energy Efficiency and Renewable Energy (2018a), ‘Combined Heat and Power Basics’. Available at: <https://www.energy.gov/eere/amo/combined-heat-and-power-basics> [Accessed: 27/01/18].
- Office of Energy Efficiency and Renewable Energy (2018b), ‘Furnaces and Boilers’. Available at: <https://energy.gov/energysaver/home-heating-systems/furnaces-and-boilers> [Accessed: 31/01/18].
- Office of Energy Efficiency and Renewable Energy (2018c), ‘Heat Pump Systems’. Available at: <https://energy.gov/energysaver/heat-and-cool/heat-pump-systems> [Accessed: 31/01/18].
- Otterlei, E. T. (2014), Klimaregnskap for fjernvarme: Felles utslippsfaktorer for den norske fjernvarmebransjen, Technical report.
- Palonen, M., Hasan, A. and Siren, K. (2009), ‘A genetic algorithm for optimization of building envelope and HVAC system parameters’, *HVAC Technology, Helsinki University of Technology, P.O Box 4400, FIN-02015 HUT, Finland*. Available at: http://www.ibpsa.org/proceedings/bs2009/bs09_0159_166.pdf.
- Panagiotakopoulou, P. and Papadopoulos, C. (2015), ‘Integrated Renewable Power, Gas & Heat (DH) Systems & Markets Co-ordination and Cooptimization using PLEXOS[®] Integrated Energy Model’.

- PV Education (2018), 'Solar Radiation on a Tilted Surface'. Available at: <http://www.pveducation.org/pvcdrom/properties-of-sunlight/solar-radiation-on-a-tilted-surface> [Accessed: 07/05/2018].
- Renewable Energy World (2018), 'Photovoltaic Systems'. Available at: <http://www.renewableenergyworld.com/solar-energy/tech/solarpv.html> [Accessed: 27/01/18].
- Renewables.ninja (2018), 'Solar PV'. Available at: <https://www.renewables.ninja/> [Accessed: 07/05/2018].
- Saft Batteries (2018), 'Lithium-ion battery life: Technical sheet'. Available at: <https://www.saftbatteries.com/products-solutions/products/intensium%C2%AE-smart-rack-mounted-energy-storage-system?text=&tech=76&market=347&sort=newest&submit=Search> [Accessed: 18/05/2018].
- Sandou, G., Font, S., Tebbani, S., Hiret, A. and Mondon, C. (2005), Short term optimization of cogeneration systems considering heat and electricity demands, *in* '15th Power Systems Computation Conference'.
- Sartori, I., Napolitano, A. and Voss, K. (2012), 'Net zero energy buildings: A consistent definition framework', *Energy and Buildings* **48**, 220–232. Available at: <http://www.sciencedirect.com/science/article/pii/S0378778812000497>.
- Seljom, P. and Tomasgard, A. (2015), 'Short-term uncertainty in long-term energy system models — A case study of wind power in Denmark', *Energy Economics* **49**, 157 – 167. Available at: <http://www.sciencedirect.com/science/article/pii/S0140988315000419>.
- Selvig, E., Wiik, M. K. and Åse Lekang Sørensen (2017), Campus Evenstad – Statsbyggpilot. Jakten på nullutslippsbygget ZEB-COM, Technical report. Available at: <https://www.statsbygg.no/files/publikasjoner/rapporter/fou/CampusEvenstad-nullutslippsbygg.pdf>.
- Shapiro, A. and Philpott, A. (2007), 'A Tutorial on Stochastic Programming'. Available at: https://www2.isye.gatech.edu/people/faculty/Alex_Shapiro/TutorialSP.pdf.
- Sidelnikova, M., Weir, D. E., Groth, L. H., Nybakke, K., Stensby, K. E., Langseth, B., Fonnelop, J. E., Isachsen, O., Haukeli, I., Paulen, S.-L., Magnussen, I., Husabø, L. I., Ericson, T. and Qureishy, T. H. (2015), Kostnader i energisektoren, Technical Report 2. Available at: http://publikasjoner.nve.no/rapport/2015/rapport2015_02a.pdf.

- SINTEF and SU (2012), ‘Energy Efficiency and Risk Management in Public Buildings’, *SINTEF*. Available at: http://e2b.ectp.org/fileadmin/user_upload/documents/E2B/EnRiMa/D3.1.pdf.
- Skar, C., Doorman, G., Pérez-Valdés, G. A. and Tomasgard, A. (2016), ‘A multi-horizon stochastic programming model for the European power system’. Available at: https://www.ntnu.no/documents/7414984/202064323/1_Skar_ferdig.pdf/855f0c3c-81db-440d-9f76-cfd91af0d6f0.
- Solar Server (2018), ‘Solar Collectors: Different Types and Fields of Application’. Available at: <https://www.solarserver.com/knowledge/basic-knowledge/solar-collectors.html> [Accessed: 27/01/18].
- Statistics Norway (2018), ‘Konsumprisindeksen’. Available at: <https://www.ssb.no/kpi> [Accessed: 18/04/2018].
- Sun, Y., Huang, P. and Huang, G. (2015), ‘A multi-criteria system design optimization for net zero energy buildings under uncertainties’, *Energy and Buildings* **97**(Supplement C), 196 – 204. Available at: <http://www.sciencedirect.com/science/article/pii/S0378778815002856>.
- Tesla Inc. (2018a), ‘Powerpack’. Available at: https://www.tesla.com/no_NO/powerpack?redirect=no%20-%20/&redirect=no [Accessed: 12/05/2018].
- Tesla Inc. (2018b), ‘Powerwall’. Available at: https://www.tesla.com/no_NO/powerwall [Accessed: 12/05/2018].
- The Danish Energy Agency and Energinet (2012), Technology Data for Energy Plants, Technical report. Available at: https://ens.dk/sites/ens.dk/files/Analyser/technologydata_for_energy_plants_-_may_2012_ver_mar2018.pdf.
- The Green Age (2018), ‘Electric Boilers’. Available at: <https://www.thegreenage.co.uk/tech/electric-boilers/> [Accessed: 27/01/18].
- The Norwegian Tax Administration (2018), ‘How VAT works’. Available at: <http://www.skatteetaten.no/en/business-and-organisation/duties1/value-added-tax---vat/slik-fungerer-mva/> [Accessed: 06/05/18].
- Tonjer, A.-T. (2018), Private Communication. Elverum Vekst AS.
- U.S. Department of Energy (2018), ‘Furnaces and Boilers’. Available at: <https://energy.gov/energysaver/furnaces-and-boilers> [Accessed: 27/01/18].

- U.S. Energy Information Administration (2018), ‘Solar Thermal Collectors’. Available at: https://www.eia.gov/energyexplained/index.cfm?page=solar_thermal_collectors [Accessed: 27/01/18].
- U.S. Environmental Protection Agency (2018), ‘What is CHP?’. Available at: <https://www.epa.gov/chp/what-chp> [Accessed: 27/01/18].
- U.S. Official Inflation Data (2018a), ‘Euro Inflation Calculator’. Available at: <https://www.officialdata.org/2011-euro-in-2018> [Accessed: 16/04/2018].
- U.S. Official Inflation Data (2018b), ‘Inflation Calculator’. Available at: <https://www.officialdata.org/> [Accessed: 18/04/2018].
- Vereecken, P. and Bavel, M. V. (2016), ‘Solid-state Batteries for Sensors, Electric Cars and the Grid’. Available at: <http://www.renewableenergyworld.com/articles/2016/07/solid-state-batteries-for-sensors-electric-cars-and-the-grid.html>.
- Wallace, S. W. (2011), ‘How useful is the deterministic solution?’. Available at: <http://www.iot.ntnu.no/winterschool11/web/material/VSS-EVPI.pdf>.
- Wang, J.-C., Lin, S.-J., Chen, S.-L. and Lee, W.-S. (2005), ‘Charge and discharge characteristics of a thermal energy storage device’, *Experimental Heat Transfer*. Available at: <https://doi.org/10.1080/08916150590884844>.
- Wang, W., Zmeureanu, R. and Rivard, H. (2005), ‘Applying multi-objective genetic algorithms in green building design optimization’, *Building and Environment* **40**(11), 1512 – 1525. Available at: <http://www.sciencedirect.com/science/article/pii/S0360132304003439>.
- Xu, B., Oudalov, A., Ulbig, A., Andersson, G. and Kirschen, D. (2016), ‘Modeling of Lithium-Ion Battery Degradation for Cell Life Assessment’, *IEEE Transactions on Smart Grid* **PP**(99), 1–1.
- Yang, H., Lu, L. and Zhou, W. (2007), ‘A novel optimization sizing model for hybrid solar-wind power generation system’, *Solar Energy* **81**(1), 76 – 84. Available at: <http://www.sciencedirect.com/science/article/pii/S0038092X06001836>.
- ZEN Research Centre (2018), ‘Ydalir, Elverum’. Available at: <http://fmezen.no/ydalir-elverum/> [Accessed: 05/04/18].

Ånestad, A. (2014), Net electricity load profiles of zero emission buildings: A cost optimization investment model for investigating zero balances, operational strategies and grid restrictions, Master's thesis. Available at: <http://hdl.handle.net/11250/258104>.

Appendix A

$$\min z = \sum_{i \in I} \frac{1}{(1+R)^{(i-1) \cdot N}} \left(\sum_{t \in T} C_{ti} x_{ti} + \sum_{\omega \in \Omega} \pi_{\omega} \sum_{s \in S} \frac{1}{(1+R)^{\lfloor \frac{s-1}{|S|} \rfloor}} \alpha_s \sum_{o \in O_s} c_{i\omega so}^{totO} \right) + C^G + C^{DH} \cdot \delta^{DH} \quad (\text{A.1})$$

where

$$c_{i\omega so}^{totO} = P_{i\omega so}^{el_imp} \cdot y_{i\omega so}^{imp} + P^{bio} \cdot (r_{(CHP)i\omega so} + r_{(BB)i\omega so}) + P_{i\omega so}^{heat} \cdot q_{i\omega so}^{imp} + P^{gas} \cdot r_{(GB)i\omega so} - P_{i\omega so}^{(el_exp)} \cdot y_{i\omega so}^{exp} \quad (\text{A.2})$$

s.t.

$$q_{ti\omega so} - r_{ti\omega so} \cdot \eta_t^H = 0, \quad t \in T^H \setminus \{CHP, DH, ST\}, \quad (\text{A.3}) \\ i \in I, \omega \in \Omega, s \in S, o \in O_s$$

$$q_{ti\omega so} - K \cdot \sum_{\tau=i'}^i x_{t\tau} \leq 0, \quad i' = \max\{1, i - \lfloor \frac{L_i}{N} \rfloor + 1\}, \quad (\text{A.4}) \\ t \in T^H \setminus \{ST, DH, CHP\}, \\ i \in I, \omega \in \Omega, s \in S, o \in O_s$$

$$q_{CHPi\omega so} - r_{i\omega so}^{CHP} \cdot \eta_{CHP}^H \leq 0, \quad i \in I, \omega \in \Omega, s \in S, o \in O_s \quad (\text{A.5})$$

$$y_{CHPi\omega so} - r_{i\omega so}^{CHP} \cdot \eta_{CHP}^E \leq 0, \quad i \in I, \omega \in \Omega, s \in S, o \in O_s \quad (\text{A.6})$$

$$q_{(CHP)i\omega so} - \frac{\eta_{CHP}^H}{\eta_{CHP}^H + \eta_{CHP}^E} K \cdot \sum_{\tau=i'}^i x_{(CHP)\tau} \leq 0, \quad (A.7)$$

$$i' = \max\left\{1, i - \left\lfloor \frac{L_i}{N} \right\rfloor + 1\right\}, i \in I, \omega \in \Omega, s \in S, o \in O_s$$

$$y_{(CHP)i\omega so} - \frac{\eta_{CHP}^E}{\eta_{CHP}^H + \eta_{CHP}^E} K \cdot \sum_{\tau=i'}^i x_{(CHP)\tau} \leq 0, \quad (A.8)$$

$$i' = \max\left\{1, i - \left\lfloor \frac{L_i}{N} \right\rfloor + 1\right\}, i \in I, \omega \in \Omega, s \in S, o \in O_s$$

$$q_{(DH)i\omega so} - q_{i\omega so}^{imp} \cdot \eta_{DH}^H = 0, \quad i \in I, \omega \in \Omega, s \in S, o \in O_s \quad (A.9)$$

$$q_{(DH)i\omega so} \leq K \cdot \bar{Q} \cdot \delta^{DH}, \quad i \in I, \omega \in \Omega, s \in S, o \in O_s \quad (A.10)$$

$$q_{(ST)i\omega so} - K \cdot Q_{i\omega so}^{ST} \cdot \sum_{\tau=i'}^i x_{(ST)\tau} \leq 0, \quad i' = \max\left\{1, i - \left\lfloor \frac{L_{ST}}{N} \right\rfloor + 1\right\}, \quad (A.11)$$

$$i \in I, \omega \in \Omega, s \in S, o \in O_s$$

$$y_{(PV)i\omega so} - K \cdot Y_{i\omega so}^{PV} \cdot \sum_{\tau=i'}^i x_{(PV)\tau} \leq 0, \quad i' = \max\left\{1, i - \left\lfloor \frac{L_{PV}}{N} \right\rfloor + 1\right\}, \quad (A.12)$$

$$i \in I, \omega \in \Omega, s \in S, o \in O_s$$

$$A \cdot \sum_{\tau=i'}^i x_{(PV)\tau} + \sum_{\tau=i''}^i x_{(ST)\tau} \leq \bar{A}, \quad i' = \max\left\{1, i - \left\lfloor \frac{L_{PV}}{N} \right\rfloor + 1\right\}, \quad (A.13)$$

$$i'' = \max\left\{1, i - \left\lfloor \frac{L_{ST}}{N} \right\rfloor + 1\right\}, i \in I$$

$$y_{i\omega so}^{imp} \leq K \cdot \bar{Y}^{imp}, \quad i \in I, \omega \in \Omega, s \in S, o \in O_s \quad (\text{A.14})$$

$$y_{i\omega so}^{exp} \leq K \cdot \bar{Y}^{exp}, \quad i \in I, \omega \in \Omega, s \in S, o \in O_s \quad (\text{A.15})$$

$$\sum_{t \in T^H} q_{ti\omega so} + \eta_{HS}^H \cdot s_{(HS)i\omega s(o-1)} - s_{(HS)i\omega so} = D_{i\omega so}^H, \quad (\text{A.16})$$

$$i \in I, \omega \in \Omega, s \in S, o \in O_s \setminus \{1\}$$

$$\sum_{t \in T^H} q_{ti\omega s1} - s_{(HS)i\omega s1} = D_{i\omega s1}^H, \quad i \in I, \omega \in \Omega, s \in S \quad (\text{A.17})$$

$$s_{(HS)i\omega so} - \sum_{\tau=i'}^p x_{(HS)i} \leq 0, \quad i' = \max\{1, i - \lfloor \frac{L_{HS}}{N} \rfloor + 1\}, \quad (\text{A.18})$$

$$i \in I, \omega \in \Omega, s \in S, o \in O_s$$

$$\eta_{HS}^H \cdot s_{(HS)i\omega s(o-1)} - s_{(HS)i\omega so} - \bar{V}_{(HS)} \cdot K \cdot \sum_{\tau=i'}^p x_{(HS)i} \leq 0, \quad (\text{A.19})$$

$$i' = \max\{1, i - \lfloor \frac{L_{HS}}{N} \rfloor + 1\}, i \in I, \omega \in \Omega, s \in S, o \in O_s \setminus \{1\}$$

$$\eta_{HS}^H \cdot s_{(HS)i\omega s(o-1)} - s_{(HS)i\omega so} + \bar{V}_{(HS)} \cdot K \cdot \sum_{\tau=i'}^p x_{(HS)i} \leq 0, \quad (\text{A.20})$$

$$i' = \max\{1, i - \lfloor \frac{L_{HS}}{N} \rfloor + 1\}, i \in I, \omega \in \Omega, s \in S, o \in O_s \setminus \{1\}$$

$$s_{(HS)i\omega s1} - \bar{V}_{(HS)} \cdot K \cdot \sum_{\tau=i'}^p x_{(HS)i} \leq 0, \quad (\text{A.21})$$

$$i' = \max\{1, i - \lfloor \frac{L_{HS}}{N} \rfloor + 1\}, i \in I, \omega \in \Omega, s \in S$$

$$\sum_{t \in T^E} y_{ti\omega so} + \eta_B^E v_{i\omega so}^+ + y_{i\omega so}^{imp} - v_{i\omega so}^- - y_{i\omega so}^{exp} - \sum_{t \in T'} r_{ti\omega so} = D_{i\omega so}^E, \quad (\text{A.22})$$

$$I' = \{EB, ASHP, GSHP\}, i \in I, \omega \in \Omega, s \in S, o \in O_s$$

$$s_{(B)i\omega so} - s_{(B)i\omega s(o-1)} - \eta_B^E v_{i\omega so}^- + v_{i\omega so}^+ = 0, \quad (\text{A.23})$$

$$i \in I, \omega \in \Omega, s \in S, o \in O_s \setminus \{1\}$$

$$s_{(B)i\omega s1} - \eta_B^E v_{i\omega s1}^- = 0, \quad i \in I, \omega \in \Omega, s \in S \quad (\text{A.24})$$

$$v_{i\omega so}^+ - s_{(B)i\omega s(o-1)} \leq 0, \quad i \in I, \omega \in \Omega, s \in S, o \in O_s \setminus \{1\} \quad (\text{A.25})$$

$$v_{i\omega s1}^+ \leq 0, \quad i \in I, \omega \in \Omega, s \in S \quad (\text{A.26})$$

$$\eta_B^E v_{i\omega so}^- - \sum_{\tau=s'}^i x_{(B)\tau} + s_{(B)i\omega s(o-1)} \leq 0, \quad i' = \max\{1, i - \left\lfloor \frac{L_B}{N} \right\rfloor + 1\}, \quad (\text{A.27})$$

$$i \in I, \omega \in \Omega, s \in S, o \in O_s \setminus \{1\}$$

$$s_{(B)i\omega so} - \sum_{\tau=i'}^i x_{(B)\tau} \leq 0, \quad i' = \max\{1, i - \left\lfloor \frac{L_B}{N} \right\rfloor + 1\}, \quad (\text{A.28})$$

$$i \in I, \omega \in \Omega, s \in S, o \in O_s$$

$$v_{i\omega so}^+ - \bar{V}_{(B)} \cdot K \cdot \sum_{\tau=i'}^i x_{(B)\tau} \leq 0, \quad i' = \max\{1, i - \left\lfloor \frac{L_B}{N} \right\rfloor + 1\}, \quad (\text{A.29})$$

$$i \in I, \omega \in \Omega, s \in S, o \in O_s$$

$$v_{i\omega so}^- - \bar{V}_{(B)} \cdot K \cdot \sum_{\tau=i'}^i x_{(B)\tau} \leq 0, \quad i' = \max\{1, i - \left\lfloor \frac{L_B}{N} \right\rfloor + 1\}, \quad (\text{A.30})$$

$$i \in I, \omega \in \Omega, s \in S, o \in O_s$$

$$\sum_{i \in I} \sum_{\omega \in \Omega} \pi_{\omega} \sum_{s \in S} \alpha_s \sum_{o \in O_s} \left(W_{el_imp} \cdot y_{i\omega so}^{imp} - W_{el_exp} \cdot y_{i\omega so}^{exp} + W_{heat} \cdot q_{i\omega so}^{imp} \right. \\ \left. + W_{bio} \cdot (r_{(BB)i\omega so} + r_{(CHP)i\omega so}) + W_{gas} \cdot r_{(GB)i\omega so} \right) + W^{Emb} = (1 - \gamma) \cdot W^{Ref} \quad (\text{A.31})$$

Appendix B

For the building case no loads for a family house exceed 3 kW for heat and 1 kW for electricity. The smallest available technologies with typically capacities around 10 kW are therefore chosen to represent this case. The school and the kindergarten have higher loads, and should be represented with larger technologies. An assumption is made and the smallest technologies are also used to represent the technology data used as input for the school and kindergarten in the building case. This might lead to higher technology costs for the school and the kindergarten, than what is really the case in reality. The technology costs for building technologies can be seen in Table B.1 and the efficiencies and lifetimes may be seen in Table B.2.

The costs for the technologies are handled the same way as explained in Chapter 6 for the neighborhood technologies. The cost obtained for the battery are from Tesla Inc. (2018*b*) and represent the Tesla Powerwall 2 battery. This cost is already given in 2018 NOK. Note that CHP is not an included technology for the building case, while this technology is not reasonable to install in a single building.

Table B.1: Technology costs - building size

Technology	Size	Unit	Technology cost [NOK/Unit]	Reference
EB	10	kW	12 021.71	Sidelnikova et al. (2015)
GB	10	kW	19 197.88	Sidelnikova et al. (2015)
BB	150	kW	35 044.70	Sidelnikova et al. (2015)
ASHP _{a-w}	10	kW	15 037.00	Sidelnikova et al. (2015)
GSHP _{w-w}	10	kW	27 476.08	Sidelnikova et al. (2015)
ST	6	m ²	12 050.04	Sidelnikova et al. (2015)
DH	-	-	25 000 ¹	Dahl (2018)
PV	5	kW _p	31 756.34	Sidelnikova et al. (2015)
HS	0.15	m ³	7 728.98 ²	The Danish Energy Agency and Energinet (2012)
Battery	13.5	kWh	7 280.56	Tesla Inc. (2018b)

¹ [NOK/household connected to DH grid]

² [NOK/kWh]

Table B.2: Efficiencies and lifetimes - building size

Technology	Efficiency	Lifetime	Reference
EB	0.98	20	Sidelnikova et al. (2015)
GB	1.00	20	Sidelnikova et al. (2015)
BB	0.84	20	Sidelnikova et al. (2015)
ASHP _{a-w}	2.40	15	Sidelnikova et al. (2015)
GSHP _{w-w}	2.90	15	Sidelnikova et al. (2015)
ST	-	25	Sidelnikova et al. (2015)
DH	1.00	-	Dahl (2018)
PV	-	25	Sidelnikova et al. (2015)
HS	0.99	15	Lindberg, Fischer, Doorman, Korpås and Sartori (2016) and The Danish Energy Agency and Energinet (2012)
Battery	0.90	10	Tesla Inc. (2018b)